YU, HO-SHING

THREE ASPECTS OF SANDSTONE DIAGENESIS: COMPACTION AND CEMENTATION OF QUARTZ ARENITES AND CHEMICAL CHANGES IN GRAYWACKES

University of Cincinnati PH.D. 1979

THREE ASPECTS OF SANDSTONE DIAGENESIS: COMPACTION AND CEMENTATION OF QUARTZ ARENITES AND CHEMICAL CHANGES IN GRAYWACKES

a dissertation submitted to the
Division of Graduate Studies of the
University of Cincinnati

in partial fulfillment of the
requirements for the degree of

DOCTOR OF PHILOSOPHY

in the Department of Geology
of the Graduate School of Arts and Sciences

1979

Ho-Shing Yu
B. S., National Taiwan University, 1970
M. S., Texas Christian University, 1974

UNIVERSITY OF CINCINNATI

April 27, 19 79

I hereby recommend that the thesis prepared under my supervision by Ho-Shing Yu

entitled Three Aspects of Sandstone Diagenesis: Compaction and Cementation of Quartz Arenites and Chemical Changes in Graywackes

be accepted as fulfilling this part of the requirements for the degree of Doctor of Philosophy

Approved by:

J B Maynard

Paul Edwin Potter

Warren D Huff

THREE ASPECTS OF SANDSTONE DIAGENESIS:

COMPACTION AND CEMENTATION OF QUARTZ ARENITES

AND CHEMICAL CHANGES IN GRAYWACKES

ABSTRACT

This study explores topics in both the physical and chemical diagenesis of sandstones. Two sets of quartz arenites from the Alberta and Saskatchewan basins have been studied to illustrate the effects of compaction and cementation upon the grain packing and loss of porosity with depth. Additionally, the changes during diagenesis in the major element composition in graywackes were investigated by studying a suite of Recent and ancient turbidite sandstones.

Grain packing and porosity in sandstones of the Cretaceous Lower Mannville Group change systematically from east to west and with depth in the Alberta basin. Two transition zones, each defined by several variables, characterize this change: 1) above 4,500 feet, floating and point contacts with but minor long contacts are typical, and characteristic values of contact strength, packing density and porosity are 1.6, 0.70 and 23 percent, respectively, 2) between 4,500 and 7,000 feet, contact strength, packing density and porosity are 2.1, 0.78 and 12 percent, and 3) below 7,000 feet, the dominant contacts are long, concavo-convex and sutured and typical values of contact strength, packing density and porosity are 2.3, 0.86 and 8 percent. These zones also coincide with breaks in the porosity-depth plot for the sandstones of the Lower Mannville. Similar transition zones defined by contact types occur at comparable depths in Mesozoic sandstones of Wyoming (Taylor, 1950). Hence, they should be looked for in other undeformed sedimentary basins.

Types of grain contacts, packing density and porosity in sandstones of the Precambrian Athabasca Formation do not change systematically with increasing depth in the Saskatchewan basin because the effect of compaction on the grain packing is obscured by cementation processes. Of the various grain contact types, long contacts are the most abundant in the Athabasca, with concavo-convex contacts being fairly common. Sutured contacts are present throughout the whole vertical section of the sandstone sequence. Sandstones of the Athabasca Formation are mainly cemented by authigenic clays and silica. Cements range from 2 to 15 percent and average about 7 percent. Grain packing and cements suggest that sandstones of the Athabasca Formation have undergone late stage diagenesis, and the maximum burial depth was probably between 12,000 and 16,000 feet.

Geochemistry of major elements of Recent and ancient turbidites was studied to investigate the relationship between sandstone composition and tectonic setting and to determine the chemical changes of graywackes during diagenesis. It was found that Recent deep-sea turbidite sands can be separated, using chemistry, into passive or trailing edge and active or leading edge basin types. The passive basin type is characterized by 78 percent SiO_2, a SiO_2/Al_2O_3 ratio of 8 and a K_2O/Na_2O ratio of 1.1, whereas active margin basin sands have typical values of SiO_2 less than 70 percent, a SiO_2/Al_2O_3 ratio around 4.5 and a K_2O/Na_2O ratio about 0.6. Further subdivision of the active margin basins was not possible using chemical variables. Deep-sea muds of these basin types show no systematic variation in oxides of Si, Al, Fe, Mg and Ca, but K and Na do show a pattern: the K_2O/Na_2O ratio decreases noticeably from passive to active tectonic settings. Thus, chemical variables such as SiO_2 content and ratios of SiO_2/Al_2O_3 and K_2O/Na_2O should generally be reliable indicators of provenance for ancient turbidite sandstones and shales, but they can only distinguish active from passive tectonic setting.

Chemical similarity between Recent deep-sea sands, ancient turbidite sandstones and average graywackes (Pettijohn, 1963) suggests that diagenetic reactions in graywacke sandstones occur in a closed system, e.g., there is no K^+-Na^+ exchange between the turbidite graywackes and associated shales.

There is a trend of increasing K_2O content with increasing geologic age in these ancient shales. This K_2O trend, which shows an abrupt increase in K_2O content in the Devonian, can be interpreted as supporting Weaver's idea (1967) that the K_2O trend observed in other shales is primary in origin, unrelated to diagenesis. This argument also suggests that dissolution of detrital K-feldspar in the turbidite graywackes does not provide additional potassium for the conversion of smectite to illite in the associated shales. Thus, the high Na_2O content of many graywackes and high K_2O content of the associated shales are not post-depositional features, as has been suggested.

ACKNOWLEDGMENTS

The writer wishes to express sincere appreciation to Dr. J. Barry Maynard as major advisor for his encouragement and advice during the course of this project. Special thanks are due to Dr. Paul Edwin Potter for his advice and suggestions. I also greatly appreciate Dr. W. D. Huff for his suggestions and critical review of the manuscript.

Appreciation is extended to Dr. I. A. Kilinc for providing USGS standards for chemical analysis. I thank Drs. J. E. Christopher and Paul Ramaeker, Saskatchewan Geological Survey, for the samples from Saskatchewan; and Drs. J. Barry Maynard and Paul Edwin Potter, for the turbidite samples.

Mr. James Harrell reviewed earlier drafts of the manuscript and helped with computation and Mrs. Lily Kao determined the organic carbon. Mr. Pete Litz kindly prepared the thin sections. I thank Mr. James Williams for his careful drafting and Mrs. Jean Carrol for her typing.

My sincere gratitude is expressed to my wife Shyu Yau, for her encouragement and assistance during my studies.

THREE ASPECTS OF SANDSTONE DIAGENESIS:
COMPACTION AND CEMENTATION OF QUARTZ ARENITES
AND CHEMICAL CHANGES IN GRAYWACKES

TABLE OF CONTENTS

TABLE OF CONTENTS (Continued)

TABLE OF CONTENTS (Continued)

LIST OF FIGURES

LIST OF FIGURES (Continued)

LIST OF TABLES

LIST OF TABLES (Continued)

THREE ASPECTS OF SANDSTONE DIAGENESIS: COMPACTION AND CEMENTATION OF QUARTZ ARENITES AND CHEMICAL CHANGES IN GRAYWACKES

Introduction

Diagenesis concerns the chemical and physical changes, modifications or transformations undergone by sediments after deposition and up to the lowest grade of metamorphism. The study of diagenesis has progresed less than other aspects of sedimentology, although recently it has received more attention than in the past. It is now recognized that information about diagenesis combined with textural, structural, mineralogic and chemical data result in a more accurate interpretation of depositional environment, provenance and sedimentation processes. For instance, Wilson and Pittman (1977) stressed that interpretation of depositional environment and provenance based on texture and composition may be inaccurate if authigenic clays are neglected. Furthermore, the influence of diagenesis may be at least as great as that of depositional processes on reservoir properties. For example, Füchtbauer (1967) clearly demonstrated that several different diagenetic processes such as cementation and compaction can be significant in modifying reservoir porosity. Hence, for petroleum exploration and reservoir development, much work has been done on the subject of diagenesis.

Generally, compaction and cementation are recognized as the major diagenetic processes which modify the grain packing and porosity of quartz

arenites. The mineralogy and chemistry of quartz arenites are not significantly changed during diagenesis because such mature sands are made up mostly of quartz grains. However, the immature sandstones, particularly the graywackes, are considered to suffer complex chemical and mineralogic alterations during diagenesis. It is interesting to compare these diagenetic alterations in graywackes with that in the clean quartz arenites. Therefore, I have decided to investigate the possible effects of diagenetic processes on reservoir properties for two types of sandstones: cratonic sandstones, for the most part quartz arenites, and turbidite sandstones, usually graywackes.

Cratonic sandstones: Compaction and cementation are two major diagenetic processes responsible for the reduction of porosity. For clean cratonic sandstones these processes are more important than formation of matrix. Under compaction, grains rotate, slip, deform and eventually move together closer and reduce pore space. Are there significant relationships between porosity, grain packing and burial depth? Can the maximum depth of burial be estimated by using packing density? Which of the contact types is the best indicator of depth? On the other hand, precipitation of carbonate, quartz overgrowths and authigenic clays are other major factors responsible for the loss of porosity. What is the paragenesis of cementation as a result of burial? What are the important geochemical conditions? How does cement destroy porosity? To answer these questions, the grain packing, cements and porosity in some buried sandstone sequences were investigated.

Sandstones of the Lower Mannville Group (Cretaceous) of the Alberta Basin and sandstones of the Athabasca Formation (Precambrian) of the

Saskatchewan Basin were studied. The Alberta basin, which extends from eastern thrust belt of the Canadian Rockies into western Saskatchewan, is ideal to examine sandstones for progressive changes in grain packing and the relation of grain packing to porosity because both abundant drilling records and core samples are available. In addition, the Lower Mannville extends from the outcrop in Saskatchewan to as deep as 10,000 or more feet in western Alberta. Moreover, there is little structural deformation. The Athabasca Formation provides an interesting comparison: fifty samples from a continuous diamond core in the Athabasca sandstone sequence (4,774 ft. in length) of the Saskatchewan basin were available for studying grain packing and porosity.

Turbidite sandstones: These sandstones are very abundant in ancient geosynclinal sequences. In some places they form important hydrocarbon reservoirs (Hsü, 1977), and in others have large amounts of matrix and/or calcite cement and consequently little porosity. The study of ancient turbidite sandstones has revealed several problems related to diagenesis. For example, Cummins (1962) was the first to claim that almost all of the matrix of turbidite graywackes is diagenetic in origin. He suggested that the matrix is the product of the alteration of the labile grains, mainly unstable rock fragments and feldspars. Recently, Galloway (1974) presented a sequence of diagenetic development of matrix in graywackes. He noticed that the geothermal gradient (temperature) plays the most important role in the sequential formation of, first, pore-filling calcite cement, second, authigenic clay coating and finally, pore filling by chlorite, montmorillonite or zeolites. In addition, Garrels, et al.,

(1971) and Reimer (1972) have emphasized the importance of ion exchange between the graywackes and associated shales during diagenesis. They suggest that at least for turbidite graywackes, sodium and potassium are exchanged between the interbedded sands and shales and consequently albite developes in the sands at the expense of K-feldspar, the potassium going into illite in the shales. This K^+-Na^+ exchange diagenetic reaction is used to explain why ancient turbidite graywackes are rich in Na_2O, whereas the interbedded shales are not.

However, many workers believe that matrix and high content of Na_2O in many graywackes is detrital. For instance, Crook (1974) proposed a hypothesis to explain the compositional variations of ancient graywackes in terms of geotectonic setting. His hypothesis is based on the mineralogic comparison between graywackes and modern deep-sea sands and chemical comparison between graywackes and some crustal materials.

Clearly, there are many aspects of the diagenesis of turbidite sandstones. In this study the possibility of K^+-Na^+ exchange between graywackes and interbedded shales was examined. Also, the geochemistry of modern deep-sea sands is emphasized here because suitable chemical data of modern deep-sea sands for comparison with ancient ones are virtually nonexistent (Crook, 1974, p. 307) and which is the key for Crook's hypothesis.

The suggestion of K^+-Na^+ exchange between graywackes and interbedded shales and hypothesis of compositional variations of ancient graywackes as indication of tectonics of source area can be evaluated by studying a number of paired sand-shale samples from a variety of tectonic settings

and ages. Closely spaced sandstone-shale pairs were first used by Glass and others (1957) to understand better the clay mineral composition of sandstone, which is strongly influenced by diagenesis. The writer has secured about 70 pairs of ancient turbidites from North and South America and Europe and 60 sand-shale pairs of modern deep-sea turbidites from the Lamont-Doherty Geological Observatory.

CHAPTER I

SANDSTONES OF THE LOWER MANNVILLE GROUP (CRETACEOUS) OF THE ALBERTA BASIN: GRAIN PACKING AND POROSITY

Introduction

This study reports on changes of sandstone grain packing in the Cretaceous Lower Mannville Group (Fig. 1) as seen in 42 samples obtained from 17 wells in Alberta and one shallow well in western Saskatchewan (Fig. 2). The purpose was twofold: first, to see how the grain packing of sandstone changes, if at all, with increasing depth of burial and, second, which of several packing parameters best correlates with the porosity of sandstones of the oil and gas pools of the Lower Mannville as it is traced from its outcrop in Saskatchewan westward across Alberta toward the foreland thrust belt of the Rockies. Other workers studied, petrographically, porosity reduction in Cretaceous sandstones of Alberta, but have not correlated the results with depth of burial (Lerbekmo, 1961 and Mellon, 1967).

The average porosity of Cretaceous reservoir rocks in Alberta ranges from 33 percent at 2,000 feet to 5 percent at 10,000 feet. The heavy oil pools (25° API gravity or less) are concentrated mainly between 3,000 to 3,500 feet in depth and the light oil pools from 3,500 to 5,000 feet. Gas pools occur at all depths, but with perhaps increasing frequency below 7,000 feet (Energy Resources Conservation Board, 1974).

A plot of porosity versus depth for Lower Mannville oil and gas pools shows a clear curvilinear decrease in porosity with depth (Fig. 3)

and, when a trend surface is fitted to the same data and plotted on a map, a very clear westward decrease is apparent (Fig. 4).

Geologic Setting

In the Alberta plains the Lower Mannville Group consists typically of three units:

1. A basal residual deposit of varying thickness, the Deville Formation or "detrital zone" consisting of red and green waxy shale with chert fragments and siderite pellets, grading upward into dark brown shale interbedded with poorly sorted quartzose siltstone and fine-grained sandstone.

2. A sandstone unit, the "Basal Quartz" of oilfield terminology, comprises the major part of the Lower Mannville. This unit is variously known as the Ellerslie Formation in central Alberta, the McMurray Formation in northeastern Alberta, the Dina Sandstone in eastern Alberta, and the Moulton, Sunburst and Cutband Sandstones in the southern plains, and is equivalent to the Gething and Cadomin Formation in the northwest plains and foothills. These sandstones are the main oil and gas reservoirs of the Lower Mannville and consist predominantly of white, fine-grained quartz arenites interlaminated with siltstone and dark gray silty shale. The sandstones are texturally mature, very fine to coarse grained, and generally well sorted with rounded to subrounded grains. The lowest

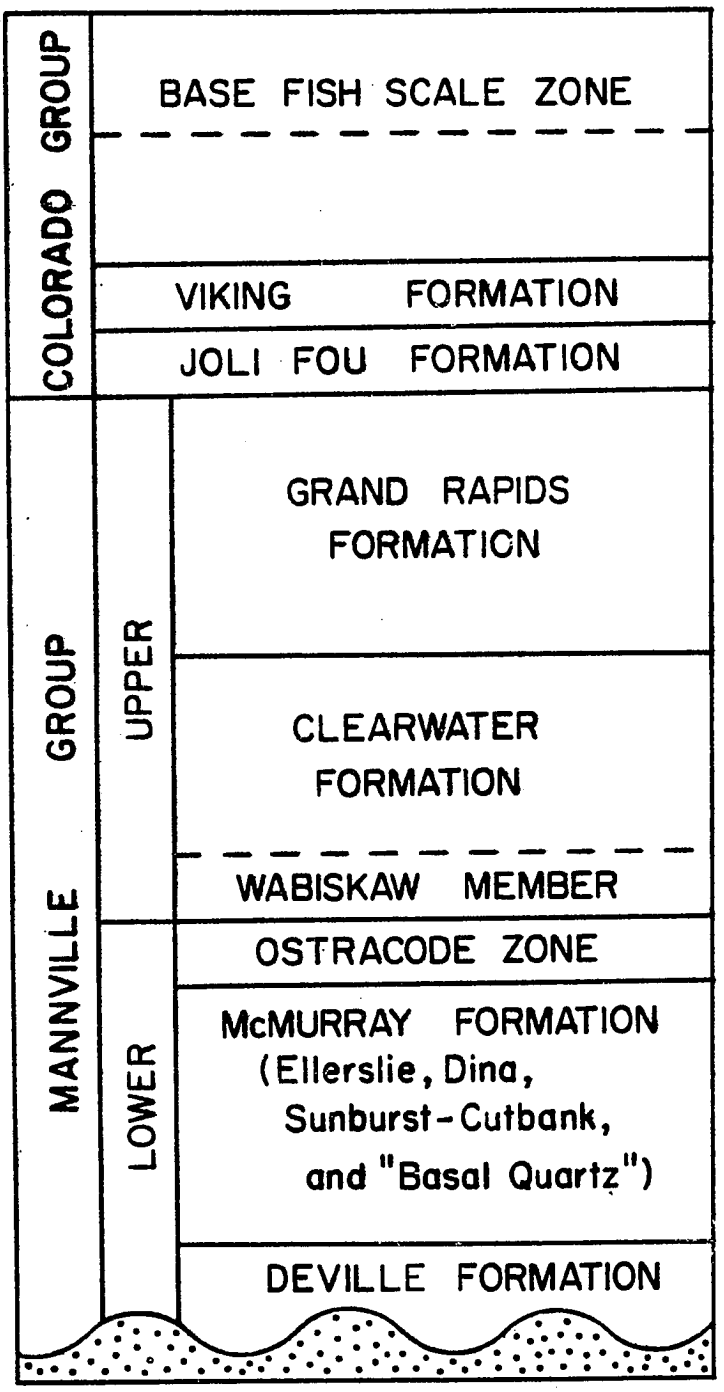

Figure 1. Stratigraphic nomenclature of the Cretaceous Mannville and Colorado Groups in the Alberta Basin.

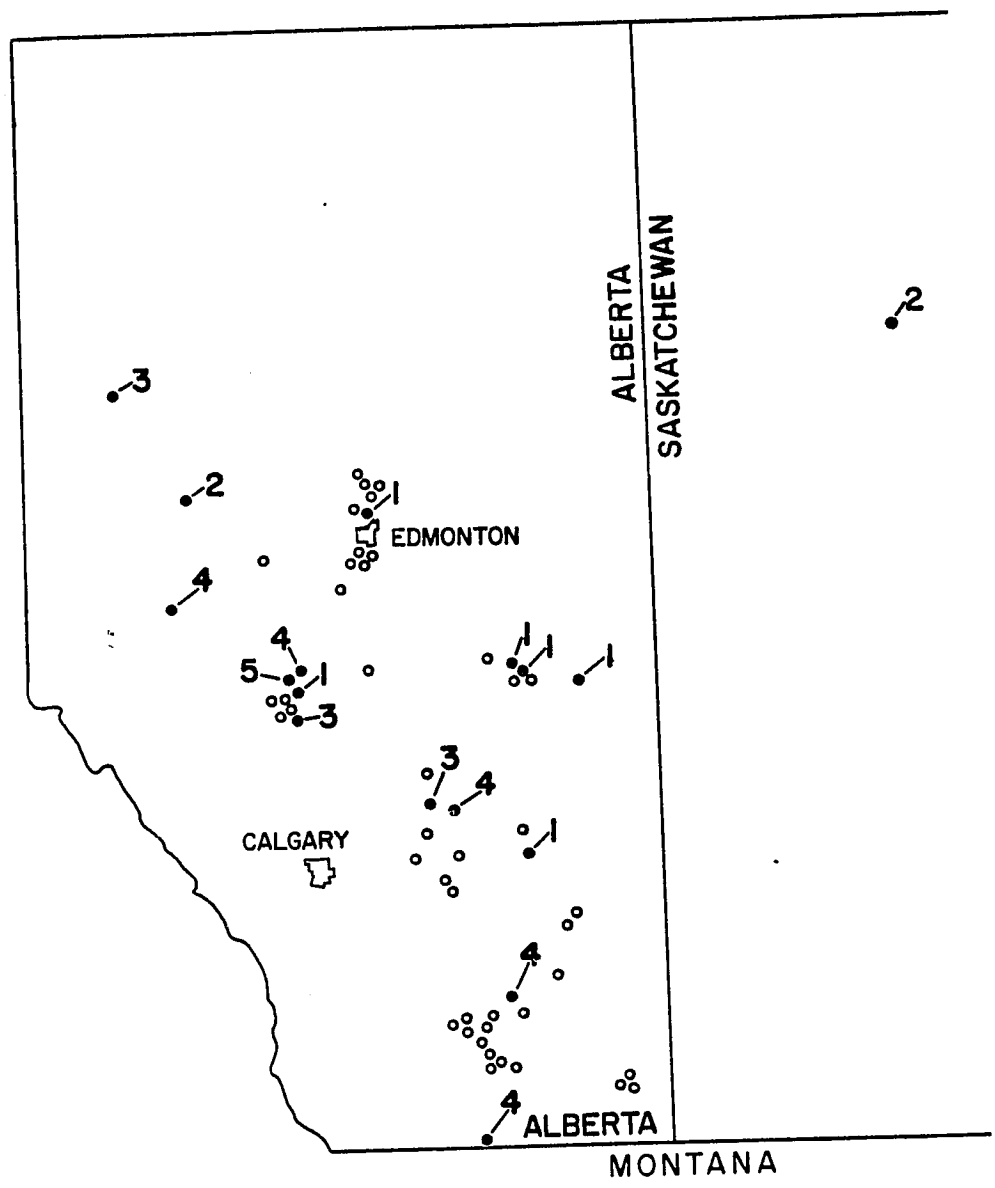

Figure 2. Samples studied in Alberta and western Saskatchewan. Numbers refer to numbers of core samples from wells of Table 1. Open circles represent oil and gas pools from which only porosity data was available.

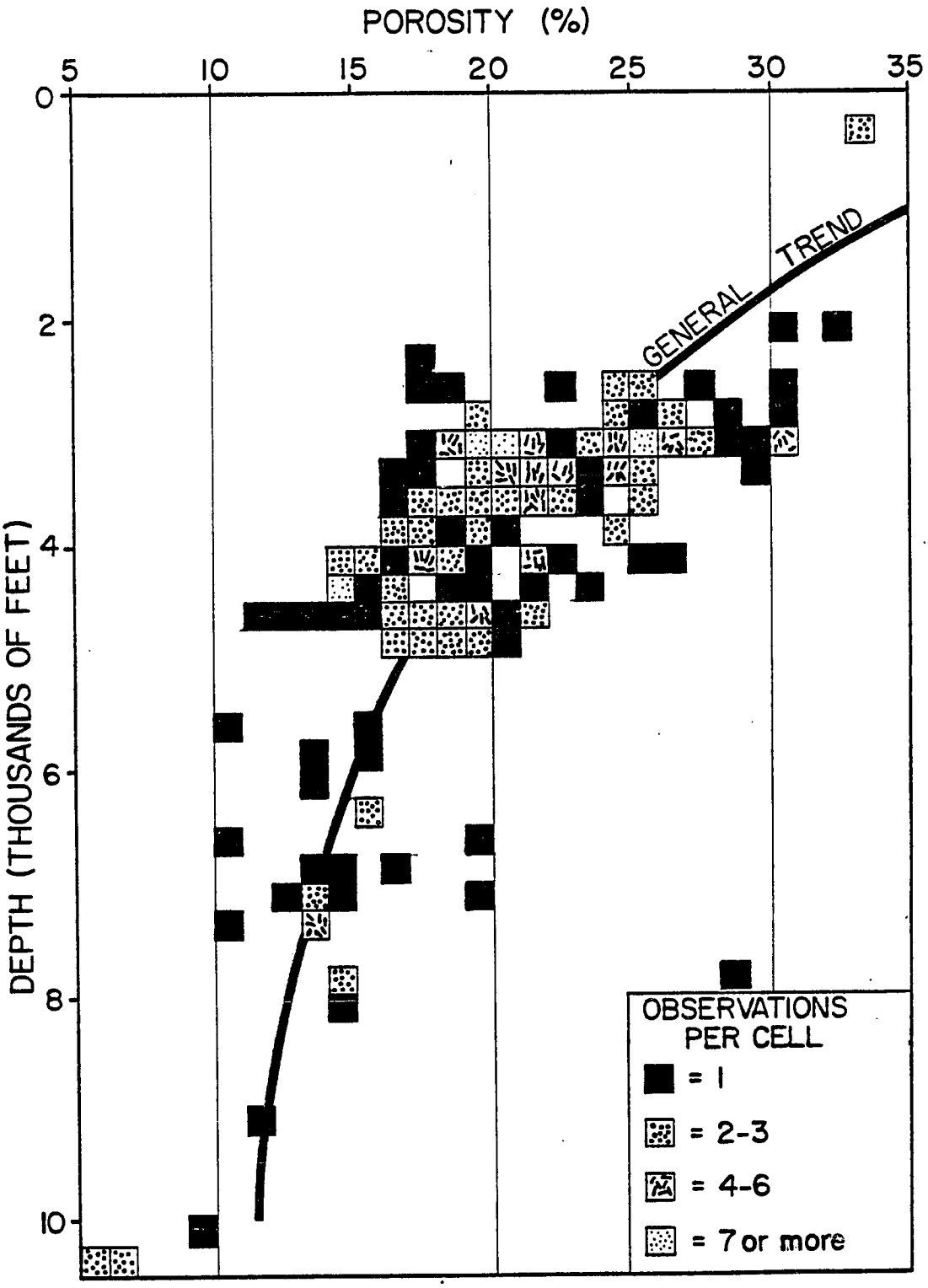

Figure 3. Porosity versus depth for 229 Lower Mannville sandstone oil and gas pools in Alberta, plus two samples from the Saskatchewan. Alberta data from Energy Resources Conservation Board (1974).

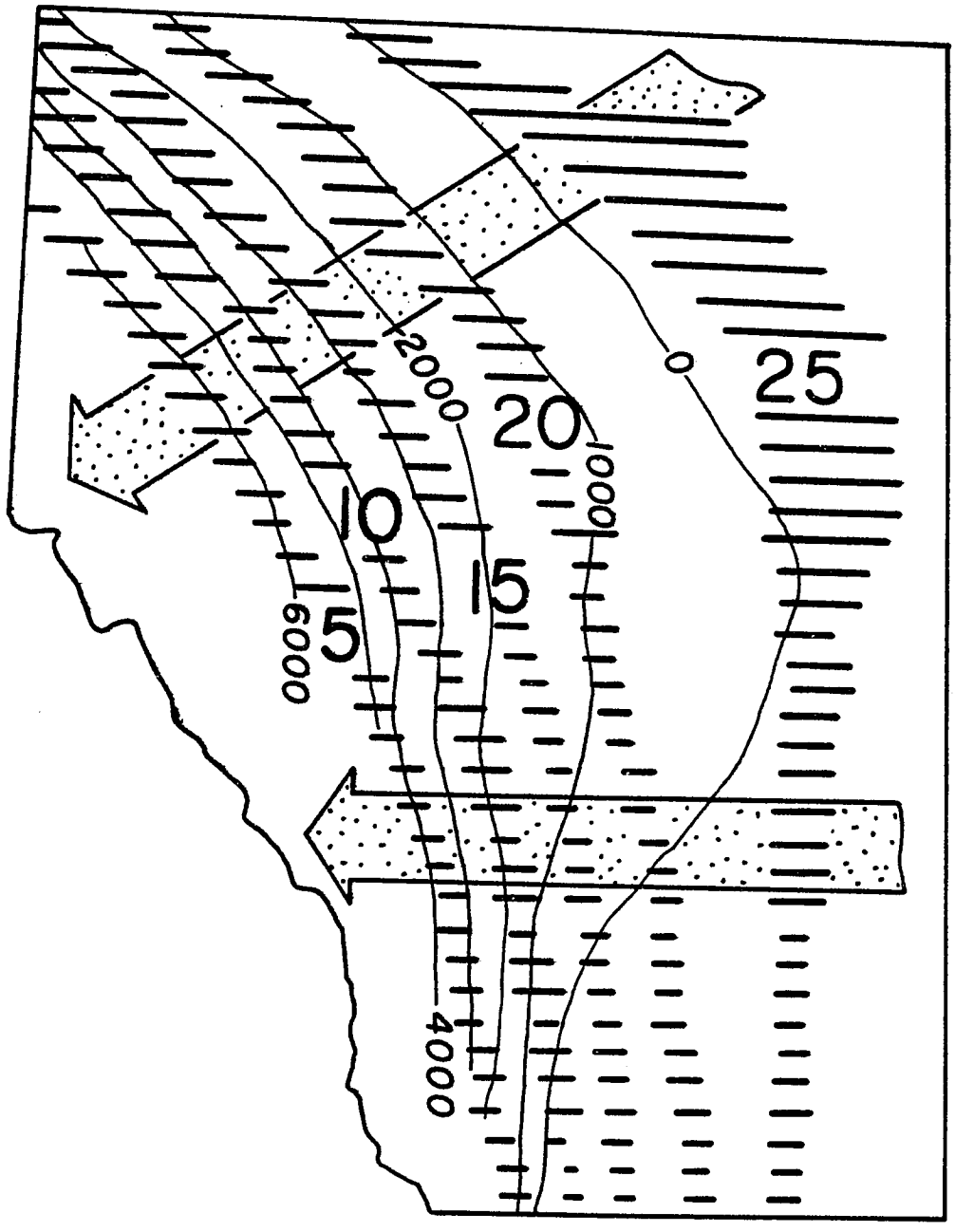

Figure 4. Trend surface of porosity based on average values of 17 pools and structure on base of the Fish Scale (Energy Resources Conservation Board, 1965), a Cretaceous horizon above the McMurray Formation. Arrows indicate general trends.

beds are the coarsest and are locally conglomeratic. These grade upward through massive fine to medium-grained sandstones into fine to very fine-grained slightly argillaceous, finely laminated sandstones which characterize the top of the unit. The McMurray Formation consists predominantly of fluvial sandstones with lesser amount of offshore siltstones and shales (Mellon, 1967 and Nelson and Glaister, 1978).

3. An upper unit, the "ostracode zone" is about 30 feet thick, and consists of gray and brown to black fossiliferous shale with minor siltstone as well as coquinal limestone and locally porous and permeable sandstone.

The Deville Formation or "detrital zone" is mainly restricted to the deeper valleys cut into the pre-Cretaceous surface. The "Basal Quartz" sandstones constitute the main part of the Lower Mannville group in central and eastern Alberta, where they average 100 to 200 feet in thickness depending upon the topography of the underlying Paleozoic erosion surface. The beds are absent over the highest parts of the surface in eastern Alberta, and thicken to 500 feet in the western plains and foothills. Its equivalents reach thickness of up to 2,000 feet in northeastern Columbia.

Petrography

Forty-four thin sections of the Lower Mannville samples were studied. Texturally, most of the samples are moderately to well sorted

and fine grained (Table 1). Mineralogically, the amount of quartz ranges from 40 to 99 percent. Minor amounts of K-feldspar and plagioclase are present. Chert is dominant among the rock fragments, with lesser amounts of siltstone, silty shale, detrital carbonates and other types of rock fragments. Chert generally occurs as framework grains, rather than cement. Some fine rock fragments such as broken shales are incorporated with clay to form matrix which competes with cement to fill the pores. Framework grains set in a featureless clay paste, which is formed of tightly squeezed clay aggregates, are common in those samples containing abundant matrix. Thin sections were stained with alizarin red dye to differentiate calcite and dolomite. Both calcite and dolomite occur as pore filling cement and also as detrital carbonate patches with erratic distribution throughout the samples. A few secondary dolomite grains occur as fine euhedral crystals in interstices. The cements consist predominately of carbonates with minor amounts of quartz overgrowths and trace clay coating. Carbonate cements commonly replace the margins of quartz grains.

The percent grains, cements and matrix were determined by point counts of 200 counts per thin section (Table 1). A triangular plot of these three end members indicates that most of the sandstone of the Lower Mannville Formation are grain-supported arenites (Fig. 5). Similarly, the percent quartz, feldspar and rock fragments were also determined and plotted (Fig. 6) and suggest that quartz arenites are dominant among the sandstones of the Lower Mannville with lesser amounts of chert arenites. Therefore, petrographically, the sandstones of the Lower

TABLE 1

POROSITY, DEPTH AND PETROLOGY OF SANDSTONES FROM THE LOWER MANNVILLE GROUP OF THE ALBERTA BASIN

Part A: Data

Sample No.	Porosity (%)	Depth (ft.)	Packing Density	Grains (%)	Cement (%)	Matrix (%)	Mean ϕ unit	Sorting	Rock Type
1	20.9	3753	0.67	71.5	2	5.2	3.55	0.45	Qtz[2]
2	21.3	3330	0.67	70.2	2	6	2.30	0.89	Subl[3]
3	23.2	2982	0.74	71	--[1]	6	2.39	0.68	Lithic[4]
4	13.9	7051	0.71	72	9.3	4.5	3.08	0.37	Subl
5	8.9	4445	0.67	70	1	20	2.95	0.55	Wacke
6	11.5	4480	0.82	79	1	8.5	2.33	0.72	Subl
7	8.3	4485	0.78	77	1	14	1.95	0.65	Lithic
8	7.4	4487	0.75	74	2	16.5	2.55	0.93	Wacke
9	8.3	7100	0.94	86	1.5	4.2	2.65	0.52	Qtz
10	9.9	7122	0.89	84.8	1.1	4.1	2.80	0.49	Qtz
11	12.6	7138	0.86	83	1.1	3.5	2.94	0.47	Qtz
12	9.9	7160	0.88	83	1	6.2	2.83	0.54	Qtz
13	12.0	7048	0.74	72	--	16	2.79	0.53	Wacke
14	10.2	7050	0.78	80.8	1	7.5	2.83	0.45	Qtz
15	10.6	6991	0.81	84	--	5	2.92	0.49	Qtz
16	12.0	6996	0.78	77.5	1.5	9	3.04	0.54	Qtz
17	21.8	7064	0.70	66	1	11	2.94	0.55	Subl.
18	26.4	3028	0.65	69	1.5	3	2.53	0.61	Qtz
19	12.5	4460	0.75	72	--	15.6	3.89	0.74	Wacke
20	8.9	4460	0.82	80	--	11	3.79	0.83	Subl
21	19.4	4460	0.68	69	3	9	3.45	0.89	Subl
22	22.7	2717	0.69	73	--	4	4.20	1.18	Subl
23	12.7	5931	0.77	81.2	4.9	1	2.18	0.97	Lithic
24	15.1	5938	0.89	82.6	2	--	1.14	0.89	Lithic
25	12.4	5951	0.78	83.5	3.2	1	3.33	0.59	Lithic
26	16.6	6501	0.59	61.5	22	--	2.41	1.03	Lithic
27	17.0	6508	0.67	78	2.5	2	2.23	0.79	Qtz
28	12.6	7453	0.86	86	--	1	2.94	0.41	Qtz
29	10.7	7426	0.85	85.5	1	2	2.77	0.47	Qtz
30	9.9	7456	0.89	89	--	1.5	3.04	0.52	Qtz

TABLE 1, Part A (Continued)

Sample No.	Porosity (%)	Depth (ft.)	Packing Density	Grains (%)	Cement (%)	Matrix (%)	Mean ϕ unit	Sorting	Rock Type
31	20.5	3162	0.72	74.5	1	3.5	2.93	0.88	Qtz
32	29.4	3173	0.70	67.6	1	2	2.23	0.55	Qtz
33	29.3	3179	0.71	69.5	--	1	2.57	0.54	Qtz
34	28.9	3180	0.71	70	--	1	2.32	0.42	Qtz
35	3.6	10281	0.87	88	5	3.5	3.31	0.85	Qtz
36	6.8	10293	0.90	86.5	2	4	2.75	0.39	Lithic
37	6.5	10298	0.85	82.5	8.5	2.5	3.10	0.93	Qtz
38	5.1	10302	0.81	88	4.4	2.5	2.64	0.59	Qtz
39	5.0	2626	0.52	56.5	38.5	--	3.05	0.74	Subl
40	13.3	2629	0.54	60	27	--	3.64	0.61	Qtz
41	16.8	2632	0.59	61	17	4.5	4.02	1.10	Subl
42	13.1	2634	0.66	72	13	1.5	4.18	1.15	Subl
43	22.1	338	0.66	63	15	--	3.15	0.43	Qtz
44	18.0	341	0.74	69	13	--	1.22	0.53	Qtz

Note:

[1]Less than 1%
[2]Quartz arenite
[3]Sublithic arenite
[4]Lithic arenite

TABLE 1

Porosity, Depth and Petrology of Sandstones from the Lower Mannville Formation of the Alberta Basin

Part B: Well Location

Sample Number	Well Location
1	6-21-54-25W4
2	2-27-25-12W4
3	2-33-41-12W4
4	12-28-39-3W5
5-8	6-22-27-20W5
9-12	6-16-41-3W5
13-14	7-29-40-3W5
15-17	3-29-40-3W5
18	6-21-41-12W4
19-21	11-36-28-20W4
22	6-21-41-7W4
23-25	8-21-63-19W5
26-27	2-2-55-13W5
28-30	4-27-36-3W5
31-34	4-20-13-13W4
35-38	10-9-46-14W5
39-42	9-6-1-16W4
43-44	4-25-68-23W2

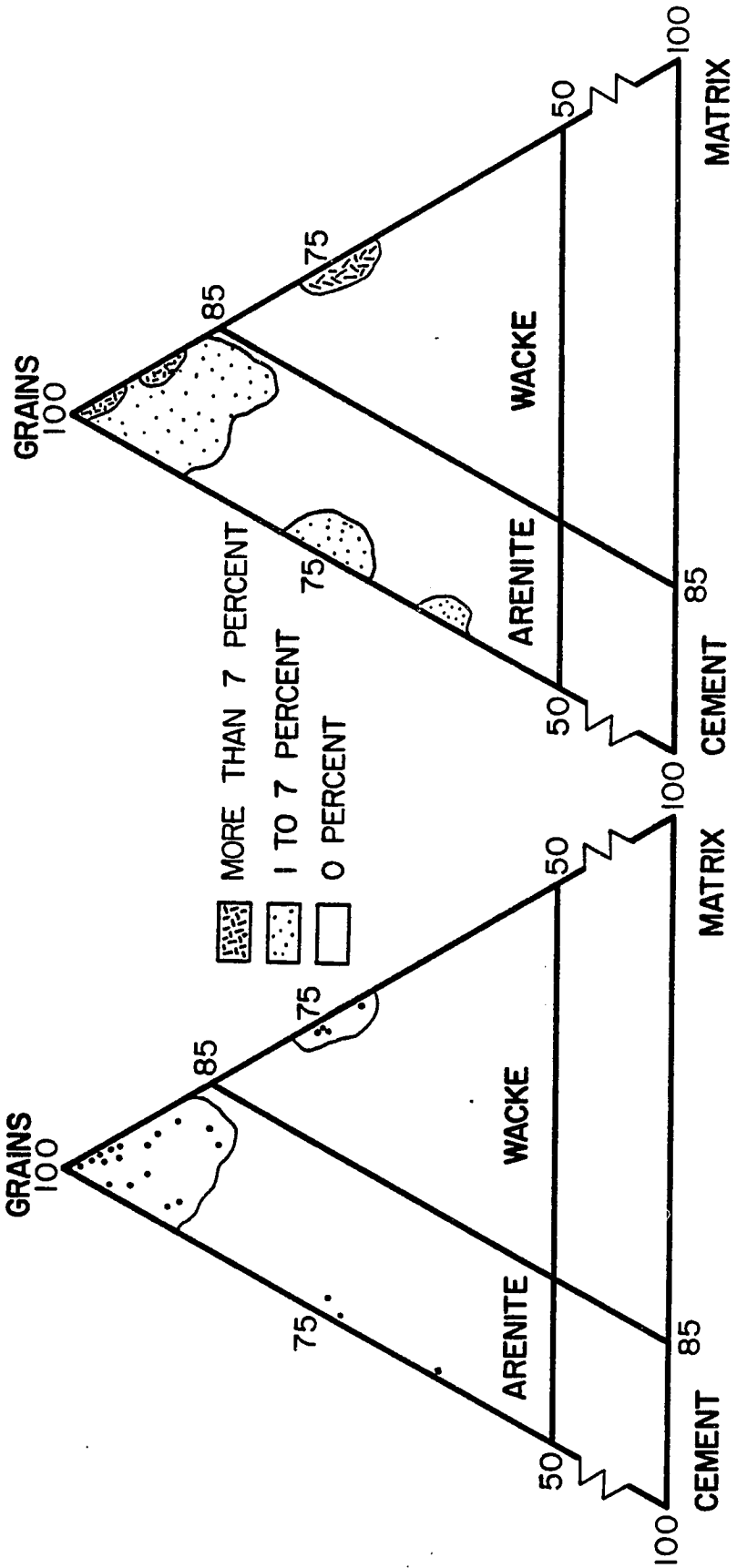

Figure 5. Texture of sandstones of the Lower Mannville Group.

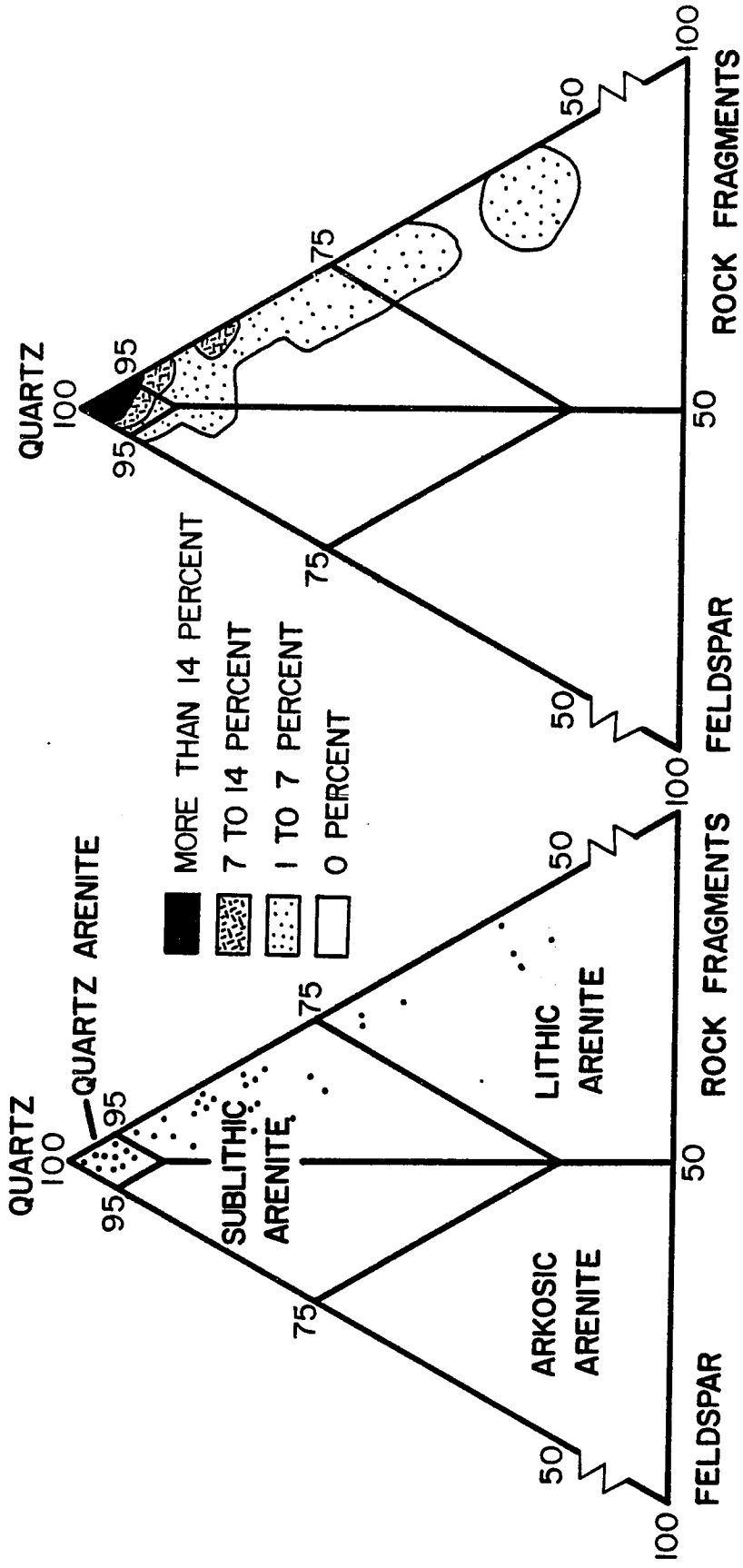

Figure 6. Mineralogic composition of sandstones of the Lower Mannville Group.

Mannville are almost all arenites and consist of about 60-percent quartz arenites, 25 percent sublithic arenites, and 15 percent lithic arenites (Table 1 and Fig. 6).

Status of Porosity-Grain Packing-Petrographic Investigations

Porosity and permeability, and their dependence on the composition, texture and packing of sandstones is a complex subject that has been sporadically studied since the 1930's so that there are today perhaps 100 or more relevant, but scattered references. Two very classic papers that are still well worth reading are those by Krynine (1940 and 1947). There are also many different approaches to the subject even though the key variables appear to be depth of burial, nature of the introduced fluids, mineralogy of the framework grains, grain size and pore water chemistry as well as the presence or absence of oil, which can inhibit diagenetic reactions. Also plate tectonics can, even in a basin such as the Alberta basin, possibly exercise broad controls on framework mineralogy, geothermal gradient, burial residence time and folding and/or faulting (Fig. 7).

Within recent years the Scanning Electron Microscope has added greatly to our knowledge of cementation in the pore systems of sandstones, because its great depth of field permits one to see details of silica, carbonate and clay mineral deposition within the individual pores of a consolidated sandstone. Indeed, a recent issue of the Journal of the Geological Society (Vol. 135, 1978) that was devoted to sandstone diagenesis may well set a predominant style of study for many years to

come--make a porosity-permeability plot of the plug data, carefully relate each plug to the different facies or subenvironments of the sandstone body, and use a combination of SEM and thin section study to petrographically explain the subfields of the plot. This method has the great advantage of linking porosity and permeability to depositional environments--mappable units on wire line logs--within a sandstone body and thus provides a major framework to which petrographic details and fluid history can be related.

The writer, however, found another path more suitable to the task at hand--use thin sections to study the contacts among the framework grains (Fig. 8) and relate the changing abundance of these types to present depth of burial and porosity. This proved to be simple and informative and was first used by Taylor (1950), who studied Mesozoic sandstones from two wells in Wyoming. Taylor found systematic variation of contact types with depth of burial. Gaither (1953) partly supported Taylor's conclusion, because he also found that less compacted sands are associated with higher percentage of floating grains. For instance, the St. Peter Sandstone (Ordovician) with a porosity of 37 percent has more than 46 percent floating grains. However, Gaither also pointed out that the numbers of contact types are dependent on grain shape; i.e., point contacts are maximal for grains with high sphericity and high roundness, whereas long contacts are most abundant when grains have low sphericity and low roundness. Later Füchtbauer (1967, p. 365) introduced the term contact strength, a quantitative expression of the relative proportion of different types of grain contacts. As used by Füchtbauer, contact strength is a single-valued parameter that defines grain packing:

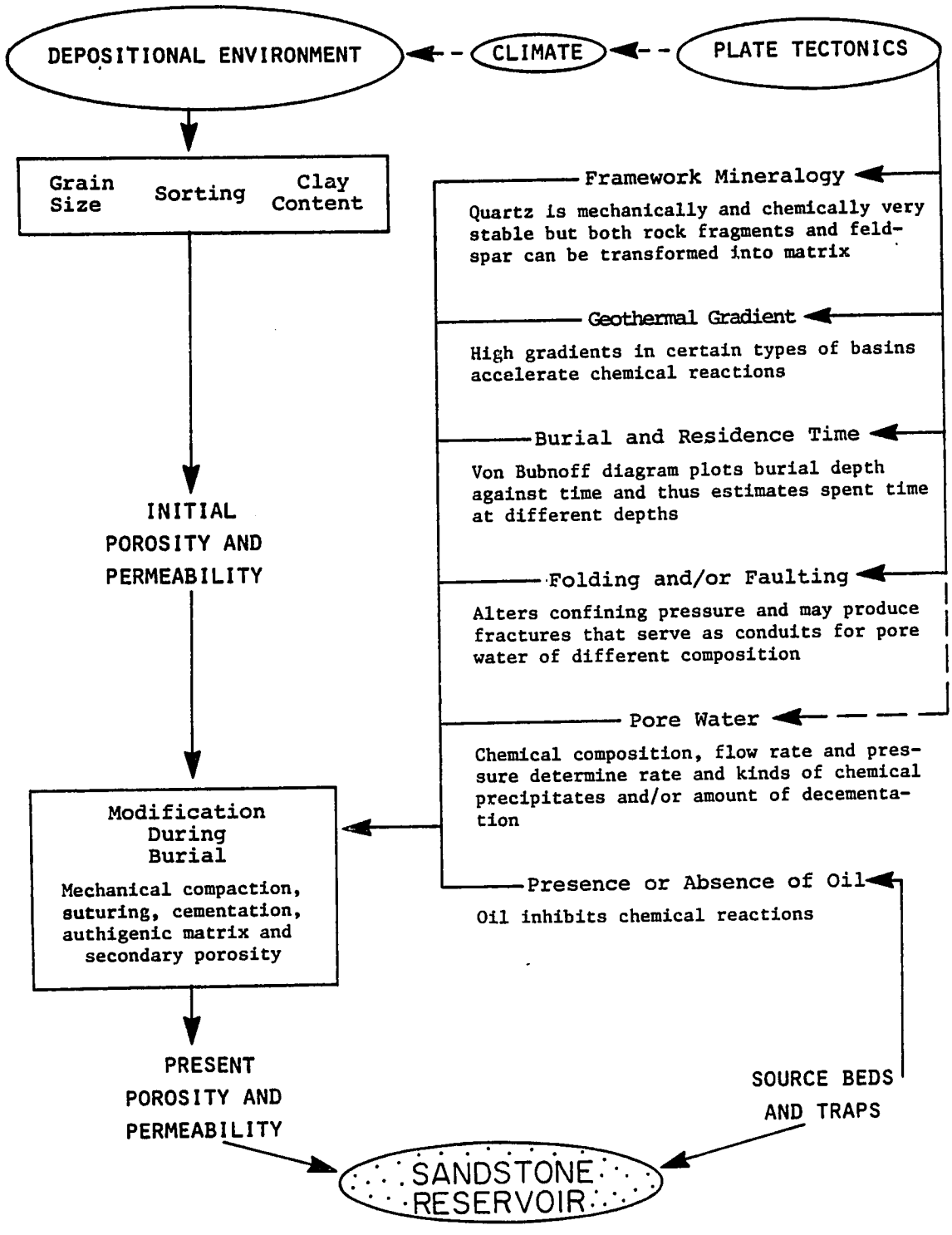

Figure 7. Principal variables of porosity evolution in sandstones and their probable interrelationships.

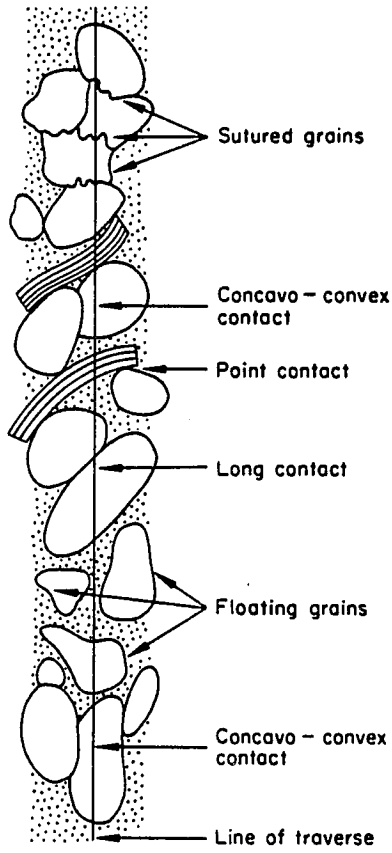

Figure 8. Definition sketch of types of contact (Pettijohn et al., 1972, Fig. 3-10).

$$\text{Contact strength} = \frac{1a + 2b + 3c + 4d}{a + b + c + d}$$

where

a = number of point contacts,

b = number of long contacts,

c = number of concavo-convex contacts, and

d = number of sutured contacts.

As defined above, contact strength increases as the grain packing becomes tighter in more compacted sandstones. While studying the Eocene section of the Maracaibo basin, Venezuela, Phipps (1969) found that long and concavo-convex contacts are dominant in sandstone buried about 13,000 feet. Prozorovich (1971, Fig. 1) also showed an increase in concavo-convex contacts with depth in Jurassic and Cretaceous sandstones of the west Siberian platform. Study of the packing in the Grimsby Sandstone (Silurian) of Ontario and New York State by Martini (1972) suggested that the compaction of sandstones can be estimated by the number and types of grain contacts and measurement of packing density and packing proximity. He found that grain size and grain orientation (imbrication) are significantly correlated with these packing parameters and further suggested that packing density and packing proximity could be used as paleoenvironmental indicators, because they are correlated with variations of other textural and structural parameters. Later, Moore (1975) related types of grain contact, total contacts per grain and porosity to depth in sandstones of the Minnelusa Sandstones of the Powder River basin in

Wyoming and identified three stages of its compactional history. Contact types have also been studied by Bell (1978a and 1978b).

Besides the forementioned general statements about porosity-petrography-grain packing, some other previous studies related to this subject are briefly summarized for reference (Table 2). This summary is alphabetical.

Methods

The Lower Mannville lends itself to the study of contact types because most of the sandstones within it are arenites--that is, the study of contact types is much more meaningful in arenites than in wackes. There are seven quantitative sandstone packing indices that can be used to study grain-to-grain relation (Pettijohn et al., 1972, Table 3-4). Of these indices, the writer used the packing density, a quantitative expression of the compaction of sands, because it can be determined simply and quickly during routine thin-section studies of sandstones. Packing density is defined as length of grains intercepted, divided by length of traverse. Packing density for the Lower Mannville samples was determined by point counts of 200 grains per thin section (Table 1). Types of contact was estimated by an additional count of 200 grains per thin section. Plug porosities of the sandstones of the Lower Mannville were determined by Chemical and Geological Laboratories, LTD., Calgary, Canada. Values of closely spaced samples are averaged (Table 3). Finally, the writer computed a matrix of linear correlation coefficients for the Lower Mannville samples to help understand the interrelationships between porosity, depth, packing density and other parameters (Table 4).

TABLE 2

A SUMMARY OF PREVIOUS STUDIES RELATED TO POROSITY AND GRAIN PACKING

Almond and others, 1976

Authigenic clays are responsible for the pore reduction in sandstones of the Horsethief Formation (Upper Cretaceous), Montana.

Backman and Hamilton, 1976

A short report of the density, porosity and grain density of the sediments from the DSDP site 222. Figure 1 shows the typical linear depth-porosity relation.

Beard and Weyl, 1973

A comprehensive study of texture, porosity and permeability based on 48 size-sorting classified artifically mixed unconsolidated Holocene barrier island sands. Grain size and sorting are closely related to porosity and permeability.

Chilingarian and Wolf, 1975 and 1976

Volume 1 contains eight chapters. Chapter 1 is a general introduction to sands and sandstones and its physical properties and origin. Role of compaction in delineating geometry and distribution of fluvial and deltaic sandstones and of special interests as is Chapter 7. Identification of sediments--their depositional environmental and degree of compaction--from well logs. Part II combines six chapters: Introduction (with many flow diagrams), Diagenesis of sandstones and compaction (375 pages and virtually a book) and Ore genesis influenced by compaction. Summing up, a very comprehensive, well illustrated compendium.

Currie and Nwachukwu, 1974

Present porosity results from fractures of reservoir rocks at depths of great geothermal temperature and accompanied with tectonism. Table 1 summarizes fractured reservoir and its characteristics.

Dapples, 1972

A comprehensive review of cementation and lithification. Many microphotographs demonstrates different stages in cementation.

Deelman, 1975

An experiment of compaction of dry mineral grains suggests that sutured grain contact is caused by plastic deformation rather than pressure solution.

TABLE 2 (continued)

Fox and others, 1975

Detailed log and petrographic analysis related to porosity in sandstones. Quartz overgrowth is main cause for the porosity reduction. Silica source is migrating solution rather than pressure solution as suggested.

Füchtbauer, 1967

Comprehensive study of diagenesis of sandstones based on 734 thin sections and many porosity measurements in Lower Triassic Redbeds of Germany. Defines a useful linear combination of contact strength of framework grains (p. 171).

Heald, 1950

Suggesting authigenic minerals as an important aspect of cementation.

Heald, 1956

Emphasizes the importance of pressure solution which triggers the formation of secondary quartz and then destroys porosity. Also noticed that the most pressure solution occurs in the clay-bearing sandstones. Defines a useful term of "minus-cement" porosity.

Heald and Larese, 1973

A development of secondary porosity resulting from the solution of feldspars is stressed. Sanidine-bearing sandstones are the most likely ones.

Kahn, 1956

A short but good review of packing of sands. Defines two useful parameters for measuring packing properties: packing proximity and packing density.

Lowry, 1956

Fracturing and welding--one mode of cementation of secondary silica--are two major factors which control the loss of porosity of the Paleozoic quartzose sandstones of Virginia.

Manger, 1963

A rather complete tabulation of porosity and bulk density data of sedimentary rocks. One hundred seventy-five references are cited from American, British, German and Swiss literatures. In general, porosity of sandstones decreases with increasing depth of burial.

TABLE 2 (continued)

Maxwell, 1964

It is probably the first paper which relates porosity, depth, temperature and age together. Many porosity-depth-temperature curves.

Morrow, 1971

A property of texture which is defined as "packing heterogeneity" is related to the irreducible saturation of porous rocks. However, it is not in widespread use.

Pittman and Lumsden, 1968

Thick chlorite coating on quartz grains prevents pressure solution and retards quartz overgrowth and then preserves the porosity.

Rittenhouse, 1971

A mathematical treatment of pore reduction by plastic deformation of ductile grains. A rare but unique study.

Sibley and Blatt, 1976

Luminescence petrography of 185 thin sections of Silurian Tuscarora orthoquartzite confirms the concept that pressure is the chief mechanism for silica cement. However, source of silica other than pressure solution still plays an important role in the silica cementation.

Sprunt and Nur, 1976

An experiment of the compaction of water-saturated St. Peter sandstone under nonhydrostatic stress suggests that porosity reduction is due to pressure solution.

Stephenson, 1977

How can the individual effect of many factors on the porosity reduction be determined? Here is a demonstration of how to set the limit of temperature effect on the porosity variation.

Swardt and Towel, 1974

A rather rare investigation in the relationship between diagenesis and folding in the sandstones and shales of a large basin, most of the sediments being in the greenschist facies.

Weller, 1959

A preliminary investigation of the compaction of sedimentary rocks--shale, sandstone, limestone and coal. Many equations and porosity-depth curves.

TABLE 2 (continued)

Weyl, 1959

A theoretical approach to the solution alteration of mineral grains at points of contact. Diffusion is the key idea, but other factors must be considered together.

TABLE 3

Average Number and Types of Grain Contacts, Contact Strength, Packing Density, Porosity and Depth in Lower Mannville Sandstones of Alberta Basin

Depth (ft.)	Types of Contacts (percent)					Contact Strength	Packing Density	Porosity (%)	Samples Averaged
	Floating	Point	Long	Concave-Convex	Sutured				
340	35	45	20	--	--	1.30	0.70	34*	No. 43, 44
3175	5	24	67	4	--	1.77	0.71	27	No. 31-34
3753	7	46	42	5	--	1.56	0.67	20.9	No. 1
4468	--	15	69	14	2	2.03	0.75	11.0	No. 5-8, 19-21
5940	--	7	77	14	2	2.11	0.81	13.4	No. 23-25
7096	--	6	78	14	2	2.12	0.83	12.1	No. 9-14, 17
7460	--	--	71	22	7	2.36	0.87	11.0	No. 28-30
10293	--	3	70	25	2	2.26	0.86	5.5	No. 35-38

*In order to complete the compaction pattern of the vertical sequence of the Lower Mannville sandstone, the concept of "minus-cement porosity" is introduced here. Pettijohn et al. (1972, p. 424) defined it as "the porosity which would be present if a specimen contained no chemical cement." Thus, the minus-cement porosity of the samples at 340 feet is 20 + 14 = 34 percent and then they would belong to the same population of the 35 low-cemented McMurray samples, and hence they could be used to evaluate the effect of compaction without the interference of cement. Thus, the 34 percent minus-cement porosity is plotted against depth of 340 feet which fits well the general trend of a progressive loss of porosity with depth (Fig. 9).

TABLE 4

Linear Correlation Coefficient Matrix of Thirty-five Samples from the Lower Mannville Sandstone with Less than 8.5 Percent Cement

	X_1	X_2	X_3	X_4	X_5	X_6	X_7
X_1	1.000	-0.725*	-0.677*	-0.279	-0.291	-0.121	0.077
X_2		1.000	0.684*	0.392*	-0.153	0.019	-0.360*
X_3			1.000	0.043	-0.248	-0.087	-0.281
X_4				1.000	-0.263	-0.051	0.354*
X_5					1.000	0.216	0.099
X_6						1.000	0.087
X_7							1.000

*Statistically significant correlation coefficient for d.f. = 33 and confidence level of 95%, critical $|r|$ = 0.335 (Crow et al., 1960, Table 7).

Note 1: X_1 = porosity, X_2 = depth, X_3 = packing density, X_4 = percent cement

X_5 = percent matrix, X_6 = mean grain size, and

X_7 = sorting.

Note 2: This matrix is based on 35 samples each of which has less than 8.5 percent cement. These 35 samples, as judged by a plot on cumulative probability paper, fits a single normal population.

Results and Interpretations

A matrix of linear correlation coefficients of the above described variables from the sandstones of the Lower Mannville (Table 4) shows that porosity, depth and packing density have the strongest correlation. However, plots of grain contacts against depth are more informative (Fig. 9).

Floating contacts, suggesting loose compaction or very early diagenetic cementation, are restricted entirely to depths above 4,500 feet in the Lower Mannville. Point contacts, also indicating loose compaction, are less abundant as the depth increases, although there are still a few found in very deep samples around 10,000 feet, presumably because of carbonate cement which prevents the further compaction of grains. Long contacts are fairly common above 4,000 feet, but greatly increase with depth and reach their maximum at 10,000 feet. They appear to be an intermediate response to burial pressure between point and concavo-convex contacts. In contrast, concavo-convex contacts, an indication of dense packing and pressure solution, are rare above 4,500 feet, but become more abundant with increasing depth. Sutured contacts of quartz grains, indicative of stronger pressure solution, are most common below 4,500 feet--a depth which Füchtbauer (1967, p. 355) also noted as being the lower limit for mechanical rearrangements of grains. Contact strength, which combines the above variables, shows a definite increasing trend with increasing depth as does the packing density, especially down to about 7,000 feet.

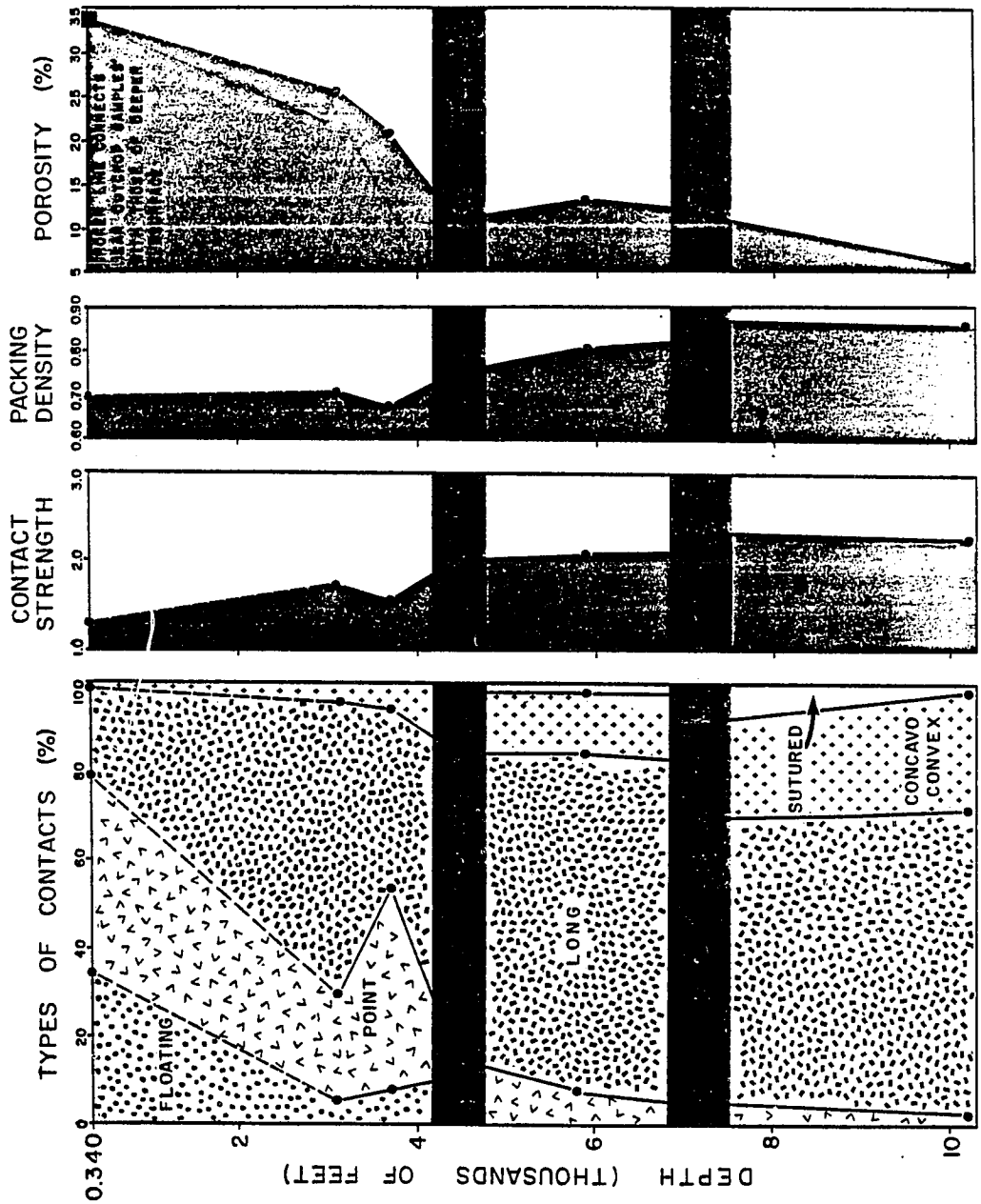

Figure 9. Vertical variations of types of grain contacts, contact strength, packing density and porosity and transition zones (gray) of sandstones in the Lower Mannville Group in Alberta basin based on data of Table 3.

There is a progressive loss of porosity with depth (Fig. 9): the porosity-depth relation has a significant linear correlation coefficient of -0.725, and the porosity-packing density correlation also has a significant linear correlation coefficient of -0.677. Clearly, the types of contacts change systematically with increasing depth of burial and, additionally, contact strength and packing density correlate well with the changing porosity of the sandstones of the Lower Mannville, whereas cement and matrix do not. Thus, the vertical variation of types of contact, contact strength and packing density strongly suggest that pressure due to depth of burial is the major factor responsible for the loss of porosity in the sandstones of the Lower Mannville.

In order to compare the grain packing of the sandstones of the Lower Mannville with that of Wyoming sandstones, the number and types of contact in Mesozoic sandstones in Wyoming (Taylor, 1950, Fig. 2) are plotted in a similar manner to those of the Lower Mannville (Fig. 10). The changes of contact types with depth in these two basins are strikingly similar--even though the observations were made by different operators separated by 25 years of time. Point contacts are dominant in the Wyoming sandstones above 3,000 feet, decreasing with increasing depth and are not present below about 7,000 feet. Long contacts, as in the Alberta basin, increase with depth, and at 8,000 feet they form about 65 percent. The concavo-convex contacts generally increase with depth. Sutured contacts are restricted to depth below 6,800 feet below which they increase; in the Alberta basin they are present over a much greater depth range, but are most abundant below 4,500 feet. Finally, contact

strength increases strongly with depth, but at a faster rate than the contact strength in the Alberta basin. Thus, the vertical distribution of types of contacts in the sandstones of the Lower Mannville is very similar to that found in the Wyoming sandstones.

Another point deserved special mention--there are two transition zones in both the Lower Mannville and Wyoming sandstones. The first one occurs in the Lower Mannville at about 4,500 feet where porosity decreases abruptly from a high of 34 to 11 percent, packing density increases from 0.70 to 0.75, contact strength increases from 1.3 to 2.0 and long contacts become dominant and floating contacts are absent. The second transition zone is at about 7,000 feet but is not clearly defined as the first transition zone, although all four variables clearly show it. There is also a transition zone in the Wyoming sandstones at about 4,500 feet, where point contacts decrease sharply from 60 to 20 percent long contacts are most abundant and concavo-convex contacts increase from 10 to 20 percent. The second transition zone is also at about 7,000 feet, where point contacts are absent and the sutured contacts first appear and subsequently increase with increasing depth.

The aforementioned transition zones defined by types of contact can be used to investigate--and perhaps better explain--the shape of the porosity-depth curve for the Lower Mannville. Six equations were fitted to the porosity-depth data of Figure 3: one general linear equation, three short linear equations defined by the two transition zones, and a third degree polynominal and a negative exponential (Fig. 11). The polynominal and exponential curves were constrained to pass through an

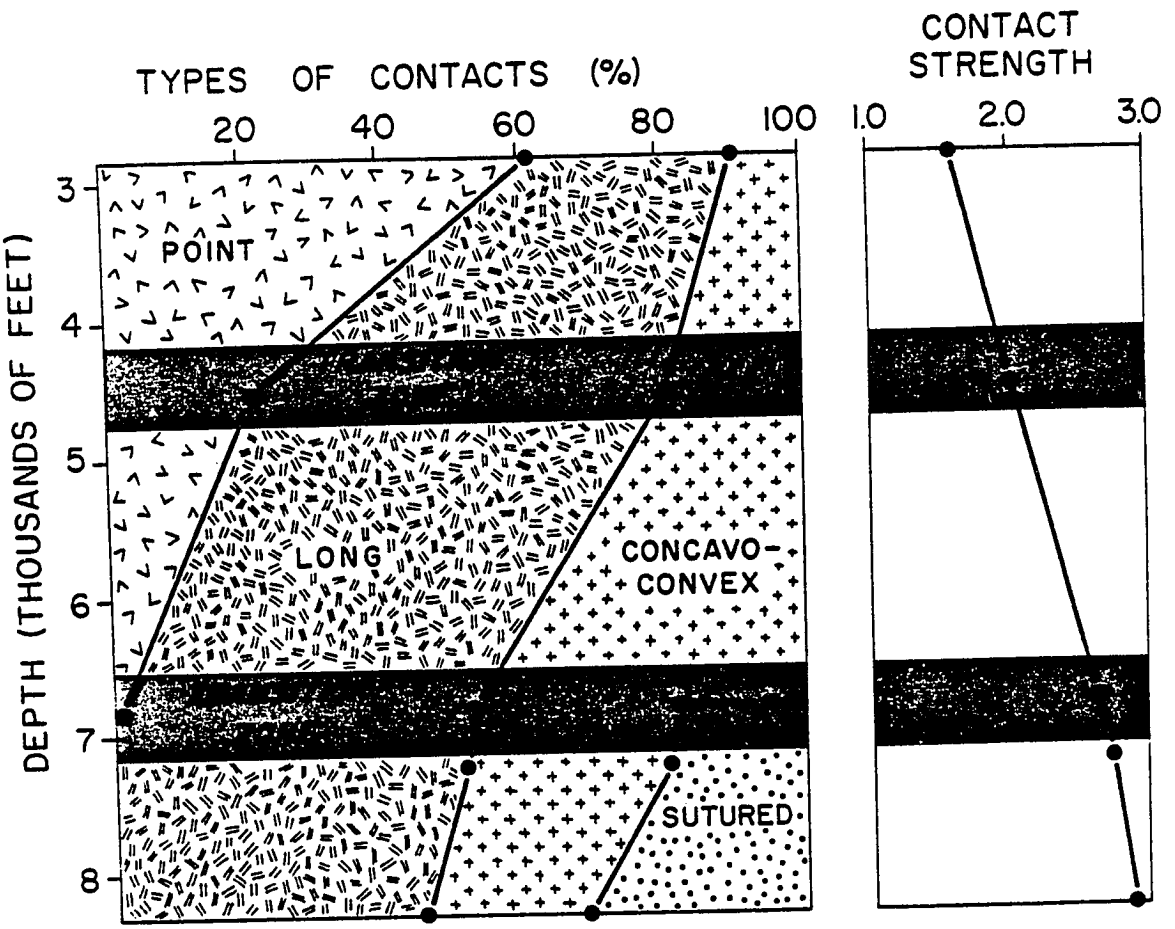

Figure 10. Vertical variation of types of grain contacts and contact strength and transition zones (gray) in Mesozoic sandstones in the Wind River and Powder River basins, Wyoming (adapted from Taylor, 1950, Fig. 2).

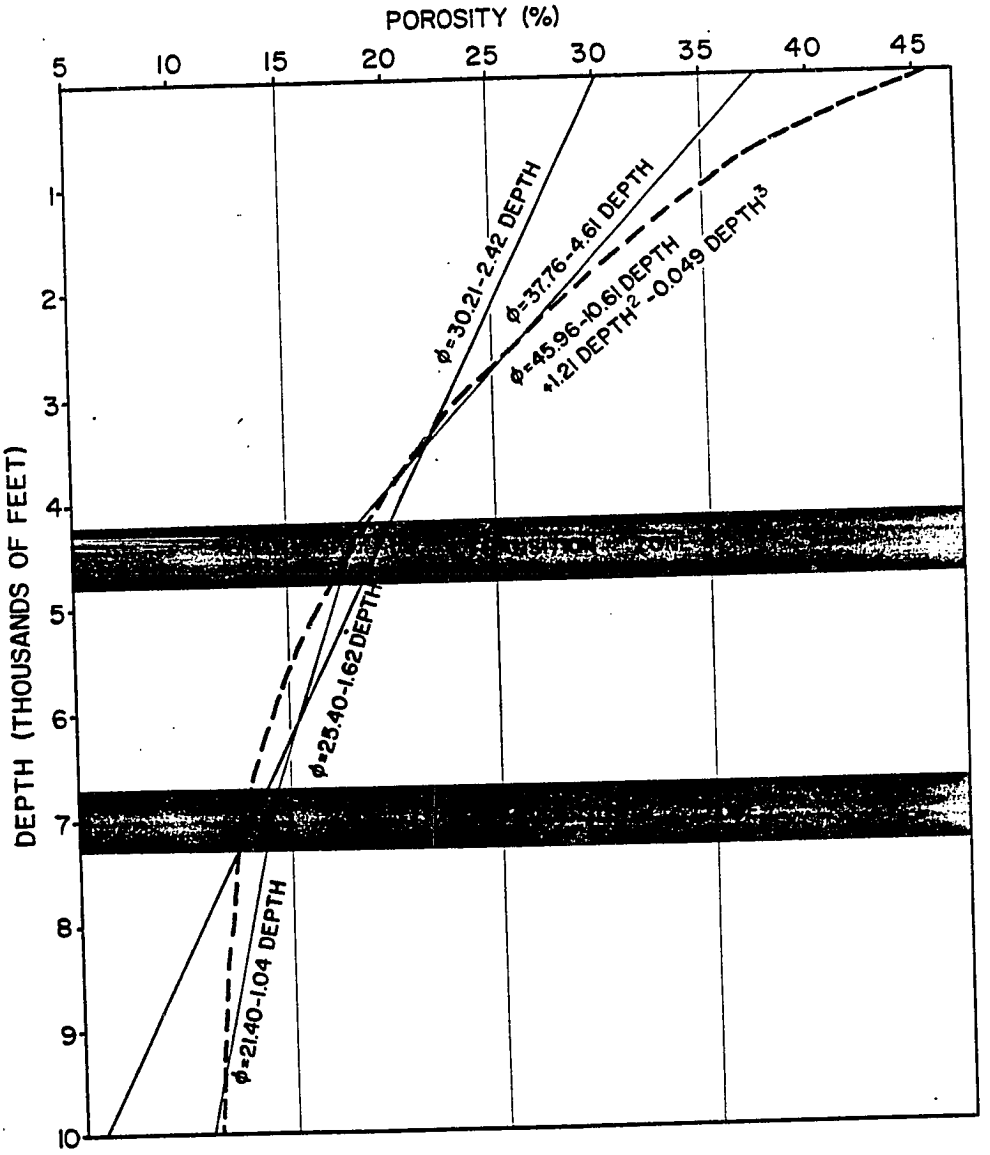

Figure 11. Linear and polynomial porosity-depth curves fitted to data of Figure 3. The three short linear lines approximate tangents to the polynomial. See Table 5 for regression constants and their statistical significance.

TABLE 5

Regression Parameters and Tests of Lower Mannville Porosity Depth Data

Part A: Regression Parameters

	Interval and Type Of Curve	Percent Variability of Porosity Explained by Depth, $100r^2$ and r, the Correlation Coefficient	Standard Error of Estimate, $s_{y/x}$	Slope (b_n)
		$100r^2$ r		
1.	0-4, 500 ft.	39.80 (-0.63)	3.33	$b_1 = 4.61$
2.	4,500-7,000 ft.	14.28 (-0.38)	2.91	$b_2 = 1.62$
3.	7,000-10,000 ft.	16.24 (-0.40)	2.31	$b_3 = 1.04$
4.	0-10,000 ft.	49.28 (-0.70)	3.42	$b_4 = 2.42$
5.	Third Degree[1] Polynomial, 0-10,000 ft.	89.45 (-0.94)	2.67	---
6.	Negative[1] Exponential, 0-10,000 ft.	87.34 (-0.93)	2.74	---[2]

Part B: Tests of Significance for Slopes, b_1, b_2 and b_3

Null Hypotheses	Value of Test Statistic[3]		Significance at 0.05 Level
	$t_{calc.}$	$t_{critical}$	
$b_1 = b_2$	3.46	(1.645 d.f. = 200)	Reject
$b_1 = b_3$	3.64	(1.645 d.f. = 173)	Reject
$b_2 = b_3$	1.50	(1.684 d.f. = 57)	Accept

[1] 100 dummy samples added at 0 feet, assuming an initial porosity of 46 percent

[2] Porosity = $43.41e^{-0.185 \text{ depth}}$

[3] $t = \frac{b_1 - b_2}{s_{(b_1 - b_2)}}$ (Crow et al., 1960, p. 161)

assumed initial 46 percent porosity at zero depth for modern sands (Pryor, 1973, Table 1).

Measure of goodness of fit were computed for these six equations (Table 5) following the standard procedures of Crow et al. (1960, p. 157-161) and Davis (1975, p. 192-221). The multiple correlation coefficient, $100r^2$, is an estimate of the percent of the variability of the dependent variable, porosity, explained by depth; and the standard error of estimate is related to the amount of variability unexplained by the predictor variable, depth.

The graphs of Figure 10 and the summary of key statistics effectively show that there is a relation in the sandstones of the Lower Mannville between contact types and the linear slope of the porosity-depth curve. Porosity decreases rapidly at first (4.61 percent per 1000 feet) and least of all below the lower transition zone (1.04 percent per 1000 feet). This is confirmed statistically by the fact that the slopes of the upper porosity-depth curve, b_1, differs significantly from that of the lower two, b_2 and b_3 (Table 5B). This suggests that much less burial pressure is needed to reduce the open, initial pore system of a sandstone than in the later stage of porosity reduction that occurs with deeper burial--a conclusion that is intuitively very clear from inspection of drawings representing typical contact types (Fig. 12). However, it should be noted that there is much variation within each of the zones defined by contact types so that the values of $100r^2$ are low for all three of their corresponding linear regression equations.

Overall, a third degree polynominal is a far better fit than a general linear curve ($100r^2$ equals 89.45 vs. 49.28), especially when it

is constrained to pass through an assumed initial porosity of 46 percent at zero depth, contrary to the generalization of Selley (1978, p. 119) that linear depth-porosity curves are the rule. The third degree polynomial is the best empirical predictor of porosity, but the petrologic results suggest that three linear segments is a more geologically reasonable relationship.

Conclusions

The systematical variations of contact types, packing density and porosity with depth strongly suggest that the sandstones of the Lower Mannville Group are affected dominantly by physical compaction during burial diagenesis.

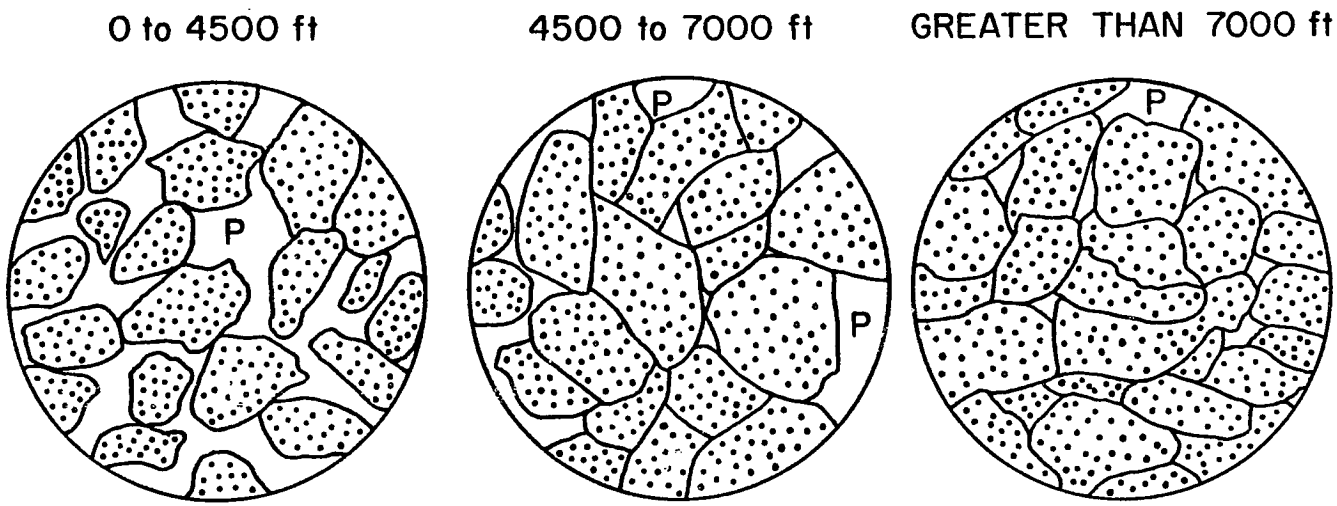

Figure 12. Schematic representation of change of grain packing of sandstones of the Lower Mannville with increasing depth. Above 4,500 feet, typical values of contact strength and porosity are 1.6 and 20 percent, between 4,500 and 7,000 feet are 2.1 and 12 percent, and below 7,000 feet are 2.3 and 8 percent. P represents porosity.

CHAPTER II

SANDSTONES OF THE ATHABASCA FORMATION (PRECAMBRIAN) OF THE SASKATCHEWAN BASIN: GRAIN PACKING AND DEPTH

Introduction

The systematic variations of types of contact, packing density and porosity with depth in sandstones of the Lower Mannville lead us to the following: should one expect the grain packing-porosity relationship of sandstones from other undeformed sedimentary basins to be similar to that of the Lower Mannville, and can contact types and packing density be used to estimate the depth of burial? In an attempt to answer these questions, the writer studied the sandstones of the Precambrian Athabasca Formation first to see how grain packing changes with increasing depth, and secondly, to estimate its burial depth.

Fifty samples from a continuous diamond core in the Athabasca sandstone sequence (4,776 ft. in length) were studied. This core is located at Rumple Lake which is about 50 miles north of Cree Lake and 39 miles west of Pasfield Lake, Saskatchewan (Fig. 13).

Geologic Setting

The Precambrian Athabasca Formation was deposited in an oval-shaped basin covering about 40,000 square miles in northwestern Saskatchewan (Fig. 13). Seismic evidence indicates that the present axis of the Athabasca basin trends northeasterly and the depth to the underlying basement complex is more than 5,000 feet (Fraser, et al. 1970, Fig. 3).

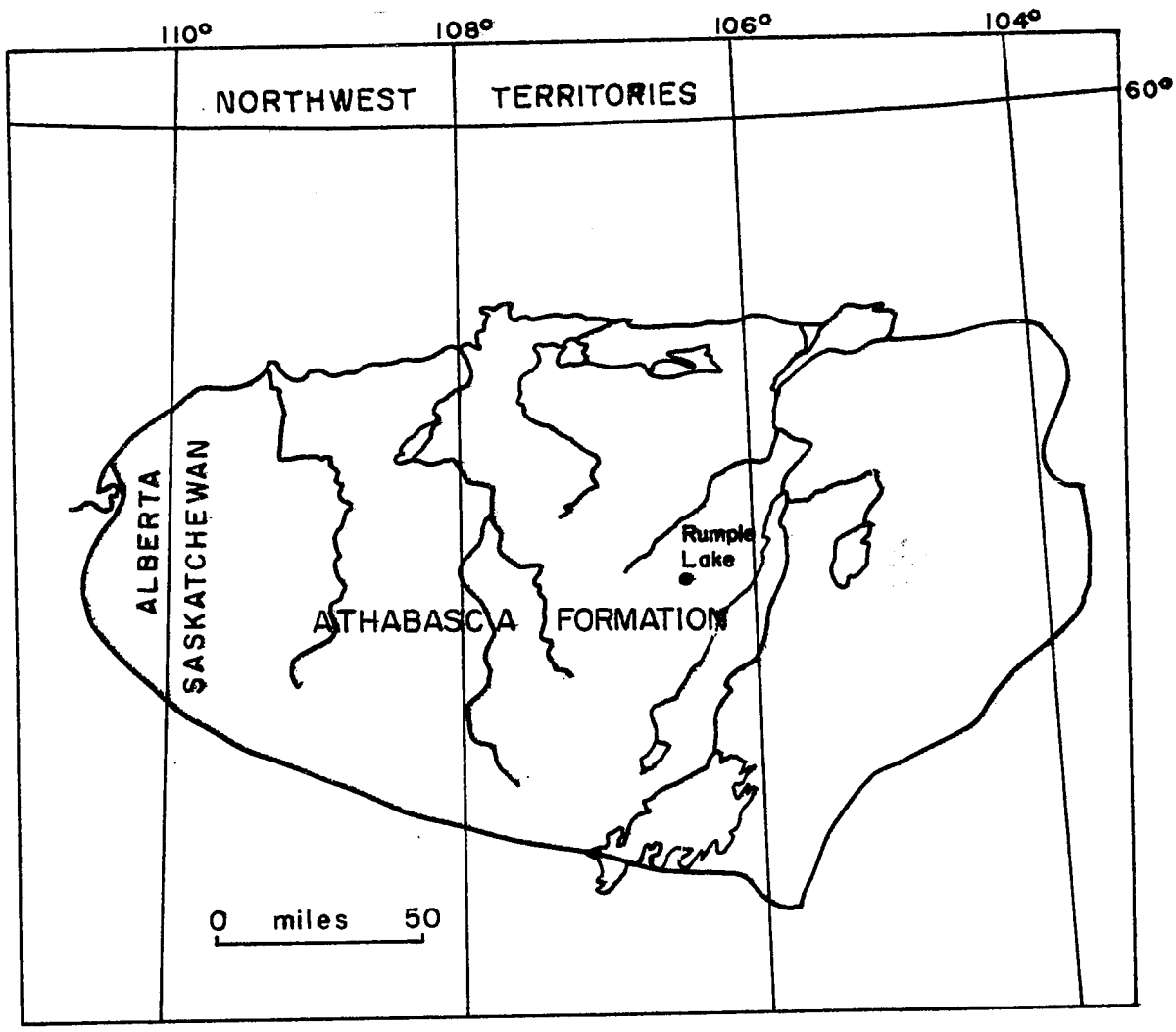

Figure 13. Location of the Rumple Lake core and distribution of the Athabasca Formation in Saskatchewan, Canada (after Fahrig, 1961, Fig. 7).

Fahrig (1961) gave a fairly detailed description of the geology of the Athabasca. More recently, Fraser et al. (1970) gave a summary of the geology of the Athabasca emphasizing its overall tectonic framework. The unmetamorphosed sedimentary rocks above the metamorphic and igneous basement complex in the Athabasca region are divided into three formations (Fig. 14): The Carswell Formation is the carbonate sequence conformably overlying the Athabasca and outcrops in a ring, which is intersected by Carswell Lake. According to Currie (1969), the Carswell Formation consists of two members: the upper member of thickly bedded, massive dolomite and the lower, of fissile dolomite with calcarenite and stromatolite zones. The maximum thickness of the Carswell Formation is more than 500 feet.

The Athabasca Formation is a flat-lying sandstone sequence south of Lake Athabasca, where it consists predominantly of quartz arenites with minor interbedded shale and conglomerate. The sandstones are mineralogically mature, fine to very coarse grained, generally moderately sorted and well rounded. The sandstones of the Athabasca show many sedimentary features of fluvial deposits and are interpreted as river deposits in a coastal plain setting.

The Martin Formation is a redbed and volcanic sandstone sequence outcropping north of Lake Athabasca. It overlies unconformably gneisses and granite of the Tazin Group. This unit is best exposed at Martin Lake area, where it is at least 13,000 feet thick.

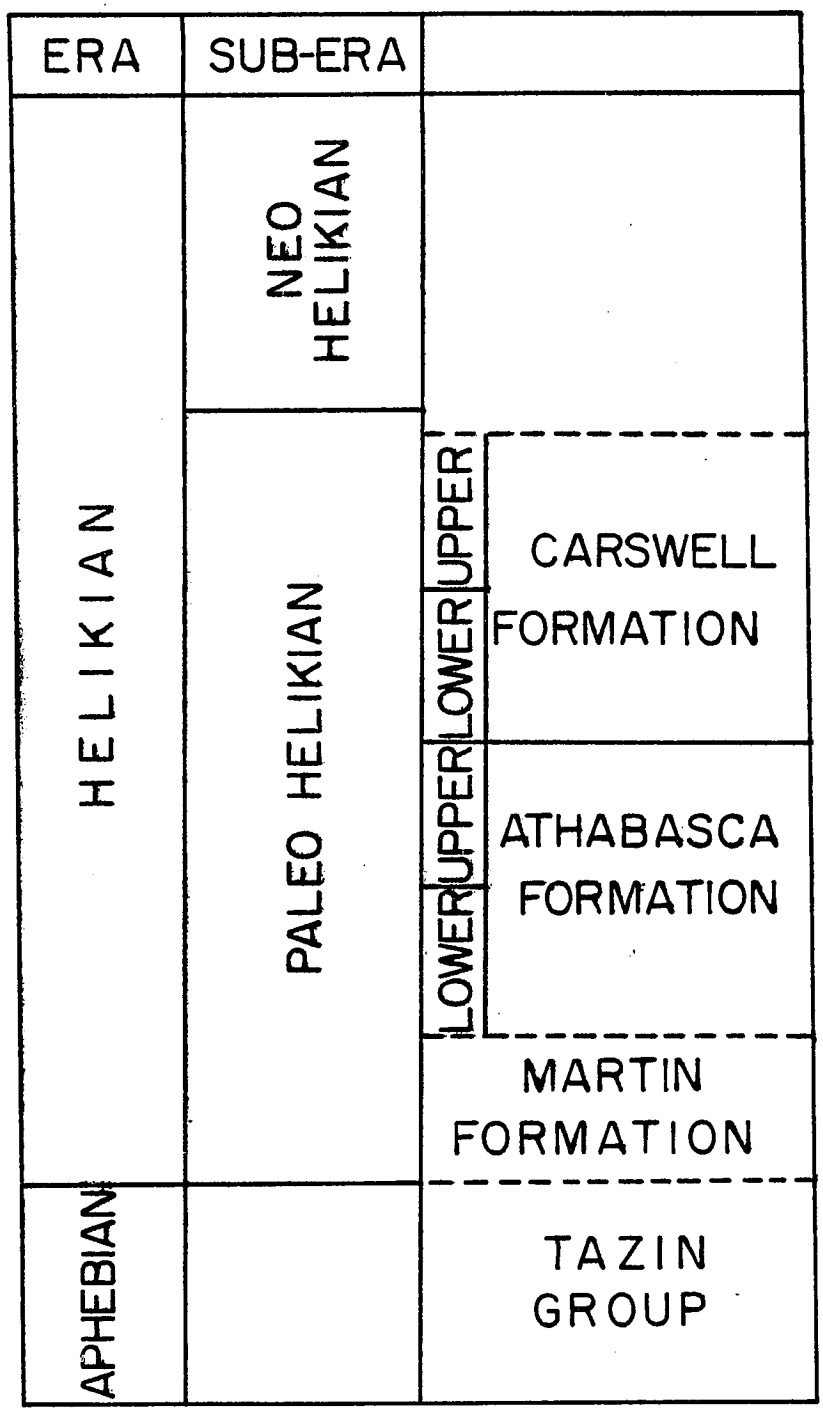

Figure 14. Stratigraphic column in the Athabasca outcrop region (after Lerand, 1970, Table 1).

Petrography

Texturally, the grain size ranges from very fine to coarse grained, the medium-grained class being the most abundant. In the upper part of the core, fine-grained sands are abundant, but coarse-grained sands commonly occur in the lower part. Sorting is highly variable and ranges from poorly to well sorted. Poor sorting is partly due to the presence of alternating laminae of contrasting grain size. However, well-sorted and moderately well-sorted sands are the most abundant. The grain size and sorting of the sandstones of the Athabasca do not show general trends with increasing depth (Fig. 15). Most of the grains appear to be subrounded to very well rounded.

Mineralogically, the sandstones of the Athbasca Formation are composed almost entirely of quartz with minor amounts of chert and mica which are squeezed and bent into the interstices of quartz grains. Monocrystalline quartz grains are more abundant than polycrystalline quartz. The sandstones of the Athabasca are cemented by a combination of secondary quartz overgrowths and authigenic clays including kaolinite, illite and chlorite. The latter occur either as pore-filling or pore-lining cement (Wilson and Pittman, 1977, Fig. 2). The kaolinite, which has a book-like pseudohexagonal crystal form with a grain size of 20 to 40 μm in diameter, is considered to be authigenic in origin. Illite and/or chlorite, also considered to be authigenic, both commonly display a radical fabric with plates normal to grain margins, or a fiberous or needle-like pore-filling habit. The presence of illite and chlorite was also confirmed by X-ray diffraction data (Lerand, 1970). Cements range from 2 to 15

percent and average about 7 percent (Fig. 16). Trace amounts of detrital matrix are present. Fractures and cracks in quartz grains are common features.

As in the Lower Mannville study, percent grains, cement and matrix were determined by 200 counts per thin section. A triangular plot of these three end members indicates that most of the sandstones of the Athabasca are grain-supported arenites (Fig. 17). In sum, sandstones of the Athabasca studied are moderately well-sorted and medium-grained quartzose sandstone.

Results and Interpretations

Types of Grain Contacts and Depth

Types of grain contact, contact strength, packing density and thin-section porosity of sandstone samples from the Athabasca were determined as with the sandstones of the Lower Mannville (Table 6), and plotted against depth in a manner similar to that for the Lower Mannville samples (Fig. 18).

Floating contacts are rare and restricted to a depth above 2,200 feet in the Athabasca sequence (Fig. 18). Point contacts are less than 30 percent at this depth and become less abundant in the Athabasca, although the concavo-convex contacts are fairly common. Both of these contacts are usually less than 10 percent throughout the whole section. Figure 18 seems to show that the vertical distribution of types of grain contacts in the Athabasca is very different from that found in the sandstones of the Lower Mannville.

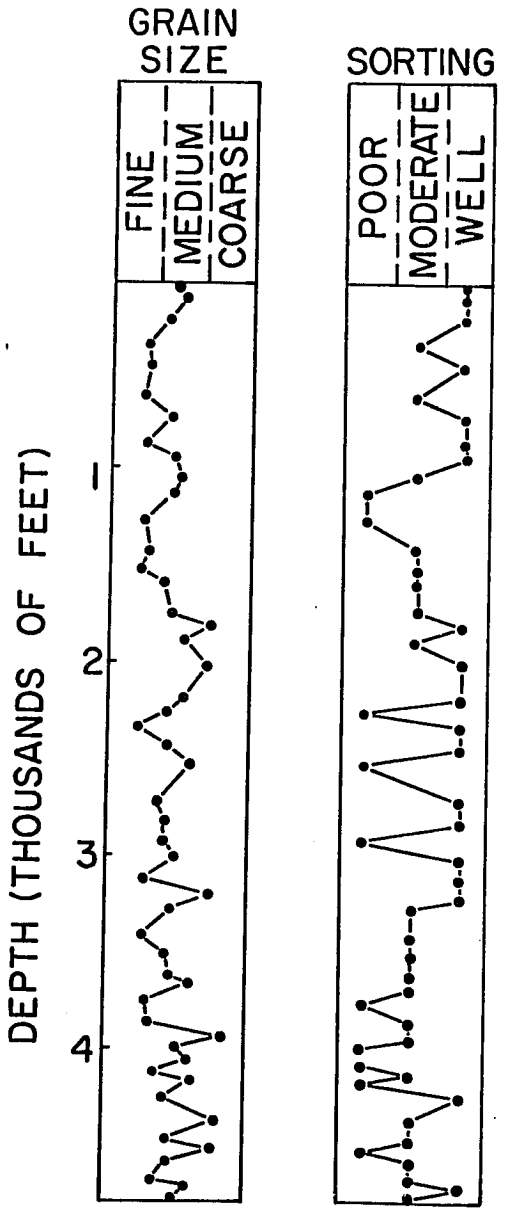

Figure 15. Vertical variation of grain size and sorting of sandstones of the Athabasca Formation. Notice that grain size and sorting do not show general trends with increasing depth.

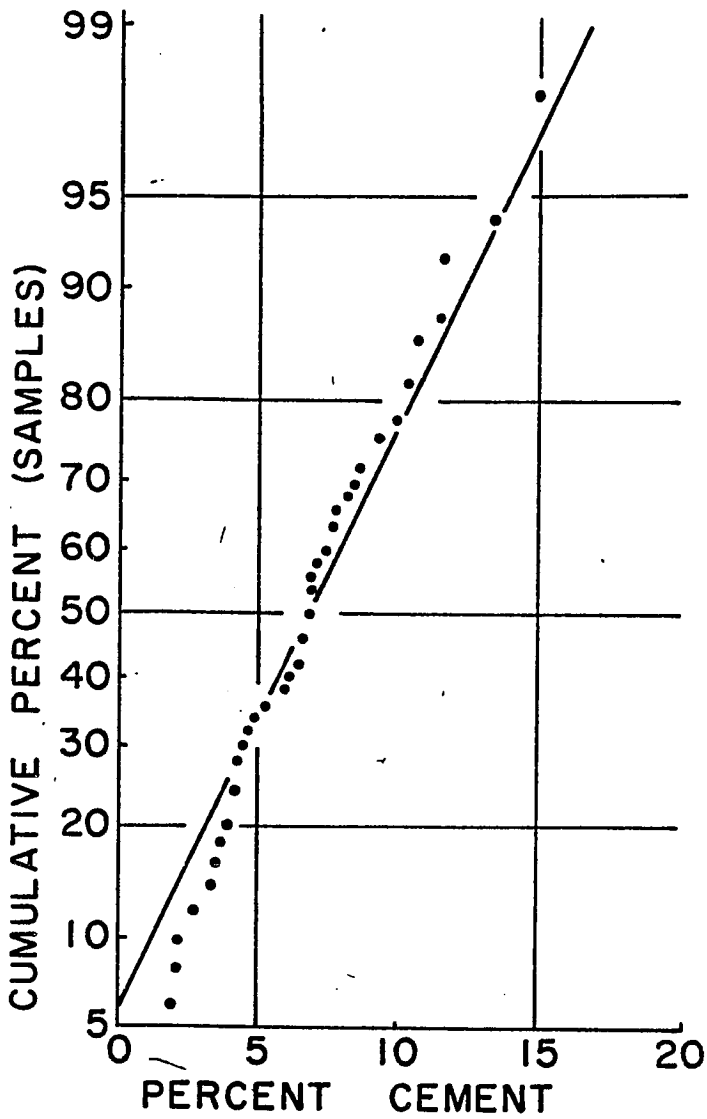

Figure 16. Percent cement for the sandstones of the Athabasca Formation plotted with a cumulative normal probability ordinate.

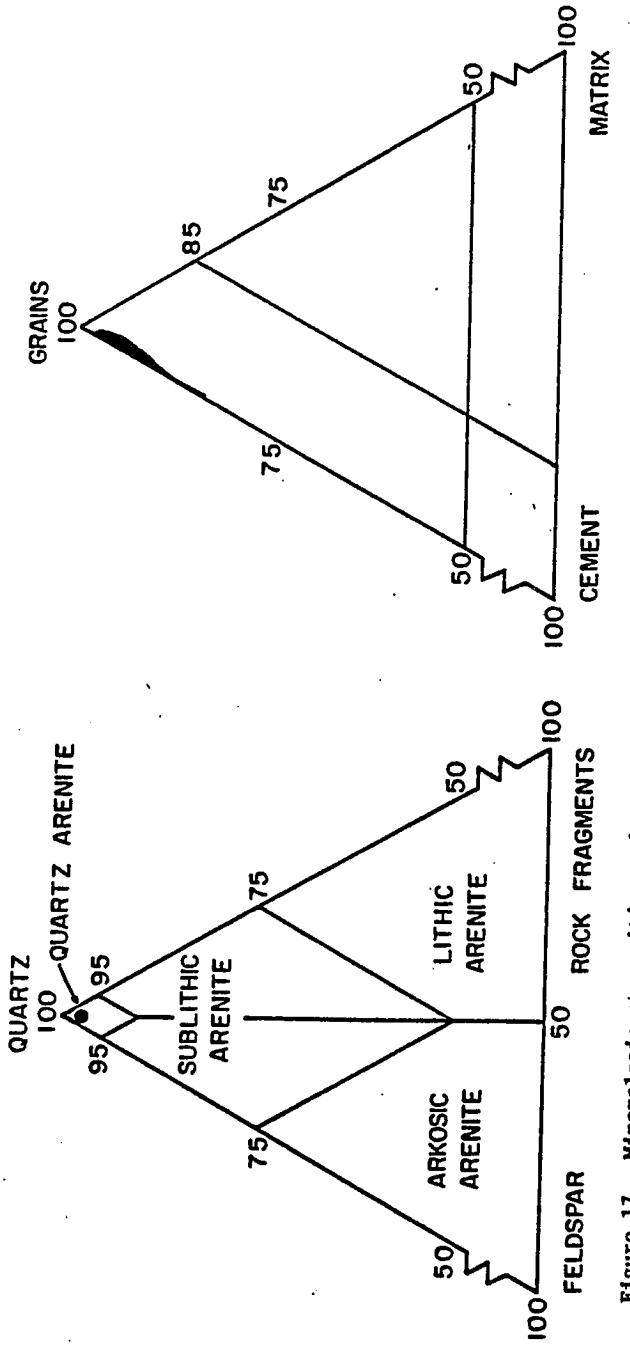

Figure 17. Mineralogic composition and texture for the sandstones of the Athabasca Formation.

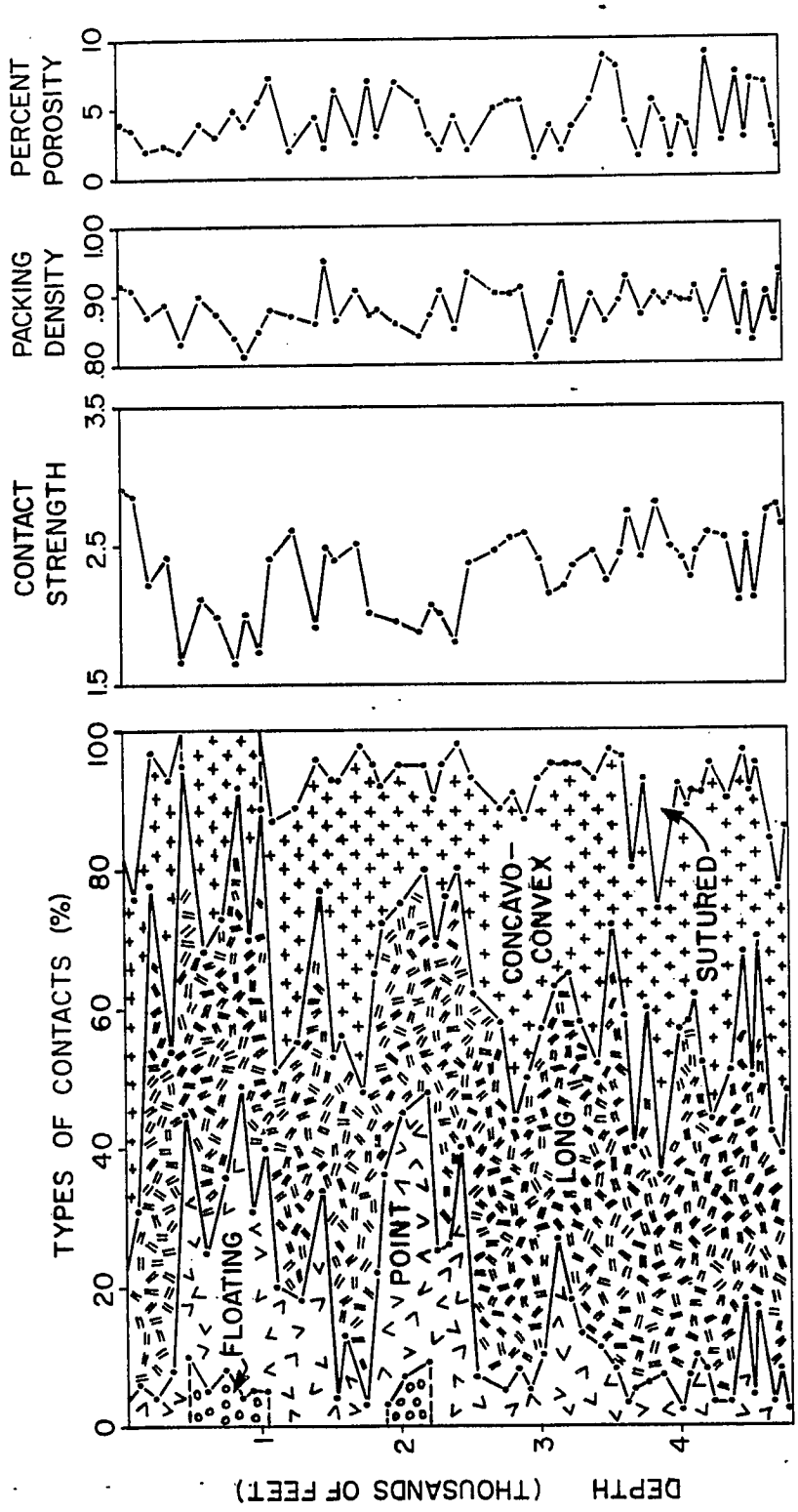

Figure 18. Vertical variations of types of grain contacts, contact strength, packing density and porosity for the sandstones of the Athabasca Formation, Saskatchewan basin.

TABLE 6

Numbers and Types of Grain Contacts, Contact Strength, Packing Density and Depth in Sandstones of the Athabasca of the Saskatewan Basin

Depth (ft.)	Types of Contacts (percent)					Contact Strength	Packing Density	Porosity (%)
	Floating	Point	Long	Concavo-Convex	Sutured			
56	--	4	20	59	17	2.89	0.92	4.2
133	--	5	26	45	24	2.88	0.91	3.5
240	--	4	74	19	3	2.21	0.87	2.1
359	--	8	47	38	7	2.44	0.89	2.3
464	10	35	50	5	--	1.66	0.83	2.1
588	5	20	44	31	--	2.11	0.90	3.8
758	8	28	37	27	--	1.99	0.87	3.0
844	4	45	43	8	--	1.61	0.84	5.0
960	5	26	40	29	--	2.03	0.81	4.2
1058	5	35	49	11	--	1.74	0.85	5.1
1097	--	20	31	36	13	2.42	0.88	7.2
1318	--	18	37	42	11	2.62	0.87	2.0
1462	--	34	43	19	4	1.93	0.86	4.5
1582	--	4	50	39	7	2.49	0.95	2.22
1658	--	13	43	37	7	2.38	0.87	6.4
1750	--	3	45	50	2	2.51	0.91	2.5
1858	3	33	36	20	8	2.03	0.88	3.0
2037	7	38	30	21	5	1.95	0.86	6.5
2191	9	39	32	15	5	1.85	0.84	5.2
2268	--	25	44	21	10	2.16	0.87	3.0
2344	--	26	50	19	5	2.03	0.91	2.1
2420	--	40	40	18	2	1.82	0.85	4.4
2616	--	7	55	31	7	2.38	0.93	2.0
2731	--	5	53	31	11	2.48	0.90	5.1
2883	--	8	38	45	9	2.55	0.90	5.5
2922	--	5	45	37	13	2.58	0.90	5.4

TABLE 6 (continued)

Depth (ft.)	Types of Contacts (percent)					Contact Strength	Packing Density	Porosity (%)
	Floating	Point	Long	Concavo-Convex	Sutured			
3040	--	10	47	36	7	2.40	0.81	1.5
3115	--	27	36	32	5	2.15	0.86	3.9
3223	--	18	47	31	4	2.21	0.93	1.9
3310	--	13	45	39	4	2.36	0.83	3.6
3465	--	11	41	41	7	2.44	0.90	5.5
3550	--	8	64	25	3	2.23	0.85	8.9
3619	--	3	56	37	4	2.42	0.89	8.0
3658	--	5	35	40	20	2.75	0.93	4.0
3812	--	6	54	33	7	2.41	0.87	1.5
3890	--	7	29	37	26	2.80	0.95	5.3
4005	--	2	55	35	8	2.49	0.90	1.2
4069	--	7	55	27	11	2.42	0.89	4.3
4121	--	10	52	29	9	2.37	0.89	3.9
4160	--	8	46	37	9	2.47	0.91	1.1
4276	--	3	40	52	5	2.59	0.86	9.0
4392	--	3	49	38	10	2.55	0.93	4.0
4470	--	18	50	29	3	2.17	0.84	7.5
4508	--	4	45	42	9	2.56	0.91	2.6
4546	--	18	52	25	5	2.17	0.83	7.0
4624	--	3	38	43	16	2.72	0.90	6.8
4689	--	8	31	38	23	2.76	0.86	3.5
4775	--	2	46	38	14	2.64	0.93	2.0

Moreover, contact strength--a quantitative expression of the relative proportion of the different types of grain contacts--does not indicate a definite trend with increasing depth, nor do packing density and porosity exhibit any trends. Clearly, the types of grain contacts do not change sytematically with increasing depth of burial. In addition, the sandstones of Athabasca, unlike the sandstones of the Lower Mannville, do not show a progressive loss of porosity and gradually increasing value of packing density with increasing depth. Thus, the sandstones of Athabasca do not have a porosity-grain packing relationship like that of the Lower Mannville.

What causes this difference? Perhaps variables such as cements, grain size or mineralogic composition and other factors have an effect on mechanical compaction and, hence, on grain packing of the sandstones of the Athabasca Formation. In contrast, grain packing in the sandstones of the Lower Mannville is mainly a response to burial depth and the mechanical compaction processes is little influenced by other factors.

The most obvious difference of vertical distribution of types of grain contacts between the Athabasca and Lower Mannville is the coexistence of floating, point and sutured contacts in the sandstones of the Athabasca. From the Lower Mannville it was concluded that point and floating contacts are indications of original packing or loose compaction of grains, and that they are restricted to shallow depths. Sutured contacts, on the other hand, are the result of pressure solution. Therefore, the coexistence of floating, point and sutured contacts in the sandstones of Athabasca needs further investigation. However, the work

of Phipps (1969) suggests a partial solution to this problem. Phipps (1969, Table 1) found that deeply buried, carbonate-cemented quartz arenites at depths of 12,834 and 12,910 feet have 34 percent floating, 58 percent point contacts, 6.7 percent floating, and 72.9 percent point contacts. In these carbonate-cemented sandstones, the calcite cement forms coarse, patchy crystals, which completely enclose the sand grains and prevent compaction, resulting in an unusually large amount of floating and point contacts. In the sandstones of the Athabasca Formation, the floating and point contacts are probably due to the early presence of quartz overgrowths and recrystallized disseminated chert which prevented further compaction, thus preserving these contact types even at great burial depths. In other words, the effect of compaction on the sandstones of Athabasca is obscured by the cementation processes.

Obviously, the present depth of the sandstones of Athabasca does not represent the maximum burial depth as revealed by the presence of abundant long and concavo-convex contacts, low porosity and tight packing of grains. This fact has also been acknowledged by engineering geologists. For example, Bell (1978a), who studied samples from a shallow core, found that the two most common types of grain contacts are the long and concavo-convex. He suggested that these sandstones were buried to an appreciable depth after deposition.

Thus, to estimate the burial depth of the sandstones of the Athabasca Formation, the vertical distribution of types of grain contacts, contact strength, packing density and porosity of the Lower Mannville is referred to as the standard for comparison. In the sandstones of

Athabasca, the dominant contacts are long and concavo-convex. Typical values of contact strength, packing density and porosity are 2.3, 0.9 and 5 percent, respectively, thus suggesting that the Athabasca sands correspond to the zone below 7,000 feet of the Lower Mannville, where the dominant contacts are long and concavo-convex and typical values of contact strength, packing density and porosity are 2.3, 0.86 and 8 percent, respectively. Therefore, the comparison of vertical distribution of types of contacts between the Athabasca and Lower Mannville suggests that the sandstones of the Athabasca Formation had at one time at least an additional overburden 7,000 feet. In other words, the sandstones of the Athabasca Formation would have been buried at least to a depth of 12,000 (5,000 + 7,000) feet.

Cements and Depth

Sandstones of the Athabasca Formation are mainly cemented by authigenic clays and silica. Dust rings of clay or iron oxides are present in almost all the quartz grains with secondary quartz overgrowth. This allows differentiation between quartz cement and framework grains. Quartz overgrowths grow outward from quartz grains into the pore space which they partly or completely fill. Morphologically, this type of quartz overgrowth displays the form of straight-edge or dog teeth. However, when quartz overgrows outward from adjacent grains and meets, filling the pore space completely, the result is a mosaic of interlocking anhedral grains.

Kaolinite typically occurs as a pore-filling cement. It forms interlocking aggregates of book-like well developed pseudohexagonal crystals with a grain size of 20 to 40 μm and usually completely infills the pore space. Authigenic illite and chlorite occur either as pore-filling or pore-lining cement. Generally, they occupy only a small part of the pore space.

In the sandstones of the Athabasca, typical sequential filling of the pores follows one of five paths:

1) Quartz overgrowths completely fill the pore space and result in an interlocking mosaic.

2) Quartz overgrowths partly fill the pores. Authigenic kaolinite precipitates as a pore-filling cement, and fills the remainder of the pores.

3) Quartz overgrowths partly fill the pores, authigenic kaolinite, the next to form, precipitates as pore-filling cement, filling a part of the remaining pore space and, finally, illite and/or chlorite fills the rest of the pores.

4) Quartz overgrowths partly fill the pores, authigenic illite and/or chlorite occur both as pore-filling and pore-lining cement, filling the rest of the available pore space.

5) Illite occurs as a pore-lining on quartz grains, then authigenic kaolinite precipitates as isolated aggregates, filling the rest of the available pore space.

In order to reveal the relationship between the cement and depth, the amount of quartz cement and authigenic clays are plotted against depth. No significant correlation between the cements and depth was found in the sandstones of the Athabasca. Füchtbauer (1974, Fig. 3-50) has shown that quartz cement of the Dogger Beta sandstones increases with depth. However, Levandowski et al. (1973, p. 2226) found that quartz cement in the Lyons sandstones is independent of depth. Thus, depth is not the only major variable controlling the amount of quartz cement. Obviously, the source of silica, depositional environment, grain size and other factors control the amount of quartz cement.

On the other hand, the sequence of clay mineral stabilities can be used as an index to the temperature-pressure conditions, and hence depth, which a sediment has undergone during burial. For instance, based on a series of clay-rich core samples, Burst (1969), Power (1959 and 1967), Perry and Hower (1970) and Hower et al. (1976) have shown that smectite is converted to illite, and randomly interlayered clays are transformed to regularly interstratified clays during burial. However, before applying the pattern of burial diagenesis of clays to interpret the clay cements in the sandstones of the Athabasca, there are two points which must be clarified. First, clay diagenesis models are based on the assumption of a uniform beginning mineral composition for the sediments prior to burial. Second, the burial diagenesis of a thick shale

sequence differs from that of a sandstone sequence. This is particularly so because during diagenesis the pore fluids play a more important role in sandstone than in shale.

Kaolinite is present throughout the Athabasca section. It generally forms later than quartz overgrowths. The paragenesis of quartz-kaolinite cements indicates that during burial, pressure solution is common and results in a supersaturation of the pore fluids with silica and consequent precipitation of quartz overgrowth. In the pore space adjacent to these overgrowths, kaolinite precipitates under slightly acid conditions where fluids still have an excess of silica and aluminum but a paucity of potassium and magnesium. It seems to the writer that kaolinite cement cannot prevent compaction. It must have formed after compaction because the kaolinite cement is not deformed. However, the quartz cement must have been early in order for the point contacts to be partially preserved. If so, it cannot be entirely from pressure solution (the source of SiO_2, that is). Therefore, SiO_2 cementation must have been at least begun early in burial history and kaolinite came in after burial to about 7,000 feet. Hence, silica and aluminum are assumed to be derived partially from feldspar leaching, or alteration of unstable rock fragments or mixed-layer clays. The lack of feldspar, rock fragments and detrital matrix in the Athabasca seems to support this argument. Additionally, hower et al. (1976, Fig. 6) and Velde (1977, Fig. 4) pointed out that the maximum depth of occurrence for kaolinite in a deeply buried shale sequence is about 16,000 feet and for montmorillonite, which becomes unstable at depth, approximately 10,000 feet

(Kisch, 1969, Fig. 2). Therefore, the absence of montmorillonite, which is generally an early diagenetic cement is sandstone, and the presence of kaolinite cement in the sandstones of the Athabasca suggests that the Athabasca section was probably buried to a depth of between 10,000 to 16,000 feet.

Illite and chlorite occur commonly as intermediate to late diagenetic cements during burial (Pettijohn et al., 1972, p. 431). Both are present throughout the Athabasca section. Under great burial depth, kaolinite is commonly altered to illite or chlorite when the pore fluids are slightly alkaline with excess amount of potassium and magnesium. In other words, the paragenesis of quartz-kaolinite-illite or chlorite in the sandstones of the Athabasca reflects the variations of pH and compositions of the pore fluids during late diagenesis. In sum, the associated facies of kaolinite, illite and chlorite and their paragenesis indicate that the sandstones of the Athabasca have undergone late stage diagenesis and have been buried to a maximum depth of approximately 16,000 feet.

Conclusions

The grain packing-porosity relationship of the sandstones of the Athabasca Formation is not the same as that for the sandstones of the Lower Mannville Group because the effect of compaction on the grain packing has been impeded by the cementation processes in the former. However, the presence of abundant long and concavo-convex contacts,

low porosity and tight packing in the sandstones of the Athabasca Formation suggests that they had an overburden at least of 7,000 feet.

Cements of kaolinite, illite and chlorite and their paragenesis indicate that the sandstones of the Athabasca have undergone late stage diagenesis and have a maximum burial depth of probably 16,000 feet. Hence, grain packing and cements of the sandstones of the Athabasca suggest that their maximum burial depth was probably between 12,000 and 16,000 feet.

CHAPTER III

GEOCHEMISTRY OF RECENT AND ANCIENT TURBIDITES: IMPLICATIONS FOR TECTONICS AND GRAYWACKE DIAGENESIS

Introduction

The matrix and soda problems related to graywacke diagenesis are probably explored better by geochemical than petrologic techniques. A suite of Recent and ancient turbidite sandstones was studied. It is necessary to divide these samples into different categories by source area because sands from low-relief continental land masses should contain fewer unstable fragments--those that can react chemically to those from autigenic matrix--than those from volcanic island arcs. That is, diagenetic patterns will be to a larger extent governed by original composition. However, before investigating the chemical changes in graywackes during diagenesis, I will briefly review the relationship between sandstone composition and provenance and then show how provenance is related to diagenesis of graywackes.

Sandstone Composition and Provenance

During the 1970's, sedimentologists have shown the usefulness of petrographic variables such as Q-F-L (Quartz-Feldspar-Lithic Fragments) and chemical variables such as the K_2O/Na_2O ratio for identifying the provenance or tectonic setting of sandstones. For instance, Dickinson (1971) showed that the modal analysis of some New Zealand Mesozoic graywackes, as expressed by a Q-F-L plot, can be used to infer a

volcanic-plutonic arc provenance. Blatt et al. (1972) were able to differentiate taphrogeosynclinal, eugeosynclinal and exogeosynclinal sandstones by means of a triangular plot of Fe_2O_3 + MgO, Na_2O and K_2O. Similarly, Harrold and Moore (1973) have shown that modern deep-sea sands from marginal basins of the northwestern Pacific can be divided into three distinct suites of volcanic, sedimentary and crystalline source terrains by means of the Q-F-L plot. Based on the framework mineralogy and volatile-free chemistry of ancient flysch arenites (graywackes), Crook (1974) divided 328 graywackes into three major groups and suggested that each corresponds to a characteristic geotectonic setting: 1) quartz-rich graywackes (> 65% quartz, average 89% SiO_2, $K_2O/Na_2O > 1$) are indicative of Atlantic-type continental margins, 2) quartz-intermediate graywackes (15-65% quartz, average 68-74% SiO_2, $K_2O/Na_2O < 1$) indicate Andean-type continental margins, and 3) quartz-poor graywackes (< 15% quartz, average 58% SiO_2, $K_2O/Na_2O << 1$) are indicative of magmatic island arcs. Crook also realized that composition of modern deep-sea sands can be more easily related to tectonic setting than that of ancient ones because the composition of deep-sea sands has not been changed by diagenesis and source areas can be determined relatively easily. Therefore, Crook further suggested that comparisons of mineralogic and chemical data of ancient graywackes with those of Recent deep-sea sands should reinforce his arguments. Unfortunately, published modal analyses of modern deep-sea sands are relatively few and chemical data of deep-sea sands are virtually nonexistent (Crook, 1974, p. 307). It is apparent that more data on modern deep-sea

sands are needed to test Crook's hypothesis on the sandstone composition of graywacke in relation to tectonics. More recently, Schwab (1975) followed Crook's idea and used the same compositional criteria to separate varieties of sandstones ranging in age from Cambrian to Quarternary into different suites of rift-valley, Atlantic, Andean and Western Pacific continental margins. However, we are still confronted by the lack of data on modern deep-sea sands to refine the concept of sandstone composition reflecting tectonics.

On the other hand, Potter (1978) has tried to relate composition of modern river sands to tectonic setting. Based on the petrologic and chemical data of 36 modern big river sands, Potter (1978) has shown that sands derived from Atlantic-type continental margins or trailing edges have a typical composition of $Q_{71}F_9L_{20}$ and K_2O/Na_2O ratio of 2.04, whereas sands from Andean-type continental margins or leading edges have a composition of $Q_{36}F_{17}L_{47}$ and K_2O/Na_2O of 1.0. Potter concluded (p. 441), "Hence the petrographic and chemical data base of this study offers promise of identifying ancient plate tectonic regimes in pre-Mesozoic sedimentary basins." The significance of Potter's work is to create a basis for comparison with ancient sediments. Moreover, it seems to support Crook's suggestion of the importance of comparison between modern deep-sea sands and ancient graywackes. Thus, ancient continental marginal sediments can be recognized by means of petrologic components ($Q_xF_yL_z$) and chemical composition (percent SiO_2 and K_2O/Na_2O) of sandstones.

The currently established compositional criteria for identifying provenance or classifying tectonic settings are summarized in Table 7. Generally, sandstones formed on a trailing edge are rich in quartz and have more potash feldspar than plagioclase, whereas those from a leading edge or island arc have an increase in lithic fragments, volcanic debris and plagioclase. However, there are some overlaps and discrepancies between these established compositional criteria because of slightly different classifications of basin types and various sands and sandstones used by different investigators. Hence, more data on modern deep-sea sands are needed to compare with that of modern big river sands and ancient sandstones, especially graywackes. This will result in a better separation of compositional variables which can be used to identify ancient tectonic regimes of sedimentary basins.

Such a procedure as relating sandstone composition to tectonic setting presumes diagenetic processes do not affect or modify the framework grains and bulk chemistry severely. However, diagenetic processes certainly will destroy some unstable rock fragments and to a lesser extent, feldspars and ultimately reduce the percentage of rock fragments and feldspars. The consequence of this could be to obscure the Q-F-L plot and the ratio of K_2O/Na_2O. Fortunately, effects of early diagenesis do not modify the framework mineralogy and chemistry of modern sands severely (Harrold, et al., 1973 and Potter, 1978). On the other hand, for ancient sandstones, particularly ancient graywackes, many investigators have shown the importance of diagenesis in transforming rock fragments into matrix in graywackes (Cummins, 1962 and Galloway, 1974). Therefore,

TABLE 7

COMPOSITIONAL VARIABLES FOR CLASSIFYING TECTONIC SETTING OF SANDSTONES

AUTHOR	TYPES OF SANDS	BASIN TYPE	Q	F	L	P/F	SiO_2%	SiO_2/Al_2O_3	K_2O/Na_2O
Dickinson (1971)	Mesozoic New Zealand Graywackes	Leading Edge	39	36	25	0.56	69.7	5.16	0.47
		Back Arc	15	45	40	0.82	--	--	--
		Fore Arc	1	19	70	1.00	55.9	3.25	0.68
Crook (1974)	Ancient Flysch Sandstones	Trailing Edge	>65	--	--	--	88.82	15.11	1.71
		Leading Edge	15-65	--	--	--	70.59	4.76	0.55
		Island Arc	<15	--	--	--	54.21	6.71	0.23
Schwab (1975)	Varieties of Sandstones	Trailing Edge	>65	--	--	--	70.0	--	>1
		Leading Edge	15-65	--	--	--	68-74	--	<1
		Island Arc	<15	--	--	--	57-59	--	<1
Potter (1978)	Modern Big River Sands	Trailing Edge	71	9	20	0.16	83.51	51.78	2.04
		Leading Edge	36	17	47	0.51	73.12	16.78	1.00
		Marginal Sea	56	11	33	0.44	79.67	12.30	1.14

diagenesis raises one question: are the petrography and chemistry of ancient graywackes as reliable indicators of provenance as they are in modern sediments? To answer that, it is necessary to investigate the possible effects of diagenesis on ancient graywackes.

The writer is interested in diagenesis not only for the possibility that it might obscure these tectonic variables but for its own sake. Diagenetic changes are severe in graywackes, at least for the petrologic variables; hence, the writer tries to test for chemical changes by using Recent sediments data to set some limits on diagenetic changes. The following section briefly summarizes two essential problems of graywacke diagenesis: matrix and soda problems.

The Matrix Problem

By definition graywackes have a matrix content that exceeds 15 percent and may reach 50 percent (Pettijohn et al., 1972, p. 206). However, Recent deep-sea sands rarely have more than 10 percent of detrital matrix. Cummins (1962) questioned why many ancient turbidites have more fine-grained matrix than Recent deep-sea turbidite sands and suggested that the clayey matrix in many turbidite graywackes was diagenetic in origin and not detrital at all. Hollister and Heezen (1964) also indicated that graywackes are not commonly found in Recent deep-sea turbidite sands. Kuenen (1966) conducted flume experiments which also indicated that original fine matrix of coarse-grained turbidites is below 10 percent. Based on these studies a diagenetic origin of matrix in graywackes has become popular. Cummins' idea is strongly supported by

evidence presented by Brenchly (1969) who showed that Ordovician volcanicgenic graywackes have 40 to 60 percent diagenetic matrix and also found that early pore-filling carbonate cements may prevent the transformation of unstable rock fragments to matrix. While investigating immature deep-sea feldspathic sands (graywackes), Hayes (1971) confirmed the formation of diagenetic chlorite and also recognized pore-filling carbonate cement playing an important role in determining the degree of authigenesis of minerals.

The significance of carbonate cement as a matrix inhibitor is not clear, however, Pettijohn, et al. (1972, p. 210) asked why the Paleozoic and older graywackes are generally matrix-rich and contain abundant carbonates. Reimer (1972) provided some clues for this question. He suggested that calcium derived from destruction and partial albitization of the plagioclase in the graywackes, and especially in the interbedded shales, forms dolomite within the graywackes which replaces the original grains. The interbedded shales, therefore, are depleted both in Ca and Sr. This carbonate is not strictly a cement because it is not confined to pore-fillings (Galloway, 1974).

A series of hydrothermal experiments on Columbia River sands chemically similar to graywackes produced matrix minerals such as montomorillonite and zeolite at relatively low temperature and pressure (150-300°C, 1-2 Kbar) (Hawkins and Whetten, 1969, Whetten and Hawkins, 1970). This textural resemblance to graywackes supports the idea that graywacke matrix is largely diagenetic. However, there is a difficulty in applying these experimental studies to ancient graywackes because the unstable

grains may be completely destroyed through diagenetic processes and leave no relic texture at all (Rahmani, 1968 and Whetten and Hawkins, 1971).

Galloway (1974) has made a careful study of the diagenetic sequence in a series of core samples from different depths from three Tertiary arc-related basins. He found the following diagenetic sequences with increasing depth: 1) early calcite pore-filling cement that forms only in some sandstones and inhibits further diagenesis when present, 2) authigenic clay coating on sand grains, 3) pore-filling silicates, either chlorite or laumontite, 4) replacement of rock fragments and heavy minerals by calcite and chlorite, and 5) appearance of phrenite-pumpellyite or albite-epidote stages of metamorphism. The progressive stages of diagenesis led him to infer a diagenetic origin of the graywacke matrix. Hence, evidences from ancient graywackes and Recent deep-sea sands and experiments with modern river sands strongly suggest that matrix in many graywackes is diagenetic.

On the other hand, many other workers believe that matrix in graywackes is detrital. For instance, Edward (1950) studied some Cretaceous graywackes from Papua in which matrix is high (15-50%) and which he presumed to be detrital. Walton (1955) thoroughly investigated Silurian graywackes in Peebleshire, Scotland, and concluded that matrix is detrital. Based on the absence of any relic texture of grains altered to matrix in the Viqueque graywackes, Audley-Charles (1967) concluded that matrix is detrital in origin. In addition, Rust (1965) found little evidence supporting diagenetic origin of the matrix (35%) of the Silurian

turbidite graywackes in southeast Wigtownshire, Scotland. Instead, carbonate replacement is the dominant diagenetic feature. Additionally, geochemical studies of some Lower Paleozoic and Precambrian turbidite graywackes gave no evidences of a diagenetic origin for the matrix (Condie, et al., 1970 and Condie and Snansieng, 1971). On the other hand, Klein (1963) and Emergy (1964) both suggested that the clayey matrix of turbidite graywackes may be introduced mechanically into the turbidite sands from the overlying or underlying muds. However, this suggestion was seriously questioned by Kuenen (1966). In addition, Atman and Gokcen (1975) found some modern graywacke-type turbidite sands with detrital matrix over 15 percent. Therefore, evidences from ancient graywackes and modern deep-sea sands also suggest that matrix in many graywackes is detrital.

A multiple origin of this matrix has been proposed by Dickinson (1970, p. 702) who suggested four types: interstitial detrital clays (protomatrix), recrystallized fine-grained material (orthomatrix), diagenetic matrix (epimatrix) and deformed and squashed rock fragments (pseudomatrix). However, the relative importance of the roles played by each of these types in the genesis of matrix in graywackes is still uncertain, especially detrital versus diagenetic.

The Soda Problem

The high content of Na_2O is the other distinctive characteristic of graywackes. Pettijohn, et al. (1972, p. 211) suggested that the high content of Na_2O of graywackes is due to the development of diagenetic

albite at the expense of K-feldspar in the sands. Thus, the high K_2O/Na_2O ratio of the interbedded shales is also a diagenetic feature, i.e., the authigenesis of illite at the expense of mixed layer clays and montmorillonite. In a study of the Cambrian Charny sandstones, a turbidite graywacke, Middleton (1972) pointed out the overwhelming predominance of albite over K-feldspar. The albite shows film perthite structure which suggests that feldspar composition is controlled not by source area, but by the amount of replacement of K^+ by Na^+ during diagenesis. However, the argument of Middleton has been questioned by Lajoie (1973) and Lajoie et al. (1974), who felt that albite in the Charny graywackes could not be diagenetic in origin because they fail to meet the criteria for authigenetic feldspars set forth by Kastner (1971), and then concluded that the albitization may occur in the source area. In addition, Iosomi et al. (1966) pointed out that the unusually high ratio of K_2O/Na_2O of some Japan graywackes reflects a granitic and metamorphic provenance. Based on modal mineralogy and chemical analysis of some Mesozoic New Zealand graywackes, Dickinson (1971) also showed that the relatively high content of K-feldspar and percent K_2O are attributable to provenance rather than to diagenesis. Therefore, the origin of the high content of Na_2O in graywackes is still uncertain.

Both of these problems, matrix and Na_2O, are concerned with interactions between the sandstone and surrounding rocks: has Na_2O been added? Has matrix been introduced? Graywackes occur commonly as turbidites (Dzulynski and Walton, 1965 and Pettijohn et al., 1972) and hence they are interbedded with shales. Therefore, the sand-shale pair as a

unit needs to be studied to investigate the possibility of exchange of material between them.

Glass et al. (1957) were probably the first ones to consider sand-shale as a paired sample in evaluating the effects of diagenesis when they studied the Pennsylvanian sediments in the Eastern Interior basin. They suggested that greater permeability in the sandstone than that in interbedded shales resulted in better circulation of groundwater which produced authigenic kaolinite in the sandstones. Similarly, in an investigation of a core of 237 feet of interbedded sandstone and shale of the Atoka Formation, Triplehorn (1970) showed that formation of diagenetic iron-rich chlorite is confined to the sandstones because of their greater porosity and permeability. In addition, silica cementation commonly occurs close to the boundaries between sandstone and shale and the source of silica is considered to be mainly from the shale. This feature was also observed by Füchtbauer (1967). Moreover, chemical analysis suggested that the overall diagenesis occurs within a closed system, except iron which is introduced from the groundwaters. Based on the clay mineralogy and some chemical analysis of the interbedded sandstones and shales of the Desmoinesian deltaic strata in Oklahoma, Buck and Mankin (1971) recognized that diagenetic kaolinite is restricted to the sandstones. Within sandstones, K-feldspar is destroyed providing excess aluminum and silicon for the formation of kaolinite whereas the partly degraded illite is an acceptor for the K^+ released during K-feldspar decomposition and results in keeping dissolved K^+/H^+ low, a necessary condition for the precipitation of kaolinite. In other words,

ions such as Si, Al and K involved in the formation of diagenetic kaolinite were present in situ, i.e., within the sandstone itself. Recently, Wallace (1976) also has shown that interbedded shales are a source of silica for quartz cementation in the adjacent sandstones in the Precambrian Uinta Group. Hence, silica mobility is a prominent feature of diagenesis in the sand-shale sequence. In addition, considering the effects of compaction on shales, he further suggested that during progressive burial diagenesis of the interbedded shales and sandstones, Na^{+} and H_4SiO_4 concentrations in the sandstones increase relative to shales whereas K^{+}, $Al^{+}3$, Mg^{++} and Ca^{++} are held in shales. From these studies, it is postulated that diagenesis takes place within a sand-shale pair acting as a closed system and ions such as Si, Al, Na and K may have been rearranged in situ without long distance transport. From this point, it can be assumed that there may be K^{+}-Na^{+} exchange between turbidite graywackes and interbedded shales.

Objectives

This study has two main objectives: first, the chemistry of Recent deep-sea sands and associated muds will be defined and examined for any relationship to tectonics. Secondly, these compositions will be compared with data from ancient sandstones and interbedded shales to see if there has been any exchange of chemical components during diagenesis.

Sampling

The geochemistry of Recent and ancient turbidites can be investigated by studying a number of paired sand-shale samples from a variety

of tectonic settings. About 70 sand-shale pairs of Recent deep-sea turbidites were collected from the depository of the Lamont-Doherty Geological Observatory. These deep-sea samples were selected from various plate tectonic basin types: Atlantic-type continental margin basins, Andean-type continental margin basins, back arc basins and fore arc basins. Locations of these deep-sea samples are shown in Figure 19. Water depth, sub-bottom depth, longitude, latitude and basin type of these deep-sea samples are given in Appendix 1.

Around 100 pairs of ancient turbidite sandstones and shales ranging in age from Cambrian to Pliocene were also studied. Unfortunately, these ancient samples are not equally distributed by age: Paleozoic samples predominate. About one third of the ancient samples are Tertiary in age; few are Mesozoic. In addition, the tectonic settings inferred from the literature are not so clearly defined as those of the modern deep-sea sands. The stratigraphic unit, age and locations of these ancient turbidites are given in Table 8. All the ancient turbidite samples were supplied by Drs. Paul Edwin Potter and J. Barry Maynard, University of Cincinnati.

Analytical Methods

The major element concentrations of ancient turbidite sandstones and interbedded shales and Recent deep-sea sands and associated muds were determined using Atomic Absorption Spectrophometry and carbon analyzer. The elements Si, Al, Fe, Mg, Ca, Na and K were analyzed by Atomic Aborption Spectrophometry technique. The general procedure is given by Medlin et al., 1969.

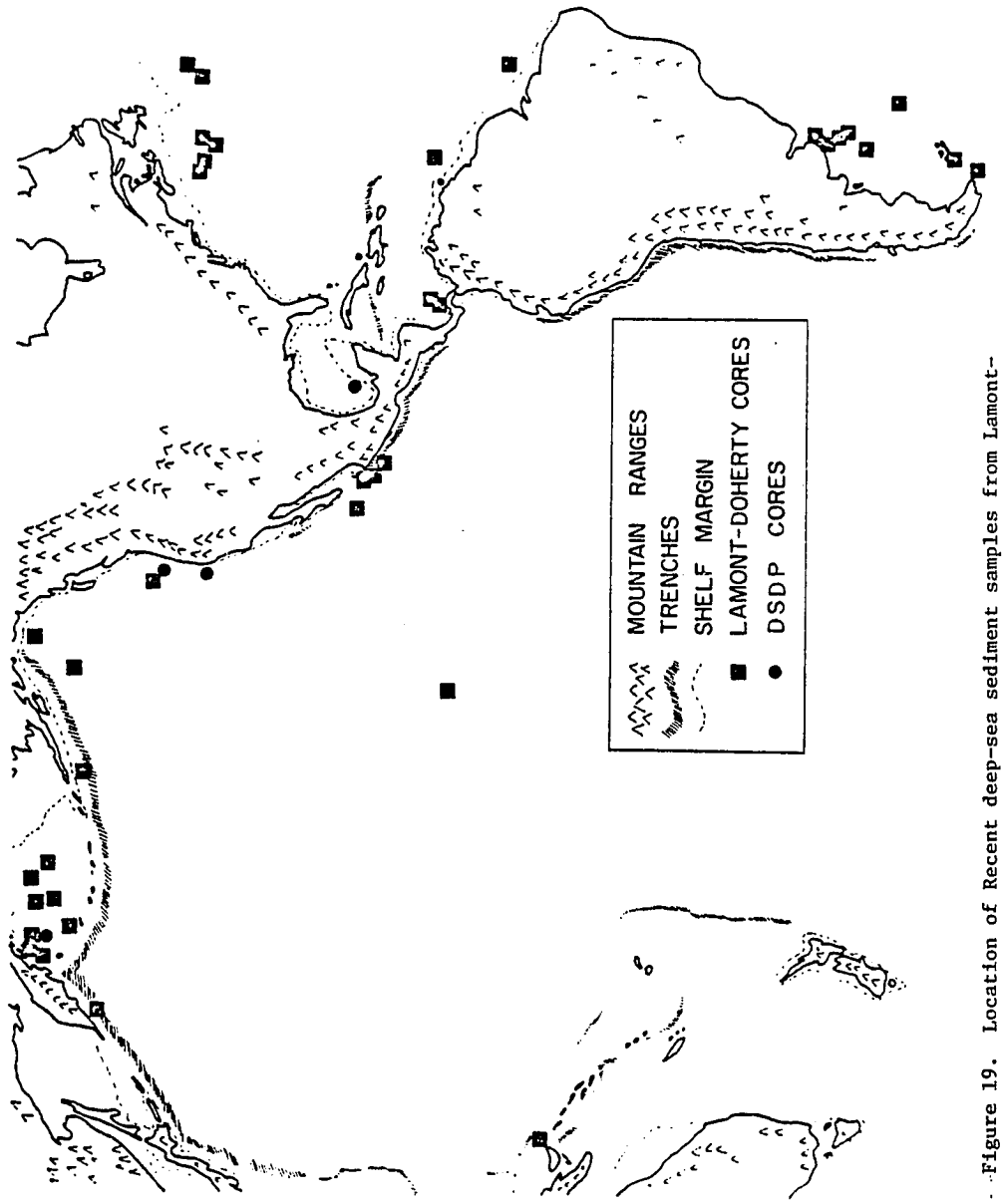

Figure 19. Location of Recent deep-sea sediment samples from Lamont-Doherty Geological Observatory and the DSDP.

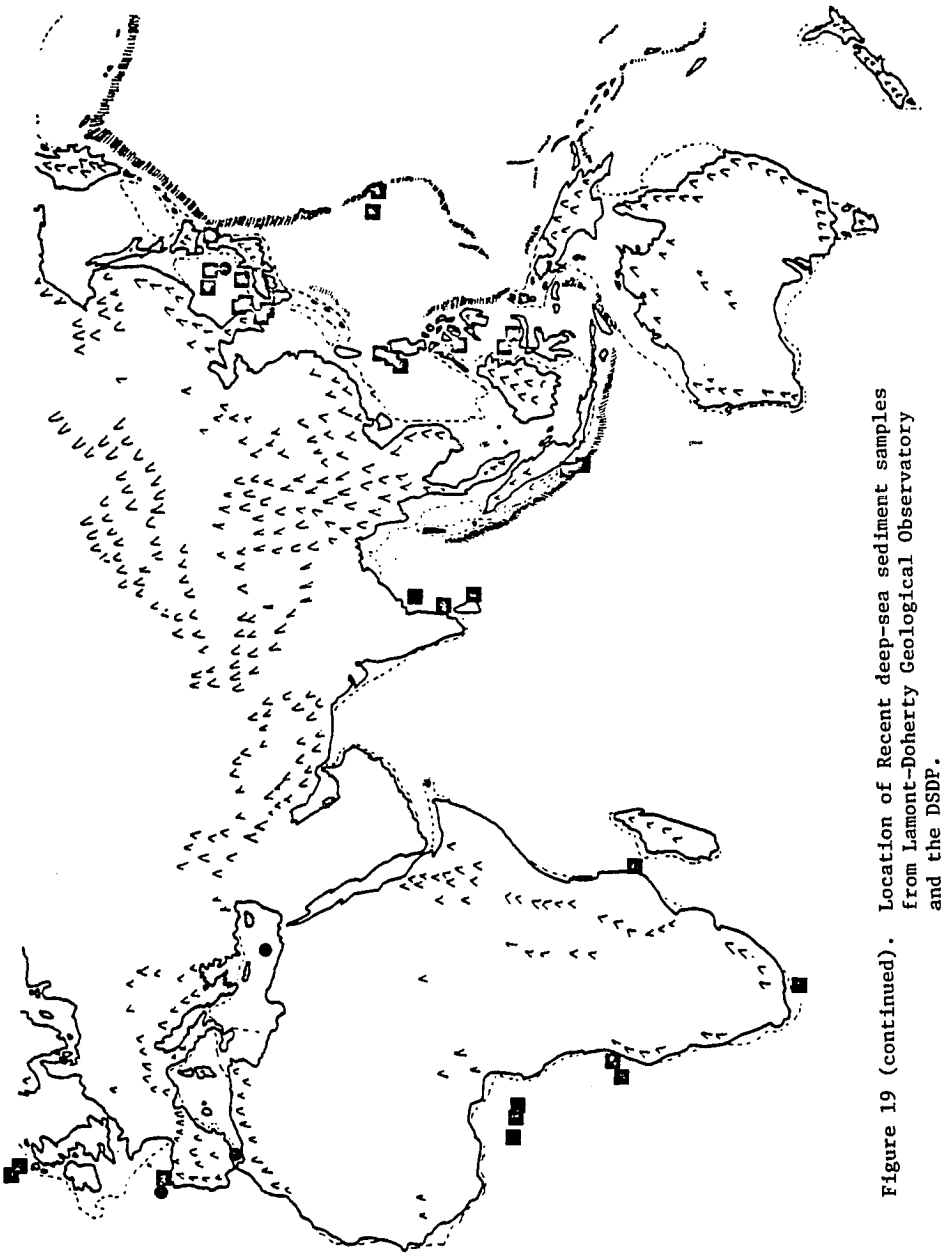

Figure 19 (continued). Location of Recent deep-sea sediment samples from Lamont-Doherty Geological Observatory and the DSDP.

TABLE 8

STRATIGRAPHIC UNIT, AGE AND LOCATIONS OF ANCIENT TURBIDITES

Stratigraphic Unit	Number of Samples	Age	Locality
Pico Formation	7	Pliocene	Ventura Basin, California
Macigno Formation	10	Early Miocene	Pievepelgo, Italy Castel di Casio, Italy
San Isidro Fm.	14	Oligocene	Punta Arenas, Chile
Sunrise Group	3	Cretaceous-Jurassic	Kenailake, Alaska
Lewes Group	4	Jurassic-Triassic	Whitehorse, Yukon Territory
Alpine Flysch	16	Mesozoic	Geneva, Switzerland
Escuminac Fm.	3	Devonian	Miguasha Ferry, Quebec
Aberstwyth Grit	15	Silurian	Wales and Prin Quarry, Scotland
Frenchville Fm.	4	Silurian	Stockholm, Maine Corners, Maine
Normanskill Fm.	4	Ordovician	Albany, New York
Utica Formation	7	Ordovician	St. Antonie, Quebec St. Nicolas, Quebec
Martinsburg Fm.	41	Ordovician	Shartleville, Pennsylvania Williamsport, Pennsylvania Lehigh Gap, Pennsylvania
Sillery Formation	9	Cambrian	St. Apollinaire, Quebec St. Romuald, Quebec

Samples were crushed with a mortar and pestle and ground to less than 200 mesh. Finely ground samples then were ignited at 1000°C about 15 minutes, mixed 1:5 with $LiBO_2$, and fused. Ignition loss was not recorded. The glass beads were dissolved with 4 percent HNO_3. The solution was further diluted with 1 percent Lanthanum Nitrate for the elements of Si, Al, Fe, Mg, and Ca. For Na and K a dilution with distilled water of 1:20 is sufficient.

USGS standard Granite, G-2, Diabase, W-1 and Andesite, AGV-1 were used for constructing the analytical curves. Selected samples with CaO content greater than 10 percent were analyzed for organic and carbonate carbon using a Perkin-Elmer 240 Elemental Analyzer. Carbonate content was determined by the difference in carbon content between whole rock samples and samples heated overnight in HCl. Thus, organic carbon and carbonate carbon can be discriminated and then the CO_2 percentage determined.

Results

One of the main purposes of this study is to compare the chemical data of Recent deep-sea samples with that of the ancient ones. However, chemical compositions of ancient flysch arenites from Crook (1974, Table 2) are presented on a volatile-free basis. Thus, for the sake of chemical comparison on a volatile-free basis, the major oxides of turbidite samples of this study are also recalculated to 100 percent. In addition, the volatile-free chemical data may minimize the interference from the carbonate cements. Recalculated bulk compositions of Recent and ancient turbidites are given in Appendix 2.

The arithmetic average chemical compositions of Recent and ancient turbidite samples are given in Table 9. Also, histograms of chief oxides of the Recent turbidite samples are given to show the ranges and scatter around the arithmetic mean (Fig. 20).

Interpretations

Chemical Compositions of Deep-Sea Sands and Provenance

The arithmetic average chemical compositions of modern deep-sea sands of this study can be compared with that of modern river sands and average ancient sandstones (Table 10). It is apparent that Recent deep-sea sands have more Al_2O_3, total iron, MgO, K_2O and Na_2O than modern river sands and ancient average sandstones. However, the SiO_2 content of deep sands is much less than that of river sands and ancient sandstones. Also, ancient average sandstones have more CaO than that of deep-sea sands probably because of their carbonate cement. This comparison suggests that modern deep-sea sands of this study are immature sands. This is confirmed by the petrographic evidence from Valloni and Maynard (in press, Sedimentology, 1979). They showed that these deep-sea sands contain more feldspars and rock fragments than Potter's (1978) river sands.

It is particularly noteworthy that the average chemical composition of modern deep-sea sands is very close to the average ancient graywacke except with higher CaO content. In addition, a ternary plot of Fe_2O_3 + MgO, K_2O and Na_2O also shows that the average modern deep-sea sands fall into the graywacke field (Fig. 21) based on the chemical

TABLE 9

AVERAGE CHEMICAL COMPOSITION OF RECENT AND ANCIENT TURBIDITE SAMPLES

	Recent Deep-Sea Sands	Recent Deep-Sea Muds	Ancient Turbidite Sandstones	Ancient Shales
SiO_2	69.74	66.90	68.07	62.17
Al_2O_3	13.40	14.26	13.85	18.31
Fe_2O_3*	4.62	6.30	4.68	6.79
MgO	2.27	3.05	2.00	2.93
CaO	4.70	5.04	6.90	4.55
K_2O	2.08	2.15	2.04	4.00
Na_2O	3.19	2.29	2.45	1.38

*Total iron expressed as Fe_2O_3

TABLE 10

AVERAGE CHEMICAL COMPOSITION OF RECENT DEEP-SEA SANDS, MODERN RIVER SANDS AND ANCIENT SANDSTONES

	Recent Deep-Sea Sands	Modern River Sands (Potter, 1978)	Average Sandstones (Clarke, 1924)	Average Graywackes (Pettijohn, 1963)
SiO_2	69.74	80.15	78.66	66.7
Al_2O_3	13.40	6.43	4.78	13.5
Fe_2O_3	4.62	2.47	1.38	5.1
MgO	2.27	0.85	1.17	2.1
CaO	4.70	3.32	5.52	2.5
K_2O	2.08	1.20	1.32	2.0
Na_2O	3.19	1.19	0.45	2.9

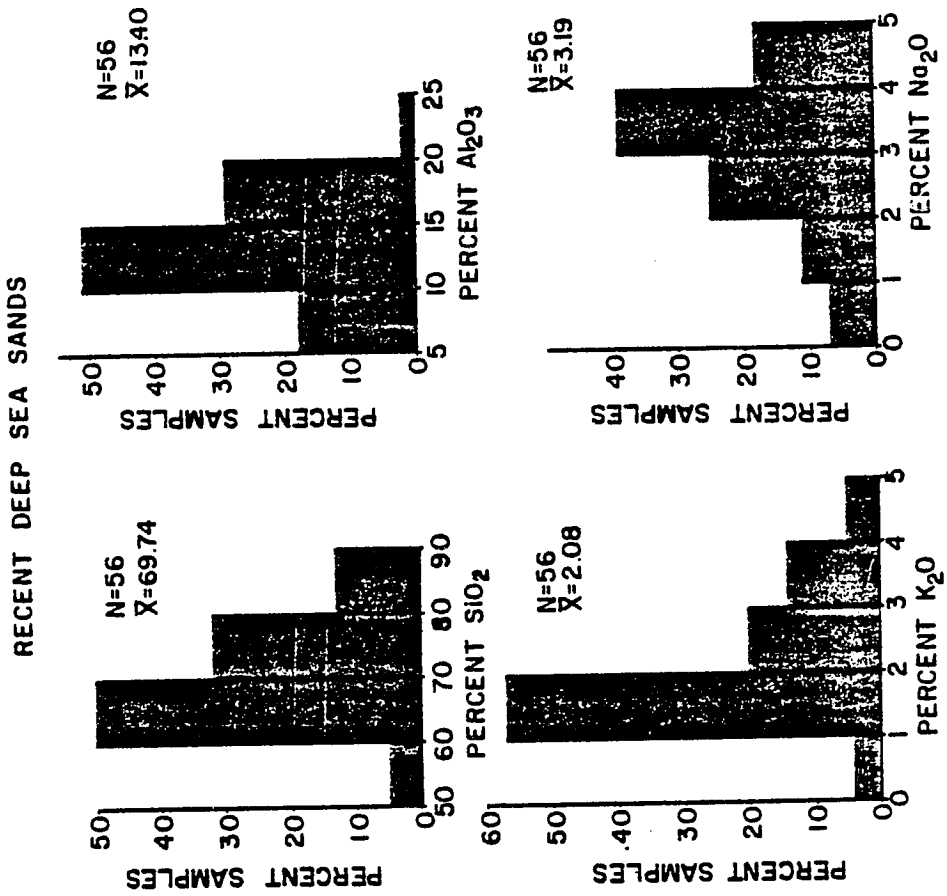

Figure 20. Histograms of major oxides of Recent and ancient turbidite samples.

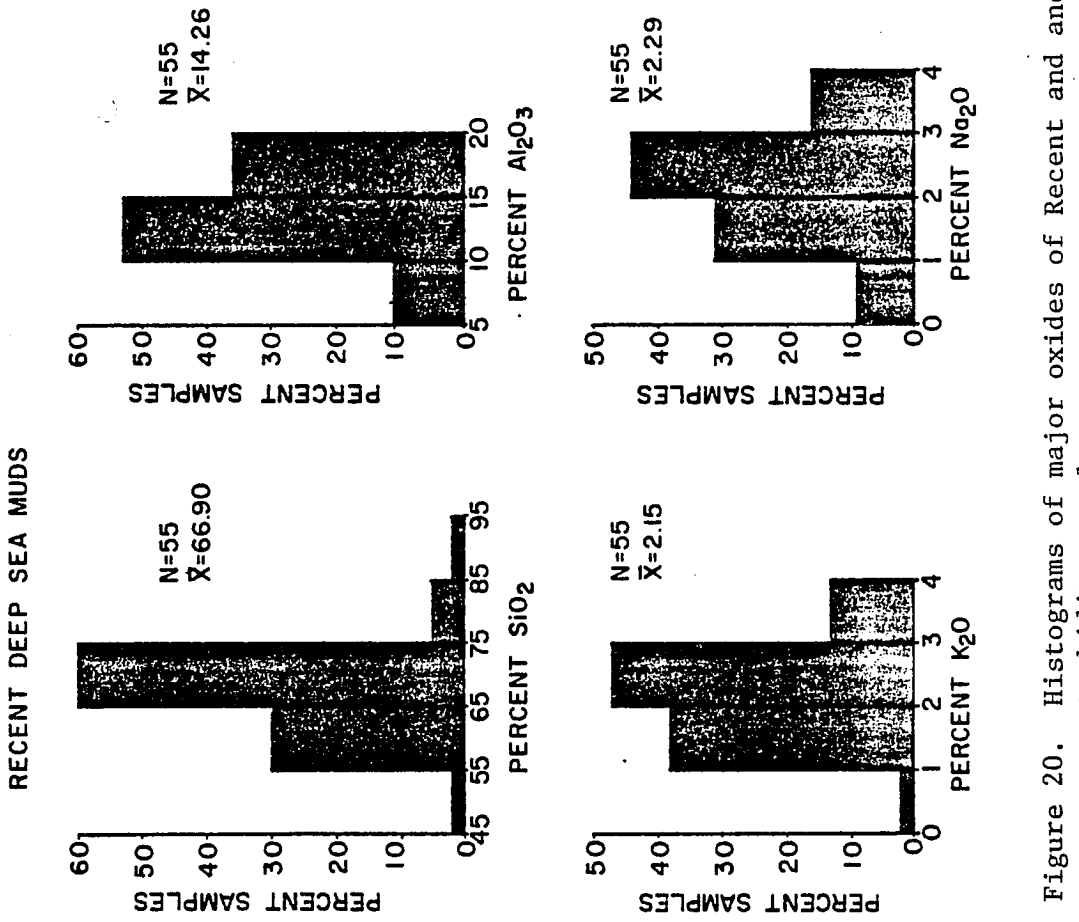

Figure 20. Histograms of major oxides of Recent and ancient turbidite samples.

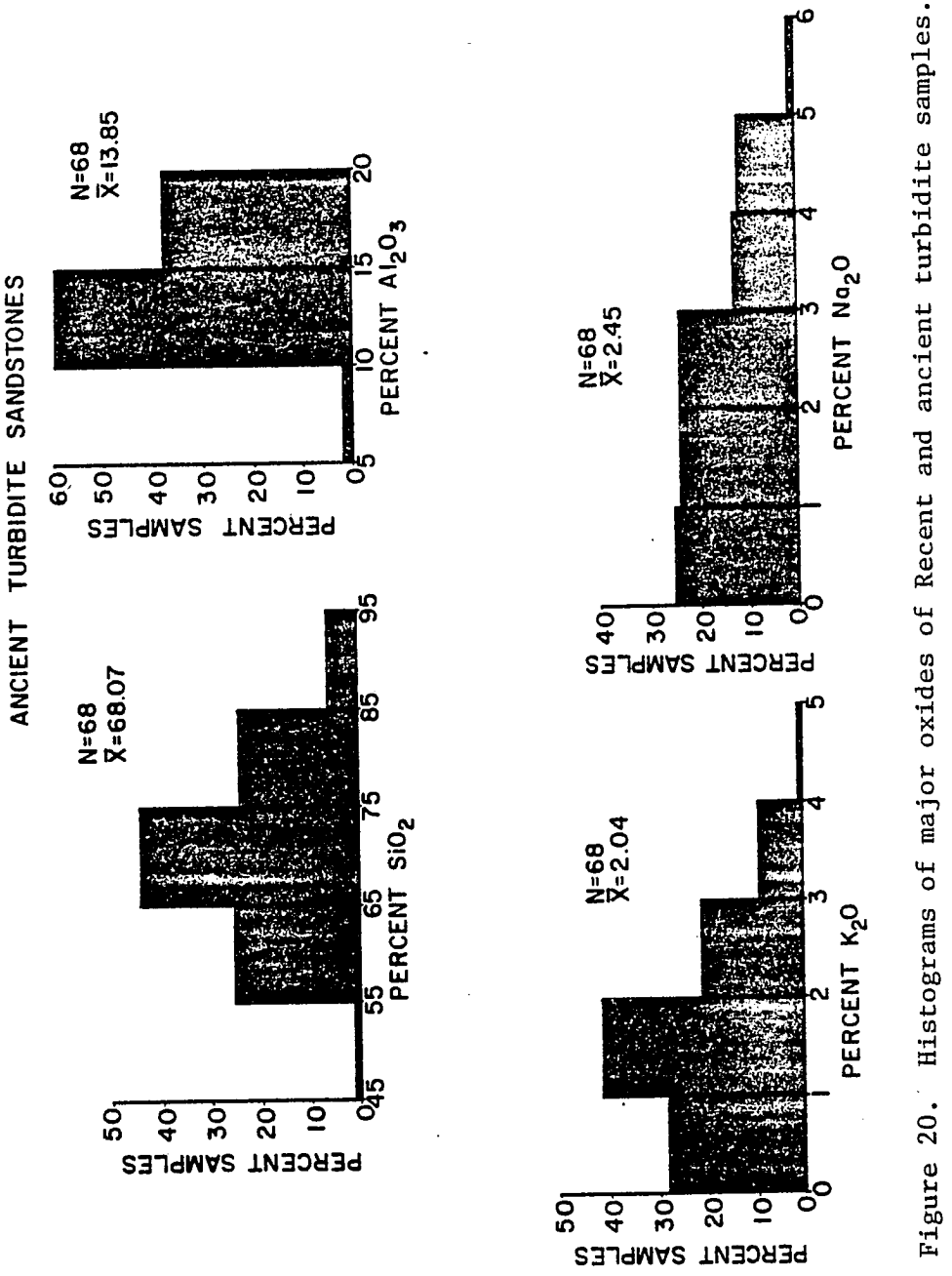

Figure 20. Histograms of major oxides of Recent and ancient turbidite samples.

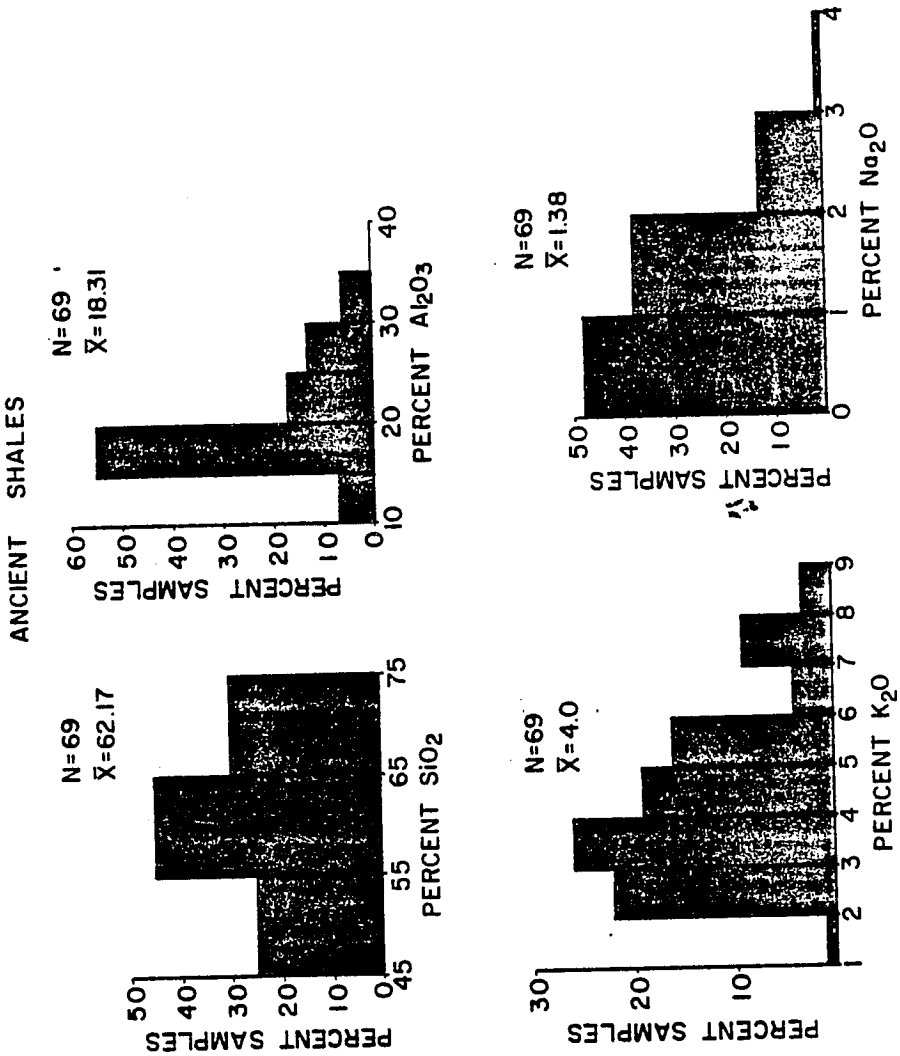

Figure 20. Histograms of major oxides of Recent and ancient turbidite samples.

classification of Blatt et al. (1972, Fig. 9-2). Thus, modern deep-sea sands and ancient graywackes seem to be very similar chemically. This significance of chemical similarity between them will be discussed later.

To explore the relationship between the chemical composition of deep-sea sands and tectonic setting, these deep-sea samples are grouped, using a four-fold plate tectonic classification of ocean basins (Table 11), into trailing edge, leading edge, back arc and fore arc basin types and then an average chemical composition for sands from each of these major basin types is calculated (Table 12).

Modern deep sea sands from trailing edges have the highest SiO_2 content and SiO_2/Al_2O_3 ratio--a chemical maturity index (Potter, 1978), and the K_2O/Na_2O ratio is slightly greater than one (Table 12). In contrast, sands from fore arc basins have the lowest SiO_2 content and SiO_2/Al_2O_3 ratio and the K_2O/Na_2O is much less than one, just as in Crook's (1974) study. Chemical variables of sands from leading edge and back arc basins are intermediate between these two extremes. However, sands from these two basins cannot be separated by chemical compositions. Clearly, modern deep-sea sands become less mature, chemically, going from stable cratonic basins to tectonically active settings, and this general trend agrees well with previous studies (cf. Table 7).

On the other hand, the range of SiO_2 content of deep-sea sands is not as great as that of Crook's ancient graywackes. The SiO_2 content of Crook's graywackes ranges from 54 to 88 percent whereas in these samples the range is 64 to 79 percent. It is also noticed that deep-sea sands

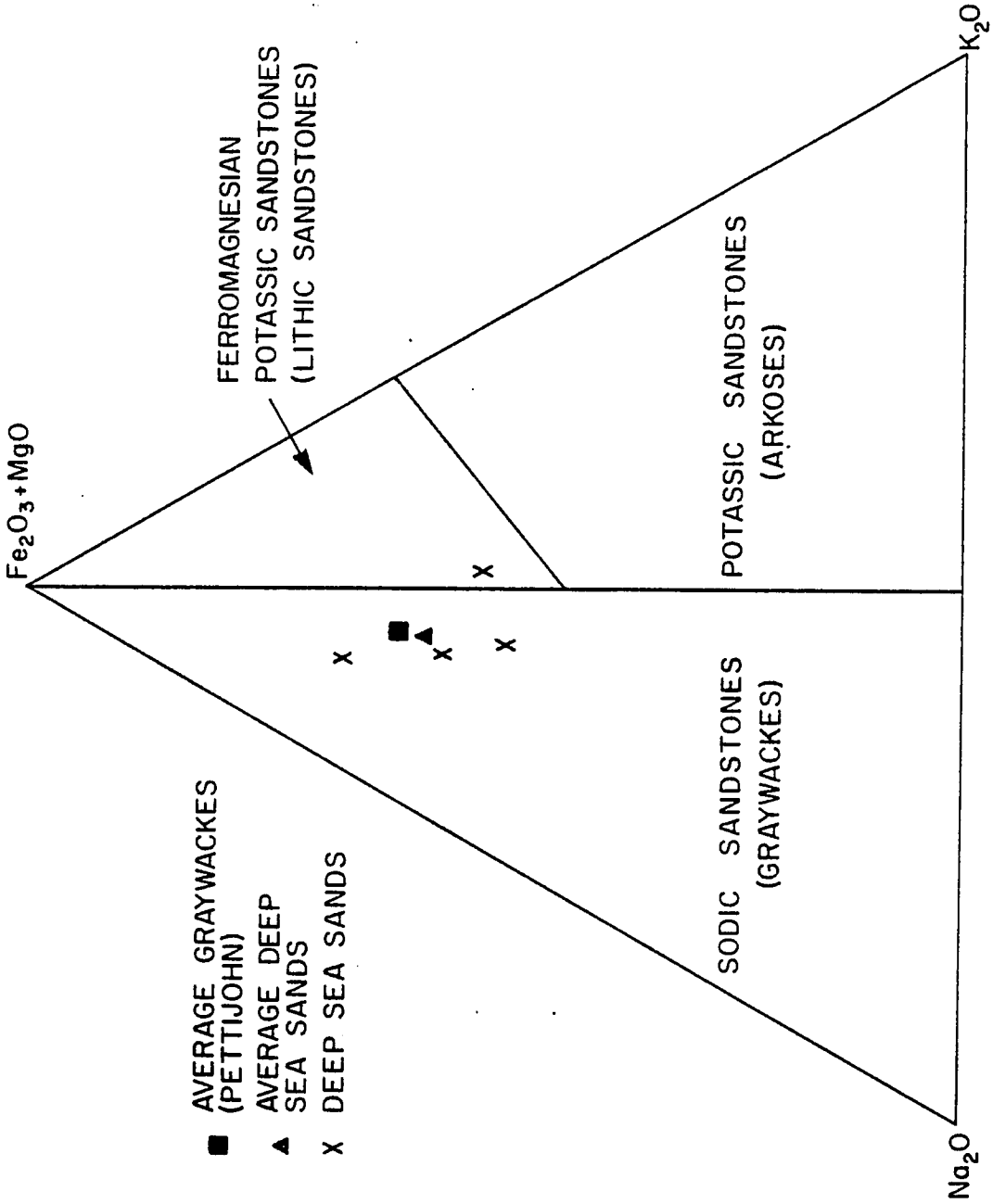

Figure 21. Chemistry of Recent deep-sea sands expressed in the Fe_2O_3+ MgO-Na_2O-K_2O system. Notice that average deep-sea sands fall into the graywacke field.

TABLE 11

FIRST-ORDER PLATE TECTONIC
SUBDIVISION OF OCEAN BASINS

Name Abbreviation	Definition	Example
Trailing Edge (TE)	Passive, intraplate continental margin facing a spreading center	Atlantic Coast, South America
Leading Edge (LE)	Active, plate boundary continental margin over-riding oceanic crust	Pacific Coast, South America
Back Arc (BA)	Continent side of island arc	Sea of Japan, Bering Sea
Fore Arc (FA)	Ocean side of island arc	Western North Pacific

TABLE 12

AVERAGE CHEMICAL COMPOSITION OF DEEP-SEA SANDS FROM VARIOUS TECTONIC SETTINGS

Basin	No. of Samples	SiO_2	Al_2O_3	Fe_2O_3	MgO	CaO	K_2O	Na_2O	SiO_2/Al_2O_3	K_2O/Na_2O
Trailing Edge	17	78.87	9.66	2.72	1.22	3.76	1.98	1.78	8.16	1.11
Leading Edge	9	68.11	15.10	4.09	1.91	4.38	2.56	3.85	4.51	0.66
Back Arc	21	68.29	14.15	4.81	2.49	4.64	2.09	3.47	4.83	0.60
Fore Arc	9	63.68	14.67	6.85	3.44	6.02	1.68	3.64	4.34	0.46

of this study do not separate into the quartz-rich (> 65%), quartz-intermediate (15-65%) and quartz-poor (< 15%) varieties of Crook's graywackes (see Valloni and Maynard, in press). Thus, although SiO_2 in these samples is in general in agreement with literature data on tectonics and sandstone composition, there are some discrepancies. Further chemical variables only differentiate three tectonic sand types: passive continental margin, active continental margin (including back arc basins) and fore arc basins. Fore arc sandstones are probably rare in ancient rocks exposed on the continents, so in practice there may only be two categories that can be identified by chemistry.

The K_2O/Na_2O ratio of modern river sands (Potter, 1978) from trailing edges is almost twice as large as that of deep-sea sands because the former are more mature. In addition, the SiO_2/Al_2O_3 ratio shows a distinctly higher value for the modern river sands from trailing edges than the deep-sea sands from the same settings. Therefore, a discrepancy in the chemical indices between deep-sea sands and modern river sands exists suggesting a difference in the nature of these two sands. However, these two sands from the trailing edges do have the highest SiO_2 content and the ratios of SiO_2/Al_2O_3 and K_2O/Na_2O.

In sum, modern deep sea sands show two distinct contrasts between passive and active basin types. The passive basin type is characterized by 79 percent average SiO_2, a value somewhat less than for Crook's graywackes and modern river sands from the same setting. Further, these sands have an SiO_2/Al_2O_3 ratio of 8 and a K_2O/Na_2O ratio of 1.1, whereas active margin sands have typical values of SiO_2 less than 70 percent,

SiO_2/Al_2O_3 ratios around 4.5 and K_2O/Na_2O ratios about 0.6. Moreover, the percent SiO_2, plus SiO_2/Al_2O_3 and K_2O/Na_2O ratios show a general trend decreasing from trailing edge to fore arc basin. Unfortunately, there still exist some overlaps between chemical criteria. Thus, it is necessary to be careful in using chemical compositions to assign a sandstone to the tectonic setting.

Chemical Compositions of Deep Sea Muds and Provenance

There seems to be a close resemblance of major oxides between modern deep-sea muds associated with turbidites, average shales, slates and mudrocks (Table 13). However, modern dep-sea muds have more SiO_2 and less Al_2O_3 than do the average shales, slates and mudrocks. Apparently, these deep-sea muds contain more silt than the average shale, judging from the statement of Pettijohn (1975, p. 271) that chemical compositions of shales depend on grain size, e.g., the coarser fraction is richer in SiO_2 whereas finer materials are richer in Al_2O_3. Unexpectedly, soda slightly exceeds potash in the deep-sea muds. This unusual feature is possibly due to volcanic admixtures.

Although information about the relation between the chemical composition and provenance of muds is fragmental and the reliability of chemical variables as indicators of provenance of shales still remains controversial, it is interesting to see how the chemistry of modern deep-sea muds responds to tectonic influences. Similarly to the deep-sea sands, individual chemical analyses of deep sea muds are grouped into trailing edge, leading edge, back arc and fore arc basin types (Table 14). Deep

TABLE 13

AVERAGE CHEMICAL COMPOSITION OF MODERN DEEP-SEA MUDS AND RELATED AVERAGE SHALES, SLATES AND MUDSTONES

	Modern Deep Sea Muds	Clarke (1924) Shales	Shaw (1956) Shales	Pettijohn (1975) Slates	Ronov et al. (1966) Mudstones	
					Plat.	Geosyn.
SiO_2	66.90	58.10	61.54	58.5	56.2	53.4
Al_2O_3	14.26	15.40	16.95	17.3	15.1	16.4
Fe_2O_3	6.30	6.47	6.26	7.4	5.7	6.2
MgO	3.05	2.44	2.52	2.6	2.1	2.4
CaO	5.04	3.11	1.76	1.3	4.4	5.8
K_2O	2.15	3.24	3.45	3.7	1.1	1.1
Na_2O	2.29	1.30	1.84	1.2	2.6	2.7

TABLE 14

AVERAGE CHEMICAL COMPOSITION OF DEEP-SEA MUDS FROM VARIOUS TECTONIC SETTINGS

Basin	No. of Samples	SiO_2	Al_2O_3	Fe_2O_3	MgO	CaO	K_2O	Na_2O	M*	K_2O/Na_2O
Trailing Edge	21	65.31	13.58	5.51	2.77	8.75	2.45	1.59	3.68	1.54
Leading Edge	8	65.31	15.89	6.68	3.37	3.88	2.22	2.64	3.01	0.84
Back Arc	8	68.13	14.54	6.47	3.11	3.11	2.14	2.51	2.97	0.85
Fore Arc	18	68.86	13.04	6.52	2.95	4.42	1.77	2.43	2.75	0.73

*$M = \frac{Al_2O_3 + K_2O}{MgO + Na_2O}$ (Björlykke, 1974, p. 263)

sea muds of each of these basin types show no systematic variation in oxides of Si, Al, Fe, Mg, and Ca, but K and Na do show a pattern: the K_2O/Na_2O ratio decreases noticeably from passive to active tectonic settings. Bjorlykke (1974, p. 263) has demonstrated that the ratio of $Al_2O_3 + K_2O/MgO + Na_2O$ is a good provenance indicator for shales, using it to demonstrate an island arc provenance within the 1000 m thick Paleozoic seqnence in the Oslo, Norway, region. This ratio was computed for my deep-sea muds (Table 14), but because Al and Mg are essentially constant, the $Al_2O_3 + K_2O/MgO + Na_2O$ ratio simply parallel to the pattern of K_2O/Na_2O. Obviously, active and passive margins can be distinguished by these two ratios. Further, these two ratios cannot separate back arc basins from leading edges, just as was found for sand chemistry. Thus, the K_2O/Na_2O is as reliable as Bjorlykke's ratio.

Chemical Composition of Ancient Turbidite Sands and Provenance

Chemical analyses of some ancient turbidite sandstones from various stratigraphic units ranging in age from Cambrian to Pliocene have been made for comparison with the modern sands (Table 15). Chemically classified, using method of Blatt et al. (1972), almost two thirds of ancient turbidite sandstones fall into the graywacke field. One sample (Pico Fm.) falls in the arkose field, and the remaining samples are in the lithic sandstones field. However, the average of these turbidite samples falls into the graywacke field and resembles very closely the composition of the modern deep-sea sands and average graywacke (Fig. 22).

In fact, from the similarity of chemistry between Recent and ancient turbidite sands and average graywackes, it may be inferred that if low matrix modern deep-sea sands were to undergo burial diagenesis or low-grade metamorphism and be converted to matrix-rich graywackes, then the diagenetic clay matrix is a result of transformation of reactive grains within the sandstones rather than the introduction of material. In other words, the diagenetic reactions of graywackes occur in a closed system. The high Na_2O content of many ancient graywackes would then be inherited from the source area, rather than introduced by diagenesis.

It is also noticed that the average chemical composition of Crook's ancient graywackes are close to those of the Recent and ancient turbidite sandstones of this study and average graywackes, although Crook's have more MgO and less K_2O than the others because his samples include serpentine graywackes which are rich in magnesium (Table 15 and Fig. 22). This chemical comparison suggests that modern deep-sea sands can be regarded as the contemporary analogues of ancient graywackes and then the chemical criteria determined in Table 12 for identifying the tectonic settings of modern sands are applicable to ancient graywackes.

Based on the chemical criteria such as SiO_2 content, SiO_2/Al_2O_3 and K_2O/Na_2O ratios, more than three fourths of the ancient turbidite sandstones of this study belong to active tectonic settings, the remaining samples belong to passive (Table 16). Of these chemical parameters, SiO_2 content combined with SiO_2/Al_2O_3 ratio seems to be the best indicator of tectonic setting. Turbidite samples assigned to active

TABLE 15

AVERAGE CHEMICAL COMPOSITION OF ANCIENT TURBIDITE SANDSTONES, RECENT DEEP-SEA SANDS AND AVERAGE GRAYWACKES

	Ancient Turbidite Sandstones	Recent Deep Sea Sands	Average Graywackes (Pettijohn)	Average Graywackes (Crook)
SiO_2	68.07	69.74	66.7	66.26
Al_2O_3	13.85	13.40	13.5	13.43
Fe_2O_3	4.68	4.62	5.1	5.41
MgO	2.00	2.27	2.1	7.27
CaO	6.90	4.70	2.5	2.48
K_2O	2.40	2.08	2.0	1.08
Na_2O	2.45	3.19	2.9	3.19

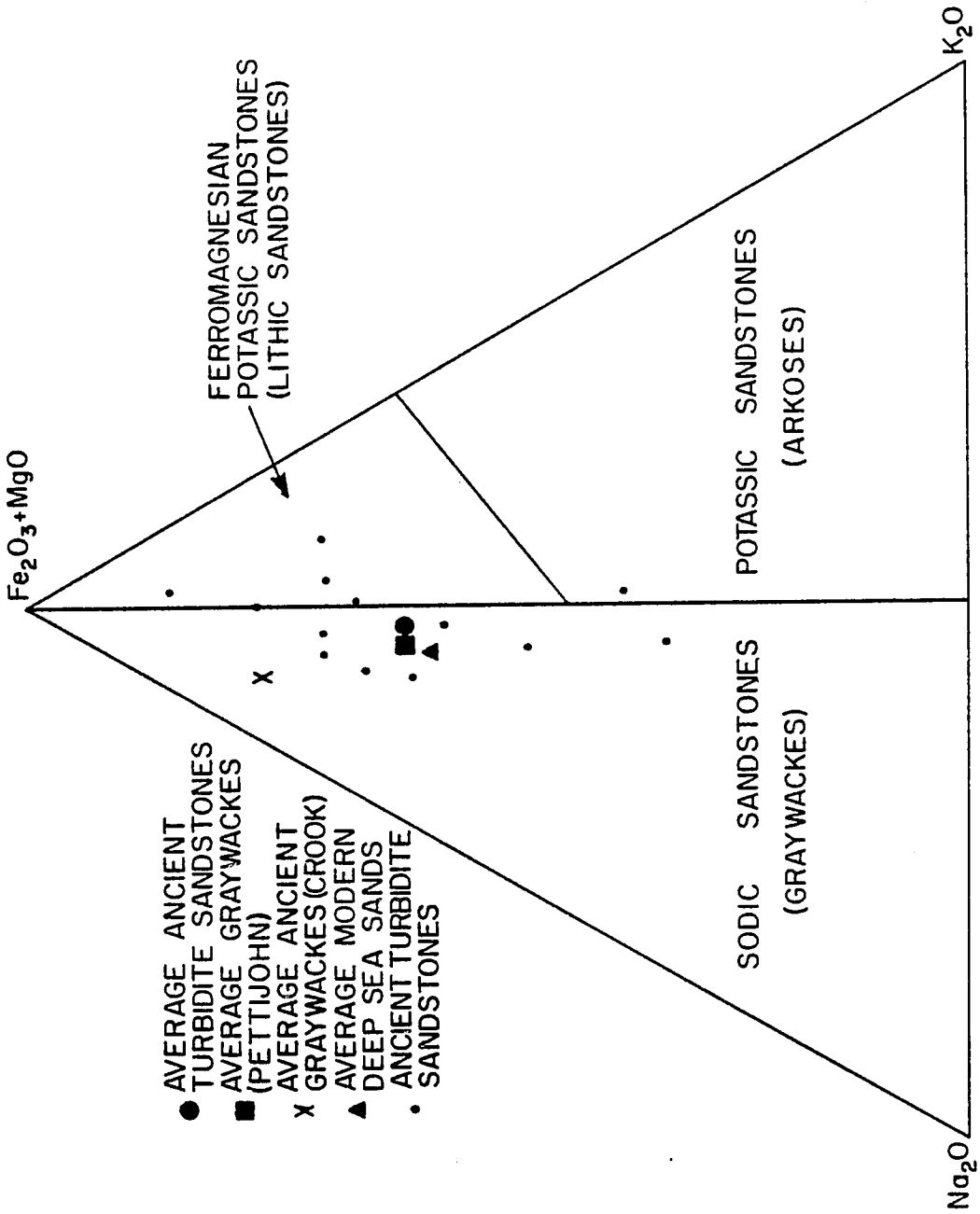

Figure 22. Chemistry of ancient turbidite sandstones expressed in the Fe_2O_3 + MgO–Na_2O–K_2O system. Notice that average turbidite sandstone also falls into the graywacke field.

tectonic settings have typical SiO_2 content less than 70 percent and a SiO_2/Al_2O_3 ratio around 4.5. K_2O/Na_2O ratio is equal to or less than one, whereas samples grouped into passive tectonic settings are characterized by SiO_2 content greater than 70 percent and a SiO_2/Al_2O_3 ratio about 7.0; K_2O/Na_2O ratio is greater than one. Inferred tectonic settings based on the literature of these ancient turbidite sandstones are also shown in Table 16. It is clear that inferred tectonic settings match quite well with that based on the chemical composition, except for the Martinsburg samples, for which I have no explanation. Therefore, chemical variables such as SiO_2 content and ratios of SiO_2/Al_2O_3 and K_2O/Na_2O seem to generally be reliable indicators of provenance for ancient turbidite sandstones, but they can only distinguish active and passive tectonic settings. It should be pointed out that these conclusions are limited by the fact that only one sample (Escuminac Fm.) happened to be from a passive tectonic setting. Hence, more data from passive margin sands are needed to support the conclusions above, although Crook's more extensive sampling is, in general, consistent with these observations.

Chemical Composition of Ancient Shales and K_2O Trend

Chemical analyses of ancient shales associated with turbidite sandstones from various stratigraphic units ranging in age from Cambrian to Pliocene show that major oxides are similar to those of average shales, slates and mudrocks (Table 17). However, there does seem to be a trend of increasing K_2O content with increasing geologic age (Fig. 23). Recent

TABLE 16

AVERAGE CHEMICAL COMPOSITION OF ANCIENT TURBIDITE SANDSTONES
AND THEIR CORRESPONDING TECTONIC SETTINGS

Stratigraphic Unit	No. of Samples	SiO_2	Al_2O_3	Fe_2O_3	MgO	CaO	K_2O	Na_2O	SiO_2/Al_2O_3	K_2O/Na_2O	Tectonic Setting From Composition	Tectonic Setting Inferred
Pico Fm.	3	66.57	14.99	2.62	0.88	8.84	3.14	2.94	4.44	1.07	Active	Active
Macigno Fm.	3	64.72	14.92	3.19	2.41	10.95	2.10	2.39	4.53	0.88	Active	Active
San Isidro Fm.	14	66.16	16.37	6.47	2.70	3.20	1.73	3.40	4.04	0.51	Active	Active
Lewes Group	4	63.99	15.47	5.75	2.67	6.28	2.00	3.79	4.14	0.53	Active	Active
Alpine Flysch	7	64.43	13.73	3.35	3.33	12.24	1.28	1.74	4.69	0.73	Active	Active
Escuminac Fm.	1	68.32	10.46	4.13	2.00	12.30	1.98	0.77	6.53	2.57	Passive	Passive
Aberystwyth Grit[1]	3	67.25	14.99	5.35	2.18	1.67	3.61	4.91	4.49	0.73	Active	Active
Aberystwyth Grit[2]	3	71.78	15.02	6.70	1.80	2.03	1.35	1.41	4.78	0.96	Active	Active
Frenchville Fm.	1	57.06	11.85	2.70	1.15	19.27	3.57	4.39	4.82	0.81	Active	Active
Utica Fm.	4	69.12	14.95	4.51	2.15	5.72	1.84	1.70	4.62	1.08	Active	Active
Martinsburg Fm.[3]	4	73.47	11.31	5.80	1.71	4.11	2.06	1.51	6.50	1.36	Passive	Active
Martinsburg Fm.[4]	16	82.96	11.44	3.93	0.63	0.29	0.48	0.30	7.25	1.60	Passive	Active
Sillery Fm.	5	69.05	15.18	6.36	2.48	2.84	1.43	2.63	4.55	0.54	Active	Active

[1]Pirn Quarry, Scotland
[2]Wales
[3]Williamsport, Pa.
[4]Lehigh Gap, Pa.

TABLE 17

AVERAGE CHEMICAL COMPOSITION OF ANCIENT SHALES ASSOCIATED WITH TURBIDITE SANDSTONE

Stratigraphic Unit	No. of Samples	SiO_2	Al_2O_3	Fe_2O_3	MgO	CaO	K_2O	Na_2O	K_2O/Na_2O
Pico Fm.	4	67.52	15.94	5.47	2.51	3.11	2.92	2.54	1.15
Macigno Fm.	7	56.30	15.87	5.29	4.51	13.39	2.94	1.45	2.03
Sunrise Group	3	63.86	18.24	8.43	2.28	2.13	3.22	1.86	1.73
Alpine Flysch	9	56.91	16.17	5.82	3.17	14.25	2.67	1.00	2.67
Escuminac Fm.	2	68.06	16.30	6.86	3.06	3.72	3.06	0.94	3.29
Aberstwyth Grit[a]	2	67.73	15.74	5.43	3.23	1.20	3.97	2.65	1.50
Aberstwyth Grit[b]	7	66.72	17.44	7.22	2.02	1.25	4.19	1.29	3.25
Frenchville Fm.	3	65.72	12.51	5.80	3.12	8.01	3.07	1.77	1.73
Normanskill Fm.	4	56.87	19.57	8.00	3.66	7.14	4.09	0.71	5.76
Utica Fm.	3	63.29	16.82	6.41	4.37	3.31	4.72	1.06	4.45
Martinsburg Fm.[c]	4	61.93	21.78	7.53	2.07	0.66	5.22	0.82	6.36
Martinsburg Fm.[d]	17	58.72	25.87	6.26	1.66	0.36	6.51	0.53	12.28
Sillery Fm.	4	54.64	25.79	9.74	2.44	0.64	5.42	1.37	3.95

[a] Pirn Quarry, Scotland
[b] Wales
[c] Williamsport, Pennsylvania
[d] Lehigh Gap, Pennsylvania

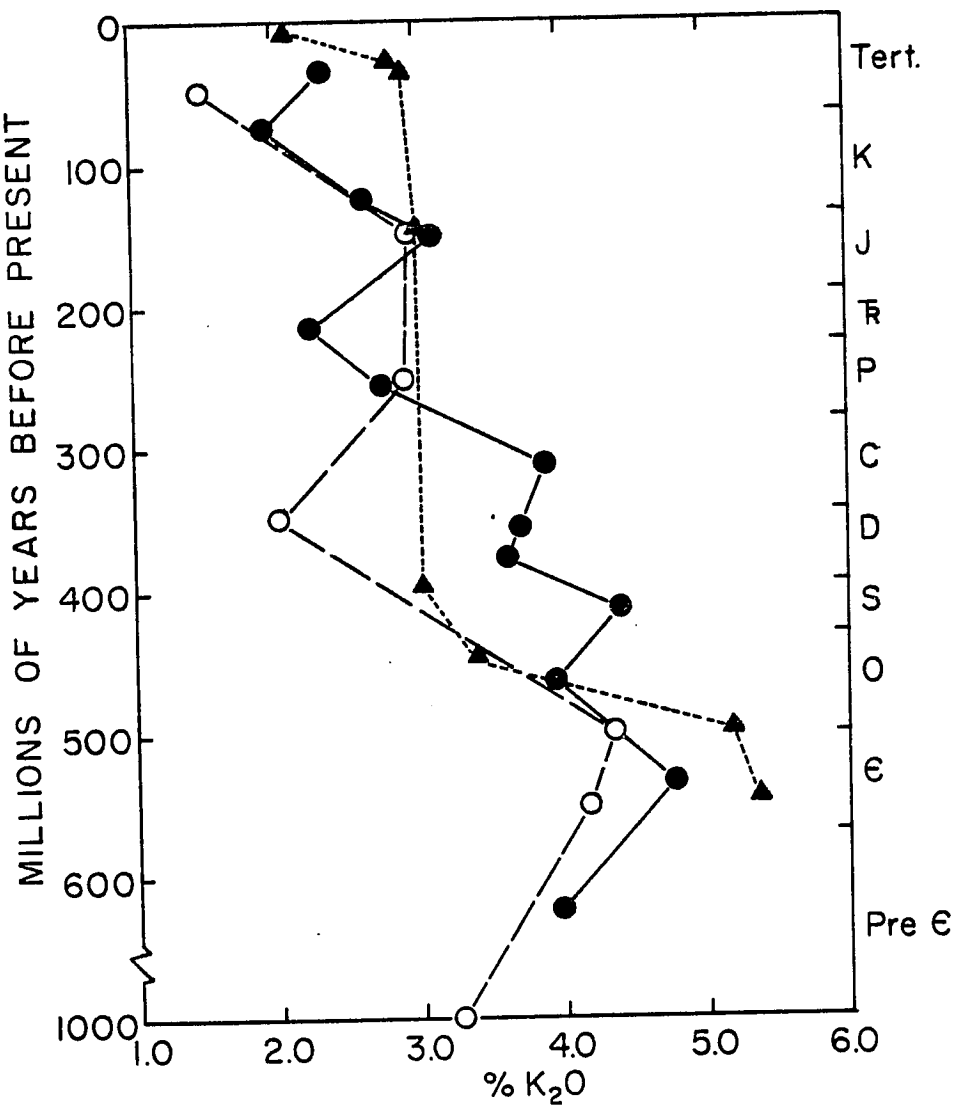

Figure 23. K_2O content in shales increases with increasing geologic age (modified after Vinogradov and Ronov, 1956, Fig. 2 and Van Moort, 1972, Table 1).

deep-sea muds have the lowest K_2O content (2.15%) and then the K_2O content increases slightly from 2.5 percent to 3.0 percent by Devonian time. There seems to be an abrupt increase of K_2O content in the Devonian, the K_2O percent increasing greatly from 3.0 to the maximal 5.4 percent in the Cambrian shales. This K_2O trend in shales with age has also been reported in clays and shales of the Russian and North America platform (Vinogradov and Ronov, 1956 and Ronov and Migdisov, 1971) and shales from Australia (Van Moort, 1972) (see Figure 23).

Vinogradov and Ronov (1956) and Ronov and Migdisov (1971) claimed that there was a greater exposure of potassium-rich crystalline rocks in earlier geologic ages. As a result of weathering of these rocks, illite was the dominant clay mineral in weathering products. K-feldspar and mica are the source of potassium for the formation of illite. Thus, high K_2O sediments accumulate and this may account for such a K_2O trend in shales. It is also noticed that the K_2O trend of shales of the Russian and North American platform are reflected in mineralogic difference (Weaver, 1967, Fig. 2). Based on over 5,000 analyses of shaly rocks from North America, Weaver showed that Paleozoic shales are approximately 90 percent illite and chlorite but Meso-Cenozoic shales have a complex clay assemblage with montmorillonite, mixed layer clays and kaolinite. Furthermore, he emphasized that there exist abrupt changes both of clay mineral suite and K_2O content at the end of the Paleozoic. These changes he interpreted as a result of rapid development of plant life and an increase in soil acidity on the continents during Devonian time, which accounts for the increase of kaolinite and montmorillonite at the

expense of illite. Hence, data of clay mineralogy of North American shaly rocks strongly suggest that the K_2O trend in shales is caused by a major change in the nature of source area. In other words, the K_2O trend in shales is mainly of detrital origin.

On the other hand, Van Moort (1972) suggested that the enrichment of K_2O in Paleozoic shales results from the introduction of potassium from altering sandstones, especially from volcanogenic sediments within the sedimentary piles, because of the lower abundance of volcanic clastics in the ancient sediments. In addition, Mackenzie (1975) suggested that chemical trends in shales are secondary and result from loss of Cao and MgO during burial and uplift and from long-term diagenesis, e.g., montmorillonite-rich mixed-layer clays take up potassium to form illite-rich mixed-layer clays or illite. In other words, Van Moort and Mackenzie favored a secondary origin for the K_2O trend in shales.

However, it is generally accepted that the progressive increase in K_2O content in shales with geologic time reflects the prevalence of illite in the older shales. The illite may be inherent or formed by diagenetic reactions. Recently, Hower et al. (1976) provided some clues for the prevalence of illite in the Paleozoic shales. Based on the observation that the mixed-layer illite/smectite in deeply buried Gulf Coast argillaceous sediments undergo a conversion of from less than 20 percent to about 80 percent illite layers with increasing depth. Hower et al. (1976, p. 725) suggested that "compositional changes in the shale as a function of metamorphic grade closely parallel compositional changes in shales as a function of geologic age." They also suggested that K^+

of illite comes from the destruction of K-feldspar and detrital micas(?) within the shale based on the observation that the whole rock potassium content remained relatively constant with depth. In other words, the shale acts as a closed system with respect to potassium. Hence, data of clay mineralogy and chemistry of Gulf Coast shales also suggest that the K_2O content in shales reflects the source area. Thus, the K_2O trend in shales of this study, which shows an abrupt decrease of K_2O after the Devonian, might be interpreted as supporting Weaver's idea. Hence, the K_2O trend in shales would be primary in origin.

According to Van Moort's hypothesis, however, the enrichment of K_2O in shales of this study would be a result of the introduction of potassium from dissolution of K-feldspar in the interbedded turbidite sandstones. Moreover, this argument could be related to graywacke diagenesis. Garrels et al. (1971, p. 93) suggested that the high K_2O in shales interbedded with turbidite graywackes is a diagenetic feature. They suggested that potassium is incorporated into the shales resulting in the formation of illite at the expense of montmorillonite and mixed-layer clays, whereas sodium released from the shales ends up forming albite in the sands. This postulated diagenetic hypothesis has been used to explain the high K_2O/Na_2O ratios of shales associated with turbidite graywackes (Pettijohn et al., 1972, Fig. 6-21).

In order to compare the K_2O and Na_2O content of shales and associated sandstones with that of other ancient turbidite graywackes and interbedded shales, the K_2O and Na_2O content of these turbidite samples are plotted in a similar manner to Figure 6-21 of Pettijohn et al., 1972

(Fig. 24). With no exception, all the ancient shales of this study have K_2O/Na_2O ratios greater than one. Only modern deep-sea muds from active tectonic settings have K_2O/Na_2O ratios smaller than one. Thus, the plot of K_2O/Na_2O of these turbidite shale samples is quite similar to that of other ancient shales associated with graywackes and this means that the K_2O/Na_2O ratios of the turbidite samples could be explained by the model suggested by Garrel et al. (1971). In other words, data on the K_2O and Na_2O content of the turbidite samples are also consistent with the argument of Van Moort (1972), i.e., the sandstones associated with shales is the source for potassium. The K_2O trend in shales of this study, therefore, may be interpreted as diagenetic in origin. If so, it is necessary to explain the lack of evidence that the interbedded sandstones are the source for potassium and also to account for the results of other studies such as Hower et al. (1976) and Heling (1978) that show shales act as a closed system with respect to potassium during burial diagenesis. Because of this difficulty, the writer suggests that a primary rather than a diagenetic origin of the excess K_2O in older shales is more likely.

It is also noticed that there is a trend of increasing K_2O/Na_2O ratio with increasing geologic age in the shales, although there are irregularities from the Silurian and Ordovician samples (Fig. 25). This shows that the K_2O/Na_2O ratio is better correlated with geologic age than tectonic setting. Thus, if the K_2O/Na_2O ratio is to be used as a provenance indicator for ancient shales, only shales of the same age should be compared.

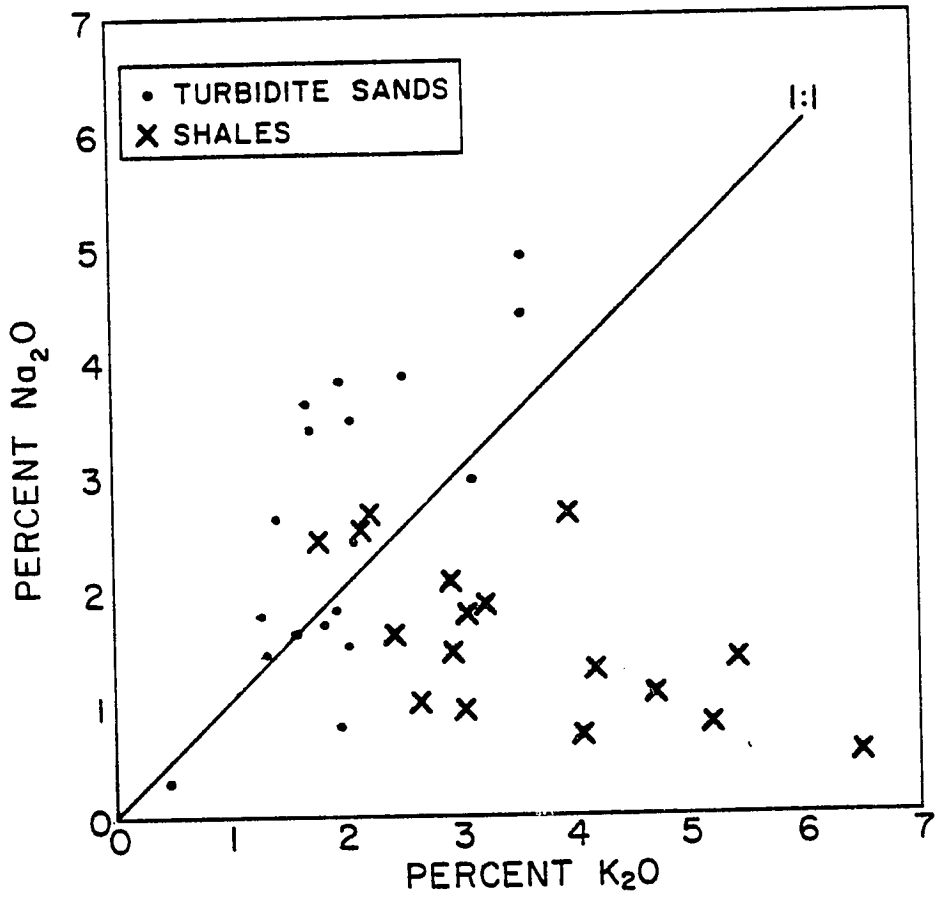

Figure 24. Na_2O/K_2O content of turbidite sands and associated shales.

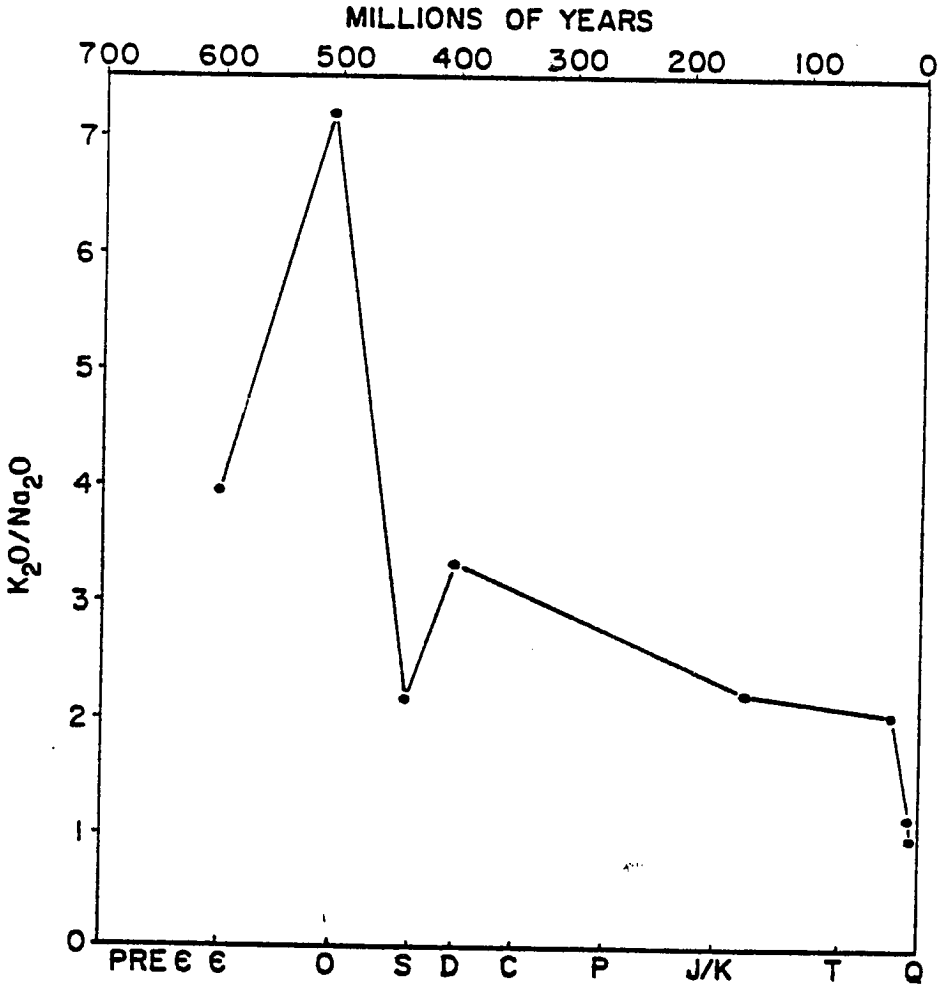

Figure 25. K_2O/Na_2O ratio of shale samples as a function of geologic age.

Conclusions

Chemical comparison between Recent deep-sea sands, modern big river sands and ancient flysch arenites suggests that chemical variables such as SiO_2 content and ratios of SiO_2/Al_2O_3 and K_2O/Na_2O seem to generally be reliable indicators of provenance for ancient turbidite sandstones, but they can only distinguish between active and passive continental margins and fore arc basins. Back arc basins and leading edge continental margins cannot be separated.

Chemical similarity between Recent deep-sea sands, ancient turbidite sandstones and average graywackes (Pettijohn, 1963) suggests that the diagenetic reactions of graywackes occur in a closed system, e.g., there is no K^+-Na^+ ion exchange between the turbidite graywackes and interbedded shales. The K_2O trend in the ancient shales, which shows an abrupt decrease of K_2O content after the Devonian, is probably primary in origin. These two arguments above suggest that the high Na_2O content of many turbidite graywackes and high K_2O content of the associated shales are not post-depositional features, as has been suggested.

Further, if this chemistry is primary, it suggests that the chemical criteria for distinguishing tectonic environments in modern sediments can indeed be applied to ancient sandstones.

CHAPTER IV

SUMMARY AND SUGGESTIONS FOR FUTURE WORK

Part A: Cratonic Sandstones from the Alberta and Saskatchewan Basins

The relationships among the grain packing, porosity, depth, composition and texture and the effects of compaction and cementation on these variables in the sandstones of the Lower Mannville in Alberta basin are summarized in a flow chart (Fig. 26). This interpretation emphasizes mechanical compaction and grain packing due to burial depth as the major control on general porosity distribution in the sandstones of Lower Mannville. A number of relevant questions for future workers can be raised, however, about this conclusion.

First, do sandy units that extend downdip in undeformed basins generally have porosity-grain packing relationships like that of the Lower Mannville?

Secondly, how common are the two transition zones of contact types? For example, are they common enough to be helpful in estimating depth of burial of sandstone sequences in undeformed basins? Or, if they are not the rule, what conditions are needed to produce them?

Certainly, a comparatively small number of additional grain packing-porosity studies in well selected basins would answer the above questions, especially if they could be made on studies from deep wells.

The Athabasca Formation in the Saskatchewan basin provides an interesting comparison. Clearly, the relationship between grain packing and porosity with depth in the sandstones of the Athabasca is not quite

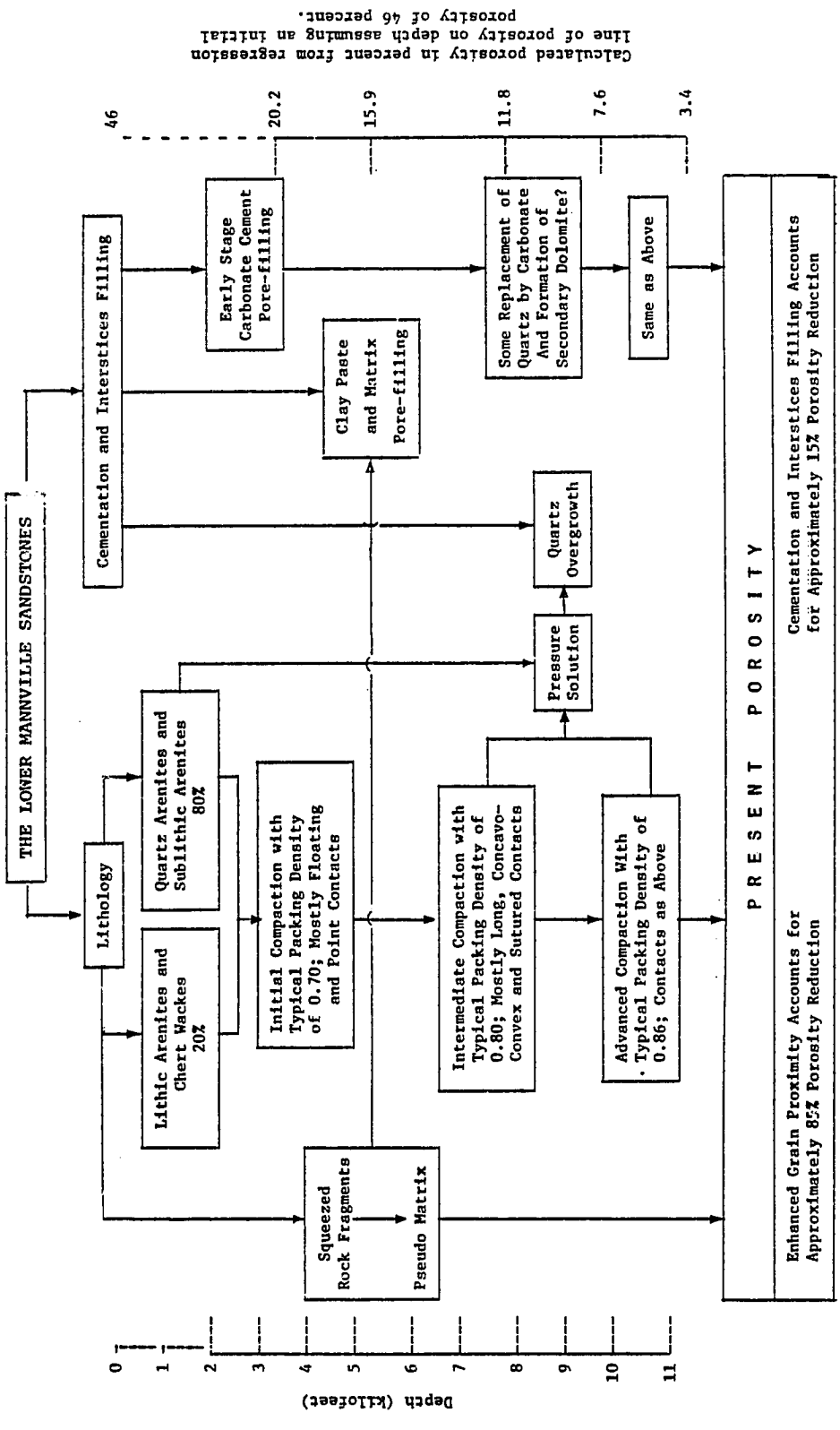

Figure 26. Flow diagram showing the interrelationships between depth, grain packing, porosity, texture and composition of the sandstones of the Lower Mannville Group.

like that of the Lower Mannville because the effect of compaction is obscured by cementation processes. However, the use of grain contact types and paragenesis of cements to estimate the depth of burial is demonstrated by the sandstones of the Athabasca.

Part B: Recent and Ancient Turbidites

The relationship between the chemical variables and tectonic setting of Recent deep-sea sands is summarized in Table 18. Clearly, Recent deep-sea sands, the modern analogues of ancient graywackes, show a distinct contrast in chemical variables between passive and active basin types. Moreover, ancient turbidite sandstones from passive continental margins are characterized by SiO_2 content greater than 70 percent, an SiO_2/Al_2O_3 ratio about 7.0 and a K_2O/Na_2O ratio greater than one, whereas samples grouped into active tectonic settings have typical SiO_2 contents less than 70 percent, an SiO_2/Al_2O_3 ratio around 4.5 and a K_2O/Na_2O ratio less than one. Thus, chemical variables such as SiO_2 content and ratios of SiO_2/Al_2O_3 and K_2O/Na_2O seem to generally be reliable indicators of provenance of ancient turbidite sandstones. However, the ancient turbidite sandstones of this study included only one sample from a passive margin tectonic setting so that for future studies, more data from passive margin sands are needed to support the conclusion above.

The K_2O and Na_2O contents of the modern deep-sea muds show a relationship with tectonic setting: the K_2O/Na_2O ratio decreases noticeably from passive to active continental margins. But, it is also noticed that

TABLE 18

MAJOR CHEMICAL VARIABLES OF RECENT DEEP-SEA SANDS AND THEIR CORRESPONDING BASIN TYPES

Types of Sand	Basin Types	Chemical Variables		
		SiO_2(%)	SiO_2/Al_2O_3	K_2O/Na_2O
Recent Deep Sea Sand	Trailing Edge	78.87	8.16	1.11
	Leading Edge	68.11	4.51	0.66
	Back Arc	68.29	4.83	0.66
	Fore Arc	63.68	4.34	0.46

there is an increase in K_2O content with increasing geologic age in the shales and the K_2O/Na_2O ratios in the shales are better correlated with geologic age than tectonic setting. However, more data of K_2O content from Mesozoic shales are needed to refine this K_2O trend for future studies.

Chemical similarity between Recent deep-sea sands, ancient turbidite sandstones and average graywacke suggests that diagenetic reactions of graywackes occur in a closed system and the high Na_2O content of many turbidite graywackes is a primary feature unrelated to diagenesis. The shale picture is less clear: the high K_2O content of ancient shales is most likely a feature they possessed at time of deposition, but there is some evidence that it could be secondary. A good test would be to measure feldspar content. If the older shales have more K-feldspar than younger shales, then the trend in K_2O is almost certainly primary because diagenetic reaction in shales leads to the destruction of K-feldspar.

More careful observations of the diagenetic textures and minerals from these turbidites will certainly be helpful in better understanding the arguments above. However, it seems to me that extensive studies of bulk chemistry, X-ray mineralogy and thin-section petrology of a series of core samples from different depths from a turbidite basin such as Ventura Basin probably is the best way to understand the two essential problems of graywacke diagenesis: matrix and soda problems.

References Cited

Almond, W. R., Fullerton, L. B., and Davis, D. K., 1976, Pore space reduction in Cretaceous sandstones through chemical precipitation of clay minerals: J. Sediment. Petrology, v. 46, p. 89-96.

Ataman, G., and Gokcen, S. L., 1975, Determination of source and paleoclimate from the comparison of grain and clay fraction in sandstones: a case study: Sediment. Geol., v. 13, p. 81-107.

Audley-Charles, M. G., 1967, Graywackes with a primary matrix from the Viqueque Formation (Upper Miocene): J. Sediment. Petrology, v. 37, p. 5-11.

Bachman, R. T., and Hamilton, E. L., 1976, Density, porosity and grain density of samples from deep sea drilling project site 222 (leg 23) in the Arabian Sea: J. Sediment. Petrology, v. 46, p. 654-658.

Beard, D. C., and Weyl, P. K., 1973, Influence of texture on porosity and permeability of unconsolidated sand: Am. Assoc. Petroleum Geologists Bull., v. 57, p. 349-369.

Bell, F. G., 1978a, The physical and mechanical properties of the Fell sandstones, Northumberland, England: Engng. Geol., v. 12, p. 1-29.

_____ 1978b, Petrographical factors relating to porosity and permeability in the Fell sandstone: Q. J. Engng. Geol., v. 11, p. 113-126.

Björlykke, K., 1974, Geochemical and mineralogic influence of Ordovician island arcs on epicontinental clastics sedimentation. a study of Lower Paleozoic sedimentation in the Oslo region, Norway: Sedimentology, v. 21, p. 251-272.

Blatt, H., Middleton, G., and Murray, R., 1972, Origin of sedimentary rocks: Prentice-Hall Inc., New Jersey, 634 p.

Brenchley, P. J., 1969, Origin of matrix in Ordovician graywackes, Berwyn Hills, North Wales: J. Sediment. Petrology, v. 39, p. 1297-1301.

Bucke, D. P., and Mankin, C. J., 1971, Clay-mineral diagenesis within interlaminated shales and sandstones: J. Sediment. Petrology, v. 41, p. 971-981.

Burst, J. F., 1969, Diagenesis of Gulf Coast clayey sediments and its possible relation to petroleum migration: Am. Assoc. Petroleum Geologists Bull., v. 53, p. 73-93.

Chilingarian, G. V., and Wolf, K. H., eds., 1975 and 1976, Compaction of coarse-grained sediment, I and II: Amsterdam, Elsevier Scientific Publ. Co., 552 p. and 808 p.

Clarke, F. W., 1924, The data of geochemistry (5th ed.): U. S. Geol. Survey Bull., 770, 841 p.

Condie, K. C., Macke, J. E., and Reimer, T. O., 1970, Petrology and geochemistry of Early Precambrian graywackes from the Fig Tree Group: Geol. Soc. Am. Bull., v. 81, p. 2759-2776.

_____ and Snansieng, S., 1971, Petrology and geochemistry of the Duzel (Ordovician) and Gazelle (Silurian) Formations, northern California: J. Sediment. Petrology, v. 41, p. 741-751.

Crook, K. A. W., 1974, Lithogenesis and tectonics: the significance of compositional variation in flysch arenites (graywackes), in Dott, R. H., and Shaver, R. H., eds., Modern and ancient geosynclinal sedimentation: SEPM Sp. Pub. 19, p. 304-310.

Crow, E. L., Davis, F. A., and Maxfield, M. W., 1960, Statistics manual: New York, Dover Publications Inc., 288 p.

Cummins, K. C., 1962, The graywackes problem: Liverpool Manchester Geol. J., v. 3, p. 51-72.

Currie, J. B., and Nwachukwu, S. O., 1974, Evidence of incipient fracture porosity in reservoir rocks at depth: Bull. Canadian Petroleum Geology, v. 22, p. 42-58.

Currie, K. L., 1969, Geological notes on the Carswell circular structures: Geol. Surv. Canada Paper 67-32.

Dapples, E. C., 1972, Some concepts of cementation and lithification of sandstones: Am. Assoc. Petroleum Geologists Bull., v. 56, p. 3-25.

Davis, J. C., 1973, Statistics and data analysis in geology: New York, J. Wiley and Sons, 550 p.

Deelman, J. C., 1975, Pressure solution or indentation: Geology, v. 3, p. 23-24.

Dickinson, W. R., 1970, Interpreting detrital modes of graywackes and arkose: J. Sediment. Petrology, v. 40, p. 695-707.

_____ 1971, Detrital modes of some New Zealand graywackes: Sedimentary Geol., v. 5, p. 37-56.

Dzulynski, S., and Walton, E. K., 1965, Sedimentary features of flysch and graywackes: Amsterdam, Elsevier Publishing Co., 274 p.

Edwards, A. B., 1950, The petrology of the Miocene sediments of the Aure Trough, Papua: Proc. Roy. Soc. Victoria, v. 60, p. 123-149.

Emery, K. O., 1964, Turbidite--Precambrian to present: Sutd. Oceanog., Tokyo, p. 486-495.

Energy Resources Conservation Board, 1965, Structure contours on the base of the Fish Scale, Alberta, 603 Sixth Ave. SW, Calgary, Alberta. Scale: 1 inch equals 16 miles.

_____ 1974, Reserves of crude oil, gas, natural gas liquid and sulphur, Province of Alberta, Dec., 31, 325 p.

Fahrig, W. F., 1961, The geology of the Athabasca Formation: Geol. Surv. Canada Bull., 68, 41 p.

Fox, J. E., Lambert, P. W., Mast, R. F., Nuss, N. W., and Rein, R. D., 1975, Porosity variation in the Tensleep and its equivalent the Weber sandstone, Western Wyoming: a log and petrographic analysis, in Bolyard, D. W., ed., Deep drilling frontiers of the central Rocky Mountains, Symposium Rocky Mountain Assoc. Geologist, p. 185-216.

Fraser, J. A., Donaldson, J. A., Fahrig, W. F., and Tremblay, L. P., 1970, Helikian basins and geosynclines of the northwestern Canadian shield, in Baer, A. J., ed.: Symposium on basins and geosynclines of the Canadian Shield, Geol. Surv. Canada, Paper 70-40, p. 213-238.

Füchtbauer, H., 1967, Influence of different types of diagenesis on sandstone porosity: Proc. 7th World Petroleum Congress, Mexico, v. 2, p. 353-369.

_____ 1974, Sediments and sedimentary rocks, 1: Part II: New York, Halsted Press, 464 p.

Gaither, A., 1953, A study of porosity and grain relationships in experimental sands: J. Sediment. Petrology, v. 23, p. 180-195.

Galloway, W., 1974, Deposition and diagenetic alteration of sandstone in northeast Pacific arc-related basin: implication for graywacke genesis: Geol. Soc. Am. Bull., v. 85, p. 379-390.

Garrels, R. M., Mackenzie, F. T., and Siever, R., 1971, Sedimentary cycling in relation to the history of the continents and oceans, in Robertson, E. C., ed., The nature of the solid earth: New York, McGraw Hill Inc., p. 93-121.

Glass, H. D., Potter, P. E., and Siever, R., 1957, Clay mineralogy of some basal Pennsylvanian sandstones: clays and shales: Am. Assoc. Petroleum Geologists Bull., v. 40, p. 750-754.

Harrold, P. J., and Moore, J. C., 1973, Composition of deep-sea sands from marginal basins of the Northwestern Pacific, in Karis, D. E., Ingle, J. C., et al., Initial reports of the Deep Sea Drilling Project: Washington, U. S. Government Printing Office, v. 31, p. 507-514.

Hawkins, J. W., Jr., and Whetten, J. T., 1969, Graywacke matrix minerals: hydrothermal reactions with Columbia River sediments: v. 166, p. 868-870.

Hayes, J. B., 1971, Petrology of indurated sandstones, Leg 18, Deep Sea Drilling Project: DSDP Initial Report, v. 18, p. 915-924.

Heald, M. T., 1950, Authigenesis in West Virginia sandstones: J. Geol., v. 58, p. 624.

_____1956, Cementation of Simpson and St. Peter sandstones in parts of Oklahoma, Arkansas and Missouri: J. Geol., v. 64, p. 16-30.

_____ and Larese, R. E., 1973, The significance of the solution of feldspar in porosity development: J. Sediment. Petrology, v. 43, p. 458-460.

Heling, D., 1978, Diagenesis of illite in argillaceous sediments of the Rhinebraben: Clay Minerals, v. 13, p. 211-219.

Hollister, C. D., and Heezen, B. C., 1964, Modern graywacke-type sands: Sciences, v. 146, p. 1523-1524.

Hower, J., Eslinger, E. V., Hower, M. E., and Perry, E. A., 1976, Mechanism of burial metamorphism of argillaceous sediment: 1. mineralogic and chemical evidence: Geol. Soc. Am. Bull., v. 87, p. 725-737.

Hsü, K. J., 1977, Studies of Ventura field, California, I: facies, geometry and genesis of Lower Pliocene turbidites: Am. Assoc. Petroleum Geologists Bull., v. 61, p. 137-168.

Isomi, H., Katada, M., Omori, E., and Omori, T., 1966, Singular characteristics of chemical composition of the Permian graywacke from the Kiso Mountains, Central Japan: J. Japan Assoc. Min. Pet. Econ. Geol., v. 55, p. 145-159.

Kahn, J. S., 1956, The analysis and distribution of the properties of packing in sand size sediment, 1: on the measurement of packing in sandstones: J. Geology, v. 64, p. 384-395.

Kastner, M., 1971, Authigenic feldspars in carbonate rocks: Am. Mineralogist, v. 56, p. 1403-1422.

Kisch, H. J., 1969, Coal-rank and burial-metamorphic mineral facies, in Advance in organic geochemistry: Oxford, Pergamon Press, p. 407-425.

Klein, G. deVries, 1963, Analysis and review of sandstone classification in the North American geological literature, 1940-1960: Geol. Soc. Am. Bull., v. 74, p. 555-576.

Krynine, P. D., 1940, Petrology and genesis of the Third Bradford Sand: The Penn. State College Bull., no. 29, 134 p.

_____ 1947, Petrologic aspects of prospecting for deep oil horizons in Pennsylvania: The Penn. State College Bull., no. 48, p. 81-95.

Kuenen, Ph. H., 1966, Matrix of turbidites: Experimental approach: Sedimentology, v. 7, p. 267-297.

Lajoie, J., 1973, Albite of secondary origin in Charny Sandstones, Quebec: Discussion: J. Sediment. Petrology, v. 42, p. 341-349.

_____ and Chagnon, A., 1973, Origin of red beds in a Cambrian flysch sequence Canadian Appalachians, Quebec: Sedimentology, v. 20, p. 91-103.

_____ Heroux, Y., and Mathey, B., 1974, The Precambrian shield and Lower Paleozoic shelf: the unstable provenance of the Lower Paleozoic flysch sandstones and conglomerates between Beaumont and Bic, Quebec: Can. J. Earth Science, v. 11, p. 951-963.

Lerand, M. M., 1970, Athabasca Formation, Rumpel Lake stratigraphic test and lithologic description: Gulf Minerals Company, Calgary, Canada, 31 p.

Lerbekmo, J. F., 1961, Porosity reduction in Cretaceous sandstones of Alberta: Alberta Soc. Petroleum Geologists J., v. 9, p. 192-199.

Levandowski, D. W., Kaley, M. E., Silverman, S. R., and Smalley, R. G., 1973, Cementation in Lyons sandstone and its role in oil accumulation, Denver basin, Colorado: Am. Assoc. Petroleum Geologists Bull., v. 57, p. 2217-2244.

Lowry, W. D., 1956, Factors in loss of porosity by quartzose sandstones of Virginia: Am. Assoc. Petroleum Geologists Bull., v. 40, p. 489-500.

Mackenzie, F. T., 1975, Sedimentary cycling and the evolution of sea water, in Riley, J. P., and Skirrow, G., eds., Chemical Oceanography, p. 309-364.

Manger, G. E., 1963, Porosity and bulk density of sedimentary rocks: U. S. Geol. Surv. Bull., 1144-E, 55 p.

Martini, I. P., 1972, Studies of microfabrics: an analysis of packing in Crimsby Sandstone (Silurian), Ontario and New York State, in Stratigraphy and sedimentology: Int. Geol. Congr. Montreal, Section 6, p. 415-423.

Maxwell, J. C., 1964, Influence of depth, temperature and geologic age on porosity of quartzose sandstone: Am. Assoc. Petroleum Geologists Bull., v. 48, p. 697-709.

Medlin, J. H., Suhr, N. H., and Bodkin, J. B., 1969, Atomic Absorption analysis of silicates employing $LiBO_2$ fusion: Atomic Absorption Newsletter, v. 8, p. 25-29.

Mellon, G. B., 1967, Stratigraphy and petrology of the Lower Cretaceous Blairmore and Mannville Groups, Alberta foothills and plains: Research Council Alberta Bull., v. 21, 270 p.

Middleton, G. V., 1972, Albite of secondary origin in Charny Sandstones, Quebec: J. Sediment. Petrology, v. 42, p. 341-349.

Moore, W. R., 1975, Grain packing-porosity relationships of Minnelusa sandstone, Powder River basin, Wyoming: The Mountain Geologist, v. 12, p. 45-53.

Morrow, N. R., 1971, Small scale packing heterogeneities in porous sedimentary rocks: Am. Assoc. Petroleum Geologists Bull., v. 55, p. 514-522.

Nelson, H. W., and Glaister, R. P., 1978, Subsurface environmental facies and reservoir relationships of the McMurray oil sands, northeastern Alberta: Bull. Can Petroleum Geology, v. 26, p. 177-207.

Perry, E., and Hower, J., 1970, Burial diagenesis in Gulf Coast pelitic sediments: Clays and Clay Minerals, v. 18, p. 165-177.

Pettijohn, F. J., 1963, Chemical composition of sandstones--excluding carbonate and volcanic sands, in Data of geochemistry (6th ed.), U. S. Geol. Surv. Prof. Paper 440s, 19 p.

_____ 1975, Sedimentary rocks, 3rd ed.: New York, Harper and Row Inc., 628 p.

_____Potter, P. E., and Siever, R., 1972, Sand and Sandstone: New York, Springer-Verlag, 618 p.

Phipps, C. B., 1969, Post-burial sideritization of calcite in Eocene beds from the Maracaibo basin, Venezuela: Geol. Mag., v. 106, p. 485-495.

Pittman, E. D., and Lumsden, D. N., 1968, Relationship between chlorite coating on quartz grains and porosity, Spiro Sand, Oklahoma: J. Sediment. Petrology, v. 38, p. 668-670.

Potter, P. E., 1978, Petrology and chemistry of modern big river sands: J. Geol., v. 86, p. 423-449.

Power, M. C., 1959, Adjustment of clays to chemical change and the concept of the equivalent level: Clays and Clay Min., v. 6, p. 309-326.

_____ 1967, Fluid release mechanism in compacting marine rocks and their importance in oil exploration: Am. Assoc. Petroleum Geologists Bull., v. 51, p. 1240-1253.

Prozorovich, G. E., 1971, Sedimentary and epigenetical trends aiding the hydrocarbon exploration in west Siberia: Sedimentology, v. 17, p. 233-241.

Pryor, W. A., 1973, Permeability-porosity patterns and variations in some Holocene sand bodies: Am. Assoc. Petroleum Geologists Bull., v. 57, p. 162-189.

Rahmani, R. A., 1968, Graywackes with a primary matrix from the Viqueque Formation (Upper Miocene-Pliocene), Timor--Comment on a paper by Audley-Charles, M. G.: J. Sediment. Petrology, v. 38, p. 271-273.

Reimer, T. O., 1972, Diagenetic reactions in Early Precambrian graywackes of the Barberton Mountain land (South Africa): Sediment. Geol., v. 7, p. 263-282.

Rittenhouse, G., 1971, Pore-space reduction by solution and cementation: Am. Assoc. Petroleum Geologists Bull., v. 55, p. 80-91.

Ronov, A. B., Girin, Y. P., Kazakov, G. A., and Ilyukhin, M. N., 1966, Sedimentary differentiation in platform and geosynclinal basins: Geochem. Internatl., 3, p. 595-608.

_____ and Migdisov, A. A., 1971, Geochemical history of the crystalline basement and the sedimentary cover of the Russian and North American platforms: Sedimentology, v. 16, p. 137-187.

Rust, B. R., 1965, The sedimentology and diagenesis of Silurian turbidites in southeast Wigtownshire, Scotland: Scot. J. Geol., v. 1, p. 231-246.

Schwab, F. L., 1975, Framework mineralogy and chemical composition of continental margin-type sandstone: Geology, v. 3, p. 487-490.

Selley, R. C., 1978, Porosity gradients in North Sea oil-bearing sandstones: J. Geol. Soc. London, v. 135, p. 119-132.

Shaw, D. W., 1956, Geochemistry of pelitid rocks III: major elements and general geochemistry: Geol. Soc. Am. Bull., v. 67, p. 919-934.

Sibley, D. F., and Blatt, H., 1976, Intergranular pressure solution and cementation of the Tuscarora orthoquartzite: J. Sediment. Petrology, v. 46, p. 881-896.

Sprunt, E. S., and Nur, A., 1976, Reduction of porosity by pressure solution: experimental verification: Geology, v. 4, p. 463-466.

Stephenson, L. P., 1977, Porosity dependence on temperature: limit on maximum possible effect: Am. Assoc. Petroleum Geologists Bull., v. 61, p. 407-415.

Swardt, A. M. J. de, and Towel, D. M., 1974, Note on the relationship between diagenesis and deformation in the Cape foldbelt: Geol. Soc. S. Africa Trans., v. 77, p. 239-245.

Taylor, J. M., 1950, Pore-space reduction in sandstones: Am. Assoc. Petroleum Geologists Bull., v. 34, p. 701-716.

Triplehorn, D. M., 1970, Clay mineral diagenesis in Atoka (Pennsylvanian) Sandstones, Crawford County, Arkansas: J. Sediment. Petrology, v. 40, p. 838-848.

Van Moort, J. C., 1972, The K_2O, CaO, MgO and CO_2 contents of shales and related rocks and their implications for sedimentary evolution since the Proterozoic: 24th IGC-section 10, p. 427-439.

Velde, E., 1977, Clays and clay minerals in natural and synthetic systems: New York, Elsevier Publishing Inc., 218 p.

Vinogradov, A. P., and Ronov, A. B., 1956, Evolution of the chemical composition of clays of the Russian platform: Geokhim., v. 2, p. 3-18 (in Russian). English translation in Geochemistry, 1960, p. 123-139.

Wallace, C. A., 1976, Diagenetic replacement of feldspar by quartz in the Unita Mountain Group, Utah and its geochemical implications: J. Sediment. Petrology, v. 46, p. 847-861.

Walton, E. K., 1955, Silurian graywackes in Peebleshire: Proc. Roy. Soc. Edinburgh, B, v. 65, p. 327-357.

Weaver, C. E., 1967, Potassium, illite and the ocean: Geochim. Cosmochim. Acta. v. 31, p. 2182-2196.

Weller, J. M., 1959, Compaction of sediments: Am. Assoc. Petroleum Geologists Bull., v. 43, p. 273-310.

Weyl, P. K., 1959, Pressure solution and the force of crystallization--a phenomenological theory: J. Geophys. Research, v. 64, p. 2001-2005.

Whetten, J. T., and Hawkins, J. W., Jr., 1970, Diagenetic origin of graywacke matrix minerals: Sedimentology, v. 15, p. 347-361.

_____ 1971, Diagenetic origin of graywache matrix minerals: a reply: Sedimentology, v. 16, p. 142-146.

Wilson, M. D., and Pittman, E. D., 1977, Authigenic clays in sandstones: recognition and influence on reservoir properties and paleoenvironmental analysis: J. Sediment. Petrology, v. 47, p. 3-31.

APPENDIX 1

SAMPLE LOCATIONS OF LAMONT-DOHERTY PISTON CORES

Sample No.	Latitude	Longitude	Water Depth m	Sub-bottom Depth cm	Location	Basin Type
V 19-284	00° 16' N	04° 46' E	3937	490	Guinea Bas.	TE
V 19-285	00° 39' N	03° 42' E	4202	35	Guinea Bas.	TE
V 19-286	00° 41' N	00° 19' E	4896	285	Guinea Bas.	TE
V 23-8	40° 33' N	60° 11' W	4991	685	Sohm Ab. Pl.	TE
V 23-15	43° 29' N	45° 15' W	4415	430	Newfoundland Bas.	TE
V 24-128	18° 11' N	120° 04' E	3189	85	South China Bas.	BA
V 24-129	19° 12' N	120° 49' E	3343	105	South China Bas.	BA
V 24-131	17° 32' N	118° 59' E	4177	110	South China Bas.	BA
V 24-137	03° 41' N	122° 59' E	5004	100	Celebes Bas.	BA
V 24-153	04° 30' S	153° 28' E	4103	40	N. Solomon Bas.	FA
V 24-258	02° 21' N	43° 18' W	4254	430	Ceara Ab. Pl.	TE
V 24-260	12° 24' N	57° 31' W	645	340	Guinea Bas.	TE
V 27-3	40° 40.2'N	62° 21.7' W	4729	625	Sohm Ab. Pl.	TE
V 27-8	40° 48.1'N	56° 36' W	5152	20	Sohm Ab. Pl.	TE
V 27-9	39° 31.5'N	57° 36.4' W	5216	90	Sohm Ab. Pl.	TE
V 27-14	41° 21.2'N	46° 49.8' W	4453	415	Sohm Ab. Pl.	TE
V 27-98	60° 39.2'N	07° 25.5' W	980	325	Rockall Trough	TE
V 27-130	45° 03.9'N	07° 59.1' W	4526	120	Biscay Ab. Pl.	TE
V 28-257	20° 37' N	146° 45' E	2681	100	Mariana Bas.	FA

APPENDIX 1 (continued)

Sample No.	Latitude	Longitude	Water Depth m	Sub-bottom Depth cm	Location	Basin Type
V 28-258	21° 33' N	143° 24' E	3387	20	Mariana Bas.	FA
V 28-264	37° 09.2'N	130° 50.5' E	2109	375	Japan Bas.	BA
V 28-271	40° 45' N	138° 27' E	3382	545	Japan Bas.	BA
V 28-272	42° 12' N	136° 02' E	3610	145	Japan Bas.	BA
V 28-273	41° 29' N	135° 43' E	3533	360	Japan Bas.	BA
V 28-275	39° 38' N	137° 27' E	2849	10	Japan Bas.	BA
V 28-283	41° 15' N	143° 39' E	2158	15	E. Japan Bas.	FA
V 28-327	02° 42' N	121° 32' E	5336	445	Celebes Bas.	BA
V 28-357	07° 21' N	103° 07' E	6454	210	Java Trench	FA
V 29-1	05° 23' N	102° 56' E	1891	95	Java Trench	FA
V 29-19	14° 42' N	83° 35' E	3182	590	Ganges Cone	TE
V 29-20	11° 32' N	81° 42' E	3557	335	Ganges Cone	TE
V 29-22	06° 58' N	82° 27' E	3950	1040	Ganges Cone	TE
V 29-94	35° 58' S	25° 36' E	4751	170	Agulhas Bas.	TE
RC 9-66	01° 57.6N	80° 26.6' W	4314	445	Panama Bas.	LE
RC 10-84	18° 10.1'N	104° 22.3' W	680	500	W. Mexico Bas.	LE
RC 10-87	19° 05.6'N	105° 30' W	4912	300	Middle Amer. Tr.	LE
RC 12-24	11° 53' N	78° 27' W	3729	290	Caribbean Bas.	BA
RC 12-25	10° 43' N	79° 03.8' W	3537	50	Caribbean Bas.	BA
RC 12-41	20° 07' N	105° 18.5' W	3837	110	Middle Amer. Tr.	LE

APPENDIX 1 (continued)

Sample No.	Latitude	Longitude	Water Depth m	Sub-bottom Depth cm	Location	Basin Type
RC 12-44	21° 02' N	113° 15' W	3662	550	S. Baja Calif. Bas.	LE
RC 12-243	40° 51' S	54° 29' W	4689	130	Argentine Ab. Pl.	TE
RC 12-245	37° 10.2'S	54° 55.2' W	99	99	Argentine C. P.	TE
RC 12-368	34° 22.2'N	129° 04.4' E	159	250	S. Korea C. P.	BA
RC 12-357	34° 45.7'N	129° 09' E	124	20	S. Korea C. P.	BA
RC 12-374	46° 39' N	130° 58' E	2111	410	Japan Bas.	BA
RC 13-220	12° 12.4'S	12° 36' E	1760	160	Angola Bas.	TE
RC 13-222	13° 34' S	09° 55.7' E	3988	870	Angola Bas.	TE
RC 14-114	51° 37.6'N	161° 54.8' E	5398	630	W. Kamchatka Bas.	FA
RC 14-117	53° 51.5'N	172° 49.6' E	3904	1430	Aleutian Bas.	BA
RC 14-122	55° 56' N	175° 05.5' W	3621	670	Aleutian Bas.	BA
RC 14-123	56° 56.4'N	179° 49' W	3782	335	Aleutian Bas.	BA
RC 14-124	58° 28.5'N	177° 23.8' E	3731	190	Aleutian Bas.	BA
RC 14-132	58° 31.8'N	167° 24.9' E	3592	550	Komandorskiy Bas.	BA
RC 14-134	57° 52.8'N	176° 34.5' E	3678	605	Aleutian Bas.	BA
RC 14-137	58° 17.1'N	164° 45.4' E	3479	120	Komandorskiy Bas.	BA
RC 14-141	57° 20.7'N	164° 26.4' E	3111	1075	Komandorskiy Bas.	BA
RC 14-151	53° 17' N	163° 32.5' W	3975	245	S. Aleutian Bas.	FA
RC 14-154	54° 36.8'N	145° 58.8' W	4111	75	Alaska Bas.	LE
RC 14-160	58° 05.2'N	142° 45' W	3729	170	Alaska Bas.	LE

APPENDIX 1 (continued)

Sample No.	Latitude	Longitude	Water Depth m	Sub-bottom Depth cm	Location	Basin Type
RC 15-2	45° 42.6'N	127° 58.8' W	2875	150	Cascadia Bas.	LE
RC 15-26	08° 59.3'N	138° 04.6' W	3780	210	Pacific Bas.	FA
RC-15-67	60° 00.9'S	80° 35.2' W	5033	140	Bellinghausen Ab. Pl.	TE
RC 15-77	55° 40.2'S	63° 20.5' W	4045	45	W. Scotia Bas.	LE
RC 15-79	52° 55.1'S	60° 27.6' W	472	250	S. Falkland Bas.	TE
RC 15-109	39° 08' S	52° 49.8' W	6430	840	Argentine Ab. Pl.	TE
RC 15-128	40° 20' S	55° 18' W	2041	50	Argentine Ab. Pl.	TE
RC 15-129	38° 31' S	56° 15' W	82	50	Argentine C. P.	TE
RC 15-132	47° 12.1'S	51° 25.1' W	6067	50	Argentine Ab. Pl.	TE

APPENDIX 2

CHEMICAL COMPOSITION OF RECENT DEEP SEA SANDS

Sample No.	SiO_2	Al_2O_3	Fe_2O_3	MgO	CaO	K_2O	Na_2O
RC 12-243*	71.06	15.02	3.15	1.25	3.82	2.08	3.62
RC 12-245*	74.17	12.23	2.79	1.16	4.27	1.84	3.53
RC 13-220	77.26	13.04	1.47	0.57	1.11	3.96	2.60
RC 13-222	76.23	13.14	2.43	0.73	2.61	2.79	2.06
RC 15-67*	69.36	15.55	4.10	1.41	3.72	1.71	4.17
RC 15-79	63.52	5.38	1.40	0.76	27.45	1.13	0.36
RC 15-109	71.48	14.80	3.12	1.29	3.63	1.93	3.73
RC 15-128*	72.17	14.94	1.80	1.06	4.21	2.04	3.77
RC 15-129*	69.82	15.84	3.23	1.15	3.99	2.17	3.86
RC 15-132*	71.82	15.43	2.82	1.21	3.20	1.89	3.64
V 19-284*	44.13	9.22	8.14	3.62	31.87	1.08	1.95
V 19-285	74.96	8.60	5.45	1.41	5.24	2.64	1.67
V 19-286	88.65	6.37	1.39	0.42	1.02	1.48	0.63
V 23-8	80.04	8.12	2.42	0.97	5.02	1.90	1.51
V 23-15	76.96	8.75	4.34	1.43	4.83	1.74	1.98
V 24-260	86.55	7.13	1.84	0.46	2.54	0.83	0.64
V 24-258	88.06	5.58	2.21	0.48	1.38	1.17	1.10
V 27-3	82.76	8.34	2.79	0.89	2.23	1.84	1.19
V 27-9	90.00	5.91	0.80	0.35	1.31	1.11	0.51
V 27-8	74.33	10.30	2.57	2.00	6.47	1.92	2.38
V 27-14	67.32	16.40	2.45	2.08	7.60	1.72	2.49
V 27-98	65.95	10.27	5.46	3.22	11.51	1.63	1.93
V 27-130	86.04	5.86	0.88	0.55	5.16	1.01	0.45
V 29-19	71.40	11.79	4.54	3.06	3.71	3.02	2.45
V 29-20	75.31	8.85	3.41	1.42	6.58	1.73	2.70
V 29-22	73.55	11.29	4.07	2.57	3.47	2.81	2.27
V 29-94	55.01	6.66	2.27	0.87	31.12	1.06	2.98

*Volcanic clastic-rich samples which are excluded for computation.

APPENDIX 2 (continued)

Sample No.	SiO_2	Al_2O_3	Fe_2O_3	MgO	CaO	K_2O	Na_2O
RC 14-123	72.79	14.65	3.61	1.60	2.84	1.67	2.83
RC 14-124	70.66	15.39	3.79	1.73	3.19	1.94	3.30
RC 14-132	67.96	14.42	5.24	2.88	4.17	1.67	3.65
RC 14-134	68.51	13.09	5.75	2.95	5.40	1.34	2.93
RC 14-137	66.12	16.49	4.49	3.09	3.35	2.01	4.45
RC 14-141	64.35	15.14	7.03	3.78	4.33	1.59	3.77
V 24-128	64.47	14.18	7.18	3.65	4.15	3.04	3.30
V 24-131	63.33	15.04	7.01	4.60	5.60	1.18	3.30
V 24-137	52.33	21.49	6.16	3.63	11.42	1.14	3.81
V 28-264	73.61	13.06	2.34	0.47	2.14	3.67	4.74
V 28-271	67.16	14.13	4.77	2.70	4.96	2.50	3.81
V 28-272	74.61	11.45	3.80	1.10	1.92	3.25	3.88
V 28-273	69.64	13.73	3.77	2.76	3.49	2.91	3.67
V 28-275	69.24	14.48	4.05	2.64	2.79	2.62	4.19
V 28-327	66.98	13.01	5.42	2.84	6.02	2.12	3.57
RC 9-66	69.72	15.41	2.35	0.99	3.31	4.45	4.67
RC 10-84	65.08	15.09	5.53	3.24	5.31	1.53	4.14
RC 10-87	72.66	13.19	3.06	1.18	3.15	3.08	3.68
RC 12-41	68.22	15.61	3.90	1.58	2.52	4.33	3.89
RC 12-44	68.70	15.05	3.97	1.64	2.73	4.19	3.76
RC 14-154	65.06	16.23	5.09	3.08	5.62	1.18	3.78
RC 14-160	67.94	15.81	4.47	1.83	4.75	1.42	3.80
RC 15-2	67.59	15.52	5.52	2.44	4.02	1.57	3.36
RC 15-77	68.10	14.92	2.89	1.21	7.98	1.32	3.62
RC 12-24	74.35	10.81	5.38	2.67	3.12	1.35	2.35
RC 12-371	75.56	10.95	2.85	1.05	2.26	3.92	3.49
RC 12-374	75.56	10.95	2.85	1.05	2.26	3.92	3.49
RC 12-374	70.50	13.59	2.31	1.08	7.58	2.40	2.55
RC 14-117	61.87	15.64	8.53	3.86	4.53	1.14	4.44
RC 14-122	72.30	13.34	4.54	1.80	3.81	1.47	2.75
RC 14-114	61.30	16.84	8.78	2.65	4.66	1.12	4.66

APPENDIX 2 (continued)

Sample No.	SiO_2	Al_2O_3	Fe_2O_3	MgO	CaO	K_2O	Na_2O
RC 14-151	63.88	14.94	6.83	2.71	5.53	1.58	4.53
RC 15-26	69.31	15.68	4.59	1.27	3.76	1.91	3.52
V 24-153	50.74	18.64	9.50	4.54	11.70	1.14	3.72
V 28-257	62.44	10.46	9.45	8.05	7.11	0.39	2.09
V 28-258	52.75	16.84	10.25	4.97	10.06	1.48	3.61
V 28-357	76.93	10.97	2.49	1.30	2.55	3.46	2.30
V 29-1	65.88	14.88	5.45	2.92	4.65	2.02	4.18
V 28-283	69.89	12.84	4.33	2.56	4.15	1.99	4.19

APPENDIX 3

CHEMICAL COMPOSITION OF RECENT DEEP SEA MUDS

Sample No.	SiO_2	Al_2O_3	Fe_2O_3	MgO	CaO	K_2O	Na_2O
RC 12-243	71.22	13.55	5.28	1.86	3.06	2.37	2.69
RC 13-220	63.94	19.02	6.84	3.09	1.58	3.94	1.55
RC 13-222	55.56	18.63	7.51	4.22	10.71	2.55	0.83
RC 15-67	71.43	13.19	4.71	1.64	3.50	1.83	3.66
RC 15-109	69.84	14.87	5.69	3.03	1.84	2.51	2.25
RC 15-132	68.56	16.55	6.11	2.55	1.64	2.46	2.17
V 19-284	45.46	12.07	10.57	3.81	24.57	1.25	1.42
V 19-286	74.31	13.83	6.66	1.54	1.10	1.83	0.70
V 23-8	65.99	12.52	5.02	3.75	8.27	2.97	1.48
V 23-15	70.91	11.51	4.79	2.50	5.88	2.64	1.77
V 24-258	85.64	7.61	2.57	0.55	1.56	1.38	0.66
V 24-260	56.09	17.23	2.37	6.48	14.91	2.27	0.73
V 27-3	66.31	14.70	6.48	2.68	5.03	3.42	1.42
V 27-8	58.74	11.86	4.61	3.75	16.95	2.39	1.72
V 27-14	64.33	10.20	3.67	4.25	13.33	2.17	2.02
V 27-98	67.43	11.15	5.76	2.09	10.01	2.09	1.44
V 27-130	64.84	8.77	2.87	1.55	18.89	2.50	0.62
V 29-19	65.75	16.25	5.97	2.64	4.24	3.52	1.69
V 19-20	66.04	15.68	7.00	2.21	4.68	2.32	2.04
V 19-22	63.87	17.59	8.26	2.71	2.87	3.58	1.12
V 29-94	55.35	8.36	3.04	1.27	29.06	1.46	1.46
RC 14-141	64.73	15.78	6.74	3.87	3.64	2.03	3.24
V 24-128	64.38	17.22	8.27	2.79	3.78	1.14	2.45
V 24-129	66.20	14.57	7.26	2.99	4.70	1.70	2.55
V 24-137	57.70	16.27	6.27	3.56	11.26	1.52	3.43
V 24-137	57.70	16.27	6.27	3.56	11.26	1.52	3.43
V 28-264	70.84	15.47	4.49	2.08	1.23	3.27	2.60
RC 9-66	67.34	14.99	5.82	2.43	5.10	1.98	2.36
RC 10-84	61.57	17.69	7.17	3.64	5.04	1.83	3.03
RC 10-87	67.34	16.64	6.04	2.95	1.94	2.55	2.54

APPENDIX 3 (continued)

Sample No.	SiO_2	Al_2O_3	Fe_2O_3	MgO	CaO	K_2O	Na_2O
RC 12-41	66.63	16.98	5.68	3.66	1.81	2.74	2.46
RC 14-154	65.61	14.33	7.43	2.94	5.00	2.07	2.61
RC 14-160	65.59	13.42	6.79	4.05	5.50	1.59	3.03
RC 15-2	64.75	14.92	7.30	4.20	3.80	2.36	2.67
RC 15-77	63.64	18.17	7.20	3.08	2.83	2.67	2.39
RC 14-114	66.55	14.41	6.61	3.30	3.94	1.86	3.34
RC 14-151	64.83	14.48	7.70	3.46	4.12	1.84	3.53
RC 15-26	74.89	11.57	5.12	1.87	2.38	2.10	2.04
V 24-153	55.14	15.38	9.70	4.93	11.18	1.24	2.41
V 28-257	74.50	7.04	9.16	2.47	4.32	0.64	1.88
V 28-357	68.12	15.31	6.97	3.52	1.93	3.27	1.85
V 28-283	77.41	9.43	4.56	1.66	3.22	1.44	2.23
V 29-1	69.41	16.71	3.32	2.39	4.27	1.76	2.15
RC 12-24	69.02	14.26	7.70	3.38	2.26	1.61	1.76
RC 14-122	69.81	14.06	6.12	2.26	3.07	2.08	2.61
RC 14-117	65.12	13.65	7.51	4.44	4.16	1.65	3.49
RC 14-123	70.39	13.23	6.37	3.28	2.42	2.23	2.13
RC 14-124	75.17	10.96	4.04	2.04	3.31	1.65	2.79
RC 14-132	66.50	16.07	6.86	3.99	2.31	2.40	1.89
RC 14-134	67.22	15.16	7.34	3.67	1.94	2.49	2.21
RC 14-137	76.93	9.80	5.23	3.05	1.58	1.50	1.93
V 28-271	68.56	14.75	8.45	2.10	1.25	2.98	1.89
V 28-272	68.54	16.16	6.14	3.00	1.09	3.16	2.00
V 28-273	67.75	15.54	6.14	3.53	1.81	2.79	2.40
V 28-275	67.45	15.74	6.01	3.46	1.44	2.63	3.23

APPENDIX 4

CHEMICAL COMPOSITION OF ANCIENT TURBIDITE SANDSTONES

Sample No.	SiO_2	Al_2O_3	Fe_2O_3	MgO	CaO	K_2O	Na_2O
T1a	61.51	15.13	3.04	0.95	13.29	3.09	2.66
T4	65.37	15.35	2.37	0.88	10.23	2.95	3.61
T5a	72.82	14.97	2.44	0.81	3.00	3.38	2.55
T7	69.00	15.44	4.17	1.60	3.13	2.19	4.32
T8	62.20	15.74	6.37	3.03	6.76	2.72	3.23
T9	61.56	15.49	5.61	2.55	10.30	1.24	3.27
T10	63.19	15.20	6.86	3.49	4.92	1.83	4.32
T12	71.09	15.01	5.92	1.95	3.28	1.24	1.42
T19	70.96	15.13	7.49	1.75	1.33	1.71	1.25
T20	73.29	14.92	6.68	1.71	1.49	1.11	1.55
T21	68.19	14.28	5.19	1.93	1.58	3.25	5.23
T22	67.40	15.25	5.08	1.99	2.03	3.13	5.23
T23	66.15	15.45	5.77	2.61	1.41	4.44	4.28
T38	71.64	14.52	4.85	1.49	3.19	1.23	2.99
T39	71.04	15.54	5.76	2.08	1.49	1.47	2.93
T40	68.93	14.81	6.91	2.51	2.05	2.66	2.58
T41	67.08	16.07	5.69	3.24	2.52	1.75	3.62
T42	72.01	16.17	5.21	1.32	1.32	1.58	2.42
T43	71.40	14.72	5.43	2.48	2.51	0.69	2.71
T44	64.72	17.38	6.41	2.60	2.29	2.32	4.18
T45	64.54	17.47	6.73	2.76	2.20	2.33	3.96
T46	61.44	19.03	7.59	2.66	2.71	2.07	4.45
T47	65.47	17.66	7.10	1.80	2.91	2.04	2.99
T48	60.27	17.94	7.15	4.86	3.17	1.65	4.93
T49	64.66	16.27	7.75	3.90	1.44	2.32	4.12
T50	64.66	16.06	9.23	3.74	1.57	1.18	3.52
T51	58.37	16.55	4.76	2.43	15.43	0.88	2.19
T54	61.14	14.90	4.83	2.42	14.04	1.12	1.51
T71	68.49	13.87	2.82	4.29	7.39	1.21	1.99
T72	65.21	14.34	4.75	2.93	10.51	1.64	1.42

APPENDIX 4 (continued)

Sample No.	SiO_2	Al_2O_3	Fe_2O_3	MgO	CaO	K_2O	Na_2O
T73	60.67	13.66	2.01	2.64	17.68	1.35	1.97
T74	56.28	13.20	4.69	3.05	20.46	1.02	1.26
T78	71.48	12.94	1.32	3.57	6.94	1.80	1.93
T89	67.75	13.23	3.06	4.38	8.67	0.79	2.08
T90	70.43	14.65	4.33	2.55	2.91	2.32	2.77
T94	63.20	14.28	2.63	2.09	13.49	2.09	2.34
T96	60.54	13.94	2.61	2.60	16.45	1.89	2.07
T102	47.43	15.80	14.63	8.70	11.07	0.22	2.13
T103	76.12	15.23	2.83	0.80	0.57	0.87	3.51
T105	78.77	13.64	2.09	0.70	0.51	1.04	3.22
T107	65.06	17.61	9.15	1.78	0.76	3.41	2.21
T109	77.88	13.62	3.08	0.43	1.28	1.60	2.09
T112	66.72	15.88	4.54	3.41	5.87	2.17	1.40
T115	67.51	13.69	4.23	2.29	9.30	1.75	1.27
T116	67.92	17.55	5.01	1.02	3.28	1.98	3.21
T118	74.32	12.68	4.24	1.87	4.44	1.47	0.93
T127	68.32	10.46	4.13	2.00	12.30	1.98	0.77
T133	69.78	11.50	5.65	6.29	2.11	1.18	3.49
T149	57.06	11.85	2.70	1.15	19.27	3.57	4.39
T175	69.41	11.17	5.82	1.74	8.39	1.82	1.65
T177	69.75	11.50	5.76	2.16	7.03	2.24	1.52
T179	74.62	12.60	6.91	1.65	0.37	2.42	1.41
T181	80.08	9.98	4.71	1.30	0.68	1.74	1.46
T188	83.35	11.86	3.62	0.53	0.16	0.27	0.29
T190	82.88	11.14	4.24	0.76	0.40	0.41	0.23
T192	84.08	10.54	4.24	0.51	0.34	0.14	0.21
T196	82.34	11.14	4.78	0.76	0.48	0.29	0.23
T198	83.71	11.74	3.18	0.41	0.44	0.24	0.23
T200	81.04	10.74	6.47	0.91	0.44	0.29	0.21
T202	82.84	10.64	4.94	0.74	0.30	0.36	0.21
T204	79.18	12.24	6.47	1.09	0.34	0.53	0.23

APPENDIX 4 (continued)

Sample No.	SiO_2	Al_2O_3	Fe_2O_3	MgO	CaO	K_2O	Na_2O
T206	83.04	11.14	3.94	0.69	0.26	0.74	0.21
T208	87.21	10.34	1.28	0.21	0.26	0.51	0.21
T210	85.82	10.14	1.96	0.27	0.44	1.22	0.21
T212	86.11	11.41	1.63	0.22	0.17	0.17	0.25
T214	80.44	13.25	4.98	0.91	0.17	0.31	0.26
T216	87.01	10.62	1.59	0.20	0.15	0.21	0.24
T218	79.86	12.78	5.59	0.94	0.15	0.36	0.28
T222	78.74	13.31	3.96	0.88	0.16	1.63	1.36

APPENDIX 5

CHEMICAL COMPOSITION OF ANCIENT SHALES ASSOCIATED WITH TURBIDITE SANDSTONE

Sample No.	SiO_2	Al_2O_3	Fe_2O_3	MgO	CaO	K_2O	Na_2O
T1	65.18	16.86	6.50	3.07	3.70	2.52	2.15
T2	64.62	16.20	6.79	3.55	3.49	3.01	2.40
T3	65.67	16.27	6.56	2.72	3.25	2.78	2.70
T5	74.61	14.43	2.02	0.68	2.03	3.35	2.91
T11	63.36	22.58	6.22	1.78	1.13	4.78	1.25
T13	69.58	15.35	6.37	1.83	1.28	4.24	1.34
T14	67.86	15.12	9.19	2.52	1.57	2.55	1.33
T15	67.06	16.04	7.65	2.09	1.21	4.69	1.18
T16	66.93	17.09	7.36	2.01	1.20	4.21	1.15
T17	63.95	19.04	7.75	2.21	1.34	4.01	1.64
T18	68.31	16.89	5.99	1.71	1.03	4.89	1.17
T26	65.64	16.13	6.57	3.85	1.21	3.97	1.64
T56	57.29	15.59	6.16	2.91	14.20	2.79	1.01
T58	58.90	16.39	4.49	4.17	12.23	2.87	0.91
T59	61.22	17.01	4.49	2.95	10.07	2.63	1.60
T64	54.95	16.61	6.30	2.65	15.98	2.50	0.96
T65	55.61	16.58	6.50	2.77	15.14	2.36	1.01
T68	55.17	17.15	7.66	3.05	11.73	4.60	0.61
T75	56.80	13.82	4.91	3.26	18.57	1.34	1.27
T76	55.40	16.46	5.90	3.22	15.84	2.41	0.72
T77	56.90	15.96	5.96	3.58	14.46	2.49	0.95
T91	65.59	15.26	5.42	3.45	3.77	3.25	2.19
T92	66.85	15.28	5.60	4.54	1.28	3.36	2.34
T93	66.73	14.51	4.96	1.86	8.06	2.71	1.37
T95	47.23	16.03	5.23	4.15	23.85	2.61	0.85
T97	49.13	16.52	5.47	6.59	18.25	3.24	0.78
T98	48.71	16.90	6.26	5.43	18.47	3.16	1.01
T99	49.88	16.62	4.09	5.52	20.09	2.25	1.63

APPENDIX 5 (continued)

Sample No.	SiO_2	Al_2O_3	Fe_2O_3	MgO	CaO	K_2O	Na_2O
T104	52.86	28.48	7.01	3.25	0.56	6.52	1.30
T106	61.21	19.65	9.86	2.53	0.53	4.84	1.52
T108	53.23	27.27	10.60	2.16	0.72	4.19	1.81
T111	51.26	27.74	11.49	1.80	0.73	6.13	0.84
T113	63.98	17.94	5.89	4.40	3.87	3.78	1.12
T114	61.20	17.73	6.38	4.53	3.75	5.28	1.10
T117	64.68	15.80	6.96	4.19	2.30	5.09	0.95
T128	69.41	16.35	6.83	1.92	1.49	3.11	0.93
T130	62.72	16.25	6.88	4.20	5.96	3.00	0.95
T148	74.52	11.27	4.11	2.53	2.41	2.92	2.22
T151	67.71	14.78	7.08	4.26	1.21	3.24	1.74
T152	54.94	11.47	6.22	2.57	20.42	3.04	1.34
T154	59.06	21.44	8.64	3.71	2.10	4.36	0.67
T156	58.28	21.55	8.13	3.58	3.36	4.41	0.73
T157	62.18	17.99	8.77	4.06	2.23	3.86	0.92
T163	47.78	17.29	6.46	3.29	20.88	3.75	0.53
T172	59.14	20.38	9.76	2.25	3.10	3.97	1.44
T173	64.81	19.13	7.86	2.39	0.53	3.08	2.07
T174	67.64	15.22	7.66	2.09	2.76	2.60	2.07
T176	56.20	25.49	7.88	2.46	0.70	7.02	0.29
T178	59.29	23.80	7.95	2.03	0.79	5.62	0.55
T180	69.08	16.87	6.92	1.78	0.37	3.54	1.46
T182	63.15	20.97	7.37	2.01	0.79	4.71	0.96
T189	67.95	16.32	9.08	0.85	0.17	4.55	0.54
T191	60.74	26.53	4.96	1.05	0.14	6.54	0.48
T193	60.74	26.28	3.99	1.11	0.15	7.13	0.46
T195	64.05	21.03	7.58	1.33	0.36	5.41	0.22
T199	54.95	30.04	4.71	1.41	0.92	7.63	0.32
T201	60.95	23.05	7.18	2.73	0.33	5.55	0.27
T203	62.40	24.26	4.76	1.60	0.35	6.15	0.48
T205	63.17	22.43	5.86	2.26	0.42	5.55	0.40

APPENDIX 5 (continued)

Sample No.	SiO_2	Al_2O_3	Fe_2O_3	MgO	CaO	K_2O	Na_2O
T207	67.37	19.70	5.28	1.89	0.35	5.11	0.28
T209	53.52	30.64	5.68	1.69	0.30	7.69	0.47
T211	59.04	24.21	7.37	2.70	0.39	5.69	0.58
T213	51.00	33.42	4.16	1.85	0.39	8.59	0.57
T215	51.15	33.33	4.69	0.99	0.39	8.39	1.09
T217	51.36	31.62	6.91	1.75	0.31	7.82	0.23
T219	54.19	29.00	6.71	1.52	0.35	7.37	0.89
T221	53.42	25.75	10.60	3.00	0.44	5.97	0.88
T223	62.61	22.15	7.27	1.11	0.41	5.52	0.93